“What I cannot build, I do not understand.”

$\sim$

Richard Phillips Feynman

University of Alberta

MINIATURIZED GENETIC ANALYSIS SYSTEMS BASED ON MICROELECTRONIC AND MICROFLUIDIC TECHNOLOGIES

by

Mohammad Behnam Dehkordi

A thesis submitted to the Faculty of Graduate Studies and Research
in partial fulfillment of the requirements for the degree of

Doctor of Philosophy

in

Micro-Electromechanical Systems and Nanosystems

Department of Electrical and Computer Engineering

Fall 2010
Edmonton, Alberta

Examining Committee

Christopher Backhouse, Electrical and Computer Engineering

Duncan Elliott, Electrical and Computer Engineering

Vincent Gaudet, Electrical and Computer Engineering

Larry Kostiuk, Mechanical Engineering

Blanca Lapizco Encinas, Microscale Bioseparations Laboratory, CINVESTAV-Monterrey, Mexico

To my great parents, wonderful sister and brothers.

Abstract

Genetic analysis is not widely used for disease diagnostics as it is costly and very labour/infrastructure intensive. We believe that by employing both microelectronic and microfabrication technologies, we are able to integrate multiple functionalities into a single, manufacturable, inexpensive instrument that performs complete genetic analysis protocols. Cost reduction (i.e. instrument and reagent costs), smaller size, and higher automation (i.e. lower labour cost) will certainly pave the way for frequent use of genetic analysis for disease diagnostics.

In this work, we develop technologies and techniques to implement a low power, inexpensive genetic analysis instrument that performs extraction of genetic material (e.g. DNA) from clinical samples (e.g. blood), genetic amplification (via polymerase chain reaction, PCR) and detection/analysis based on laser induced fluorescence (LIF)-capillary electrophoresis (CE), real-time PCR (rqPCR), and melting point analysis (MPA). This project involves integration of microfluidic and microelectronic technologies as well as molecular biology protocol adaptation. Furthermore, we develop technologies required to realize a single-use chip for genetic analysis. This chip, which is based on monolithic integration of microfluidics and microelectronics, can ultimately be mass produced using standard low-cost, high-volume microelectronic wafer fabrication equipment.

We believe that the technologies developed here, along with the molecular biology protocol adaptations, will result in a low cost portable instrument that performs genetic analysis much faster, easier, and less expensive than conventional instruments. This will certainly revolutionize the use of genetic analysis for disease

diagnostics.

Preface

The work presented in this dissertation was performed under the supervision of Dr. Christopher J. Backhouse and Dr. Duncan G. Elliott between September 2007 and August 2010 in the Electrical and Computer Engineering Department at the University of Alberta, Canada. This dissertation is in accordance with the "paper-based format" regulations of the Faculty of Graduate Studies and Research, University of Alberta, and is based on peer-reviewed journal articles that the author of this thesis lead. Publication/submission information for each of these articles is listed on the first page of each chapter in accordance with the Faculty of Graduate Studies and Research's guidelines.

Refereed Journal Publications

[1] G. V. Kaigala, **M. Behnam**, A. C. E. Bidulock, C. Bargen, R. W. Johnstone, D. G. Elliott, and C. J. Backhouse, "A scalable and modular lab-on-a-chip genetic analysis instrument," The Analyst, vol. 135, no. 7, pp. 1606-1617, 2010. ***Co-first author**

[2] G. V. Kaigala, **M. Behnam**, G. Banting, A. Olanrewaju, A. Bidulock, V. Northrup, R. Johnstone, D. M. Glerum, C. J. Backhouse, "Sample preparation, PCR amplification and analysis in a low-cost portable platform," Submitted for publication, 2010. ***Co-first author**

[3] **M. Behnam**, G. V. Kaigala, M. Khorasani, P. Marshall, C. J. Backhouse, and D. G. Elliott, "An integrated CMOS high voltage supply for lab-on-a chip systems," Lab on a Chip, vol. 8, no. 9, pp. 1524-1529, 2008.

[4] **M. Behnam**, G. V. Kaigala, M. Khorasani, S. Martel, D. G. Elliott and C. J. Backhouse, "Integrated circuit-based instrumentation for microchip capillary electrophoresis," IET Nanobiotechnology, vol. 4, no. 3, pp. 91-101 , 2010. ***Co-first author**

Manuscripts in Preparation

[1] **M. Behnam,** M. Khorasani, D. Manage, S. Martel, C. Backhouse, and D. Elliott, "Monolithic microfluidic and microelectronic chip for capillary electrophoresis," Lab on a Chip.

[2] **M. Behnam,** A. Olanrewaju, J. Martinez-Quijada, G. Banting, S. Groendahl, D.M. Glerum and C.J. Backhouse, "A bench-top integrated instrument for sample preparation, realtime PCR, and melting point analysis", Analyst.

Refereed Conference Publications

[1] **M. Behnam,** L. Luis Gutierrez-Rivera, J. Martinez-Quijada, F. Hejazi, S. Movahedian, D. Manage, S. Martel, D. Elliott, and C. Backhouse, "Monolithic microelectronic-microfluidic genetic analysis instruments: the way forward for future point-of-care diagnostics," submitted to *Annual European Conference On Micro-Nano scale Technologies for the Biosciences,* Switzerland, 2010.

[2] **M. Behnam,** A. Olanrewaju, J. Martinez-Quijada, F. Hejazi, G. Banting, A.

Bidulock, S. Groendahl, R.W. Johnstone, D.M. Glerum and C.J. Backhouse, “Inexpensive, and portable, sample-in-answer-out genetic analysis systems for point of care applications,” in *14th International Conference on Miniaturized Systems for Chemistry and Life Sciences,* Netherlands, 2010.

[3] **M. Behnam,** G. Kaigala, J. Martinez-Quijada, S. Choi, S. Ho, W. Al-Haddad, M. Khorasani, C. Bargen, D.G. Elliott, and C.J. Backhouse, “Highly compact instrumentations using CMOS technology for genetic amplification and microchip electrophoresis,” in *13th International Conference on Miniaturized Systems for Chemistry and Life Sciences,* Korea, 2009.

[4] **M. Behnam,** M. Khorasani, G. Kaigala. D. G. Elliott, and C.J. Backhouse, “Monolithic microelectronic-microfluidic integrations for lab-on-a-chip applications,” in *Gordon Research Conference on the Physics and Chemistry of Microfluidics,* Italy, 2009.

[5] **M. Behnam,** M. Khorasani, D. Manage, W. Al-Haddad, A. Hakman, P. Marshall, L. van den Berg, M. Zargham, S. Martel, P. Wright, L. Ouellet, V. Gaudet, C. Backhouse, and D. Elliott, “A microfluidic/HVCMOS lab on chip for capillary electrophoresis,” in *International Solid-State Circuits Conference (Student Forum),* USA, 2009.

[6] **M. Behnam,** G.V. Kaigala, V. J. Sieben, N. Poshtiban, A. C. E. Bidulock, C. Bergen, S. Choi, J. M. Quijada, S. Ho, A. Olanrewaju, J. Lauzon, R. W. Johnstone, D.G. Elliott, L. M. Pilarski, and C.J. Backhouse, “Medical diagnostics in your hand (and on your desk),” in *Annual European Conference On Micro-Nano scale Technologies for the Biosciences,* Switzerland, 2008.

[7] **M. Behnam,** G. Kaigala, M. Khorasani, D. Elliott, and C. Backhouse, "Genetic analysis instrument consisting of a single CMOS chip," in *12th International Conference on Miniaturized Systems for Chemistry and Life Sciences,* USA, 2008.

Technologies and systems developed in this thesis resulted in several other collaborative publications, these publications are as follows:

Refereed Journal Publications

[1] G. Kaigala, **M. Behnam,** C. Bliss, M. Khorasani, S. Ho, J. McMullin, D. Elliott, and C. Backhouse, "An inexpensive, portable and USB-powered microfluidic electrophoresis system," IET Nanobiotechnology 2009 Mar; 3(1):1.

[2] M. Khorasani, **M. Behnam,** L. van den Berg, C. Backhouse, and D. Elliott, "High-voltage CMOS controller for microfluidics," Biomedical Circuits and Systems, IEEE Transactions on , vol.3, no.2, pp.89-96, April 2009.

[3] G. Kaigala, M. Bercovici, **M. Behnam,** D. Elliott, J. Santiago, and C. Backhouse, "Miniaturized device for isotachophoresis assays," Lab on a Chip, June 2010, DOI: 10.1039/c004120c.

[4] B. J. Taylor, K. A. Martin, R. Samuel, M. Nielsen, H. J. Crabtree, **M. Behnam**, C. J. Backhouse, L. M. Pilarski, and S. K. Yanow, "Extraction of Plasmodium falciparum DNA using magnetic beads and a simple lab-on-chip sample preparation module," Submitted for publication, 2010.

Refereed Conference Publications

[1] M. Bercovici, G. Kaigala, **M. Behnam,** D. Elliott, J. Santiago, and C. Backhouse. "Portable instrument and assay for label-free detection of toxins in tap water," in *13th International Conference on Miniaturized Systems for Chemistry and Life Sciences,* Korea, 2009.

[2] G. Kaigala, M. Bercovici, R. Chambers, **M. Behnam,** D. Elliott, C. Backhouse, and J. Santiago, "Portable instrument for label-free toxin detection," in *Gordon Research Conference on the Physics and Chemistry of Microfluidics,* Italy, 2009.

[3] M. Bercovici, G. Kaigala, **M. Behnam,** D. Elliott, C. Backhouse, and J. G. Santiago, "Fluorescent finger prints for toxin detection in untreated tap water," in *Gordon Research Conference on the Physics and Chemistry of Microfluidics,* Italy, 2009.

[4] G. Kaigala, **M. Behnam,** V. J. Sieben, S. Poshtiban, A. C. E. Bidulock, A. Olanrewaju, C. H. Lim, C. Bargen, J. Booth, L. M. Pilarski, and C. J. Backhous, "Sample preparation on an inexpensive and portable genetic analysis tool kit," in *ICMEMS, International Conference on MEMS,* Chennai, India, 2009.

[5] G. Kaigala, **M. Behnam,** V. J. Sieben, S. Poshtiban, A. C. E. Bidulock, A. Olanrewaju, C. H. Lim, C. Bergen, J. Booth, L. M. Pilarski and C. J. Backhouse, "Molecular diagnostics: from clinical sample to "answer" – integration of sample preparation with genetic amplification and analysis/detection," in *Annual European Conference On Micro-Nano-scale Technologies for the Biosciences,* Switzerland 2008.

[6] S. Ho, J. Quijada, W. Al-Haddad, **M. Behnam,** G. Kaigala, C. Backhouse, and D. Elliott, "Portable USB powered and controlled lab-on-a-chip PCR platform," in *Annual European Conference On Micro-Nano scale Technologies for the Biosciences,* Switzerland, 2008.

[7] V. Sieben, C. Debes-Marun, G. Kaigala, **M. Behnam,** C. S. Sims, A. Olanrewaju, L.M. Pilarski, and C.J. Backhouse, "Integration of magnetic bead sample preparation with interphase fluorescence in-situ hybridization on a single microfluidic chip," in *Annual European Conference On MicroNano-scale Technologies for the Biosciences,* Switzerland, 2008.

[8] M. Khorasani, **M. Behnam,** L. van den Berg, C.J. Backhouse, and D.G. Elliott, "High-voltage CMOS controller for microfluidics," in *Biomedical Circuits and Systems Conference,* Canada, 2007.

[9] C. Bliss, M. Khorasani, **M. Behnam,** *et al.,* and C. Backhouse, "Towards a pocket-sized microchip capillary electrophoresis diagnostic tool," in *Annual European Conference On Micro-Nano scale Technologies for the Biosciences,* Switzerland, 2007.

Acknowledgements

First, I would like to thank my supervisors Dr. Chris Backhouse and Dr. Duncan Elliott for accepting me in their respective research groups and providing me with priceless guidance and support. Over the past five years, they have not only taught me about microelectronics and microfluidics, but taught me how to define a problem, come up with a hypothesis, and solve it in an efficient, and, most importantly, in a practical way. I am certain that these skills will help me both in my future research endeavors and in my daily life.

Dr. Backhouse, thank you for asking me "why?" after every statement I made; at first, those scientific "why?"s were not easy to answer, but over time, I learned how to support my statements with tight "because"s.

Dr. Elliott, thank you for listening to my day-to-day questions, particularly the ones that I thought did not have an answer, and showing me that "always, there is a logical answer", I just need to look for it.

Thank you both!

Thanks to my committee members Dr. Larry Kostiuk, Dr. Vincet Gaudet, and Dr. James McMullin for their support and excellent feedback. Special thanks to my external examiner Dr. Blanca Lapizco Encinas.

I would not have been able to complete this work without the help from our collaborators and lab mates, thank you all. Special thanks to members of Backhouse lab, G. Kaigala, A. Olanrewaju, A. Bidulock, R. Johnstone, J. Martinez-Quijada, V. Sieben, S. Ho, and S. Groendahl; members of VLSI lab, M. Khorasani, W. Al-Haddad, A. Hakman, P. Marshall, L. van den Berg; members of AHFMR Microflu-

idics Development group, J. Lauzon, Y. C Wong, Dr. A. Atrazhev, A. Stickel, Dr. D. Manage, and Dr. J. Crabtree; members of Glerum Lab, Dr. M. Glerum and Dr. G. Banting; ECE department technical staff, E. Tiong and R. McGregor; ECE Machine shop staff H. Dexel, M. Riedner, R. Schwarze, and T. Kugler; Nanofab staff, S. Bozic, K. Franklin, and L. Schowalter.

I would like to recognize all the engineering, fabrication, and financial support from our industrial collaborator, DALSA Semiconductor. In particular, I would like to thank S. Martel, L. Ouellet, and P. Wright.

Doing a graduate degree is hard and coping with graduate student life is much harder. I would like to thank all my friends and family in Edmonton; you made living in Edmonton more enjoyable. Edmonton's weather is cold, but you all warmed my heart. Thank you.

My sister, Hoda, and my brothers, Reza, Payam, and Ali, you are the best, thank you. Without your encouragement and support, I would not have survived. I would like to extend my thanks to my father and my mother. Thank you for letting me to take apart, disassemble (and nearly destroy) almost all things electronic that we had when I was a kid. I believe what I learned at that time has made me comfortable building the new gadgets I am building today. Thank you for being such amazing parents and friends throughout my life. My success thus far has been due to your support and advice.

Last, but not least, thanks to all the funding agencies that supported me during my graduate studies: the Natural Sciences and Engineering Research Council (NSERC), Alberta Innovates and Technology Futures (formerly Alberta Ingenuity Fund), the Informatics Circle of Research Excellence (iCORE), Association of Professional Engineers, Geologists, and Geophysicists of Alberta (APEGGA), and the University of Alberta Presidential Award.

Table of Contents

List of Figures

List of Symbols

Symbol	Definition
A	Ampere, SI unit of current
bp	Base pair
Bit	Binary digit, the basic unit of information
F	Farad, SI unit of capacitance
g	Gram, SI unit of mass
H	Henry, SI unit of inductance
Hz	Hertz, SI unit of frequency
L	Litre, unit of volume
μ	Micro = 10^{-6}
m	Mili = 10^{-3}
n	Nano = 10^{-9}
°C	Degree celsius, temperature measure
Ω	Ohm, SI unit of electrical impedance
p	Pico = 10^{-12}
s	Second, SI unit of time
σ	Standard deviation
V	Volt, SI unit of electromotive force
U	Unit
W	Watt, SI unit of power

List of Abbreviations

Abbreviation	Definition
ADC	Analog-to-Digital Converter
AML	Applied Miniaturization Laboratory
APD	Avalanche Photodiode
β2M	β2 Microglobulin
BKV	BK Virus
BSA	Bovine Serum Albumin
CCD	Charge-Coupled Device
CCI	Communication and Control Interface
CE	Capillary Electrophoresis
CMOS	Complementary Metal-Oxide-Semiconductor
DAC	Digital to Analog Converter
DC	Direct Current
DMOS	Double-diffused Metal-Oxide-Semiconductor
DMSO	Dimethyl Sulfoxide
DNA	Deoxyribonucleic Acid
dNTP	Deoxyribonucleotide triphosphate
EDTA	Ethylene Diamine Tetraacetic Acid
FDATOOL	Filter Design and Analysis Tool
FIR	Finite Impulse Response
FWHM	Full Width at Half Maximum
GaAs	Gallium Arsenide
gDNA	Genomic Deoxyribonucleic Acid
GRIN	Gradient-index
GUI	Graphical User Interface
HTML	HyperText Markup Language
HV	High Voltage
IC	Integrated Circuit
IR	Infra Red
LED	Light Emitting Diode
LIF	Laser Induced Fluorescence

Abbreviation	Definition
LOC	Lab-on-a-Chip
LOD	Limit of Detection
LP	Low-pass
LPA	Linear Polyacrylamide
MEC	Microelectronic Chip
MCU	Microcontroller Unit
MFC	Microfluidic Chip
MPA	Melting Point Analysis
MRSA	Methicillin-Resistant Staphylococcus Aureus
μTAS	Miniaturized Total chemical Analysis System
μTK	Microfluidic Tool Kit
NA	Nucleic Acid
OFAT	One Factor at a Time
PCB	Printed Circuit Board
PCR	Polymerase Chain Reaction
PDMS	Polydimethylsiloxane
PLPHM	Provincial Laboratory for Public Health
PMT	Photo-multiplier Tube
POC	Point-of-Care or Point-of-Concern
Pt	Platinum
PWM	Pulse-Width Modulation
rqPCR	Real-time Quantitative Polymerase Chain Reaction
SARS	Severe Acute Respiratory Syndrome
Si	Silicon
SMU	Source-Measurment Unit
SNR	Signal-to-Noise Ratio
SP	Sample Preparation
SPE	Solid Phase Extraction
SPI	Serial Peripheral Interface
SVR	Surface-to-Volume Ratio
TLC	Thermochromic Liquid Crystal
TTE	TRIS-TAPS-EDTA
TTK	Tricorder Tool Kit
USB	Universal Serial Bus
UV	Ultraviolet
VLSI	Very-Large-Scale Integrated
1D	One Dimensional
2D	Two Dimensional

Chapter 1

Introduction

Molecular biology techniques are used in a wide range of medical diagnostics from cancer to adverse drug reaction prevention. However, the widespread use of molecular biology tests is limited by their associated cost and complexity, constraining the availability of these tests to research facilities or very advanced hospitals. The cost and complexity of the molecular biology tests are due to the following: 1) expensive instrumentation and infrastructures, 2) non-automated procedures, 3) requirement of highly trained personnel to operate instruments, 4) large volumes of expensive reagents consumed in each operation, and 5) a long lead-time caused by batch processing. In addition, there has been a pressing need for on-site genetic diagnostic tests for infectious diseases or deficiencies such as adverse drug reactions, which require immediate test results. The most plausible path forward at this time for these onsite diagnostic tests is complete lab-on-chip (LOC) implementations, where a complete test is performed on a single self-sustained portable instrument in a timely fashion.

The goal of this project is to develop an inexpensive portable genetic analysis instrument based on microelectronic and microfluidic technologies. This instrument

needs to enable highly automated and cost-effective diagnostic tests (i.e. applying sample and obtaining result with minimum manual interventions), and provide a qualitative outcome (i.e. Yes/No answer) that will reduce the analysis time.

Through the use of microfluidic and microelectronic technologies, molecular diagnostics tests can be miniaturized and automated, thereby reducing the cost and complexity and increasing accessibility to the public. Our goal is to model our development after the microelectronics industry, wherein a combination of miniaturization, automation, and mass production has decreased the cost of computers in a way that they are now used for the most trivial tasks.

1.1 Social Relevance and Necessity

Central laboratories are the main diagnostic test providers to the health care system. Millions of diagnostic tests are performed every day in a "batch-processing" fashion in these laboratories using large and expensive equipment. The main shortcomings associated with "batch-processing" are the long latency from taking a sample to getting results and associated cost. On the other hand, there is a pressing need for a point-of-care (POC) diagnostics, especially for infectious diseases. Current statistics from the U.S. National Center for Health Statistics show the impact of infectious diseases in the U.S., with statistics such as:

- approximately one-third of Americans are exposed to hepatitis A at one point of their lives,
- around 36,000 people are killed by influenza every year in U.S.,

- sexually transmitted diseases affect more than 1.2 million people every year in U.S.
- in Canada alone, SARS reportedly cost the country over $2.6 billion in 2003 [1].

1.2 Project Scope

This Ph.D. project is a collaborative effort between the Applied Miniaturization Laboratory (AML, supervised by Dr. Christopher Backhouse) and VLSI Laboratory (supervised by Dr. Duncan Elliott) towards the integration, miniaturization, and automation of genetic analysis instruments based on microfluidic and microelectronic technologies. The Backhouse lab has been developing microfabrication techniques, microfluidic integrated chips, miniaturized systems, and biological protocols for LOC applications for almost a decade. This lab has published several papers covering microfabrication techniques (e.g. [2]), microfluidic chip design (e.g. [3]), instrument development (e.g. [4]), and LOC-based disease diagnostics (e.g. [5]). As result of these developments, the system cost has decreased by a factor of 5 per year since 2005, decreasing to hundreds of dollars for infrastructure that once could cost on the order of one million dollars. In a similar way, the Elliott lab has been developing integrated microelectronic chip for LOC applications for more than five years [6, 7, 8]. The research in this lab is directed towards developing circuits and technologies to introduce LOC instruments that can be mass-produced using conventional microelectronic fabrication equipment. The central goal for this ongoing collaboration is a single microelectronic-microfluidic chip solution for genetic analysis.

As part of a collaboration between Backhouse and Elliott labs, I have been involved in the ongoing development of bench-top LOC instruments at the AML. These general purpose platforms not only offer functionalities for various genetic analysis protocols, but also enable me to design, build, and characterize specific modules (e.g. optical detection) with ease and in a timely fashion. This level of configurability is essential for design and fabrication of miniaturized modules. Moreover, these platforms function as a test-bed for developing/porting molecular diagnostics procedures to the LOC format. At the same time, I have been assisting in the ongoing evolution of VLSI chips to ultimately replace discrete instrumentations developed at the AML. My primary role has been in spearheading the integration of the AML systems and VLSI chips to realize a "true LOC" implementation that could revolutionize healthcare. Figure 1.1 illustrates my development road-map towards a single self-contained genetic analysis instrument.

1.3 Thesis Organization

This thesis is written in a paper-based format and is structured around four peer-reviewed journal papers. As this project is a multidisciplinary project, these papers demonstrate a collaborative effort between several group members. However, this thesis demonstrates projects lead by the author of this thesis.

Projects illustrated in this thesis could be categorized in to two categories: 1) development of modular scalable bench-top genetic analysis instruments and integration of molecular diagnostics procedures into LOC format (Chapters 3 and 4)

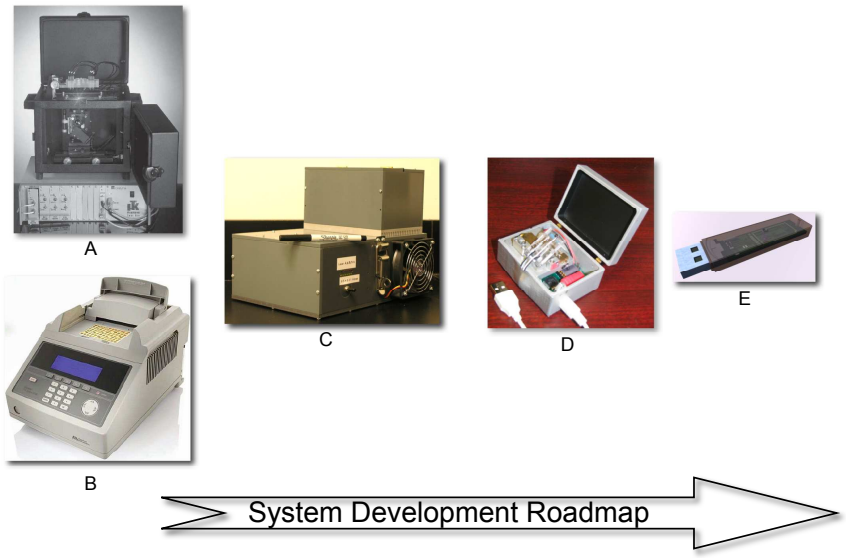

Figure 1.1: The development roadmap for LOC genetic analysis instruments. **A** and **B** are commercial electrophoresis and genetic amplification equipment. Biological protocol development and training are initially performed on these systems. **C** is one of our inexpensive, modular, scalable and general purpose platforms, these platforms are discussed in Chapters 3 and 4. **D** is a representative of our custom microelectronic chip based genetic analysis instruments, these instruments are discussed in Chapters 5 and 6. **E** depicts the future goal of this project, a monolithic microelectronic-microfluidic chip that performs all the required steps for a molecular diagnostic test.

and 2) illustration of the scalability of our bench-top instruments by introducing USB key size genetic analysis devices based on custom designed microelectronic chips (Chapters 5 and 6).

This thesis is organized as follows: in Chapter 2, the lab-on-chip technology, its current limitations and our methodology are discussed. Furthermore, a brief description of standard molecular diagnostic procedures and our design approach are presented. To do a fair comparison between demonstrations by other industrial/research groups and our demonstrations, an in-depth review of the literature related

to each project is presented at the beginning of each chapter. Chapter 3 illustrates a modular scalable genetic analysis toolkit. This toolkit is the basis of all our projects as it can be configured rapidly to develop, test, and debug new LOC techniques and modules. To demonstrate the functionality of this toolkit for real diagnostic applications, genetic amplification via PCR, and analysis using capillary electrophoresis (CE), were implemented. This PCR/CE implementation has a component cost of approximately $600 and is sensitive enough for medical diagnostic applications. Chapters 4 demonstrates a complete genetic-based diagnostic test (i.e. sample-in-answer-out) using our developed toolkit. In this demonstration, we integrated a simple inexpensive sample-preparation module to extract the genetic material from a patient's raw sample. Genetic amplification and analysis in this demonstration were done via PCR and LIF-CE. Chapter 5 describes a CMOS-based chip (3 mm $\times$ 2.9 mm) that generates high voltages (HV) and switches HV outputs for hand held CE instruments. This CMOS chip replaces bulky HV infrastructures accounting for a large percentage of the cost and size of discrete component based system. In chapter 6, we present an improvement on our HV CMOS chip by integrating an optical detection capability. The presented CMOS chip, with total silicon area of $<$0.25 cm^2, combines all the required instrumentation for LIF-based CE and can perform microchip electrophoresis analysis with minimal additional infrastructure (e.g. a laser diode). This chapter demonstrates that it is possible to integrate all the LOC support infrastructures into a single microelectronic chip, and establish a basis for "real LOC" solutions, in which all the required infrastructures are integrated into one or few miniaturized chips. Chapter 7 concludes this thesis, presents the author's contribution to the field in a list format, and discusses future research directions.

Bibliography

[1] P. Darby, "The economic impact of SARS," *The Conference Board of Canada*, vol. 403, p. 3, MAY 2003.

[2] G. V. Kaigala, S. Ho, R. Penterman, and C. J. Backhouse, "Rapid prototyping of microfluidic devices with a wax printer," *Lab on a Chip*, vol. 7, no. 3, pp. 384–387, 2007.

[3] G. V. Kaigala, V. N. Hoang, and C. J. Backhouse, "Electrically controlled microvalves to integrate microchip polymerase chain reaction and capillary electrophoresis," *Lab on a Chip*, vol. 8, no. 7, pp. 1071–1078, 2008.

[4] G. V. Kaigala, V. N. Hoang, A. Stickel, J. Lauzon, D. Manage, L. M. Pilarski, and C. J. Backhouse, "An inexpensive and portable microchip-based platform for integrated RT-PCR and capillary electrophoresis," *Analyst*, vol. 133, no. 3, pp. 331–338, 2008.

[5] V. J. Sieben, C. S. Debes-Marun, L. M. Pilarski, and C. J. Backhouse, "An integrated microfluidic chip for chromosome enumeration using fluorescence in situ hybridization," *Lab on a Chip*, vol. 8, no. 12, pp. 2151–2156, 2008.

[6] M. Khorasani, L. van den Berg, P. Marshall, M. Zargham, V. C. Gaudet, D. G. Elliott, and S. Martel, "Low-power static and dynamic high-voltage cmos level-shifter circuits," in *International Symposium on Circuits and Systems (ISCAS 2008), 18-21 May 2008, Sheraton Seattle Hotel, Seattle, Washington, USA*. IEEE, 2008, pp. 1946–1949.

[7] M. Khorasani, M. Behnam, L. van den Berg, C. J. Backhouse, and D. G. Elliott, "High-Voltage CMOS Controller for Microfluidics," *IEEE Transactions*

on Biomedical Circuits and Systems, vol. 3, no. 2, pp. 89–96, APR 2009.

[8] M. Behnam, G. V. Kaigala, M. Khorasani, P. Marshall, C. J. Backhouse, and D. G. Elliott, "An integrated CMOS high voltage supply for lab-on-a-chip systems," *Lab on a Chip*, vol. 8, no. 9, pp. 1524–1529, SEP 2008.

Chapter 2

Background

In this chapter we present an overview of lab-on-a-chip technologies and its limitations for use in point-of-care disease diagnostics. Following this, we present our methodology to overcome such limitations. We also briefly review standard molecular diagnostic techniques and end with our design approach for the projects discussed in this thesis.

2.1 Lab-on-a-Chip and its Current Limitation

Soon after its introduction in early 1990's, miniaturized total chemical analysis systems (μTAS) became a popular research field both in academia and industry [1]. The main concept in μTAS is to miniaturize, and integrate required functionalities for a complete analysis (e.g. chemical analysis, genetic analysis, and etc.) that includes but is not limited to sample preparation, fluidic handling, sample amplification, sample concentration, detection and analysis. Microfluidics, a subset of μTAS, is concerned with the design, fabrication, and the use of microchannels for manipulating small volumes of liquid. Microfluidics offers advantages such as reduced reagent volumes, shorter analysis time, and the potential for complex integration

and portability when compared with macro-scale laboratory instruments. These advantages, along with the mass-manufacturability of these devices have made them the ultimate technology for future point-of-care (or point-of-concern, POC) medical diagnostics [2, 3, 4].

There have been significant advancements in LOC technology, especially in porting and integrating conventional laboratory procedures (such as sample preparation, sample mixing, sample separation, and detection into microfluidic format [5, 6, 7, 8, 9]) on microchips. Despite these advancements and the advantages offered by LOC technology, LOC based instruments are not being used extensively in commercial settings, particularly for POC applications. This lack of use is due to the fact that most, if not all, LOC demonstrations rely on substantial external infrastructure (e.g. high voltage power supplies and switches, detection systems, valves/pumps, and thermal cyclers). In other words, most of the recent LOC demonstrations have been presented in what might be called *"chip-in-lab"* approaches (i.e. requiring extensive support equipment) rather than *"lab-on-chip"* approaches. Yager *et al.* notes that LOC technologies will be more widely used in applications such as POC disease diagnostics if and only if inexpensive, low-power and portable instruments are built [10]. In this thesis, we address this issue by developing technologies to build self-sufficient instruments that can run a complete diagnostics while being inexpensive, miniaturized, and integrated. This development addresses the cost and size of LOC support equipment and demonstrates the fact that in near future, the need for external equipment will not be an obstacle in the wide use of LOC applications.

2.2 Our Methodology

Building an integrated, inexpensive general purpose platform that can perform a wide range of molecular diagnostics is a challenging task. For this, we are required not only to introduce miniaturized and inexpensive versions of conventional laboratory equipment but also to integrate all of the functionality together into a single platform. It is important to emphasize that integrating various functionalities such as temperature control in microchambers, high voltage generation and switching, fluid handling, and sensitive detection mechanism in a single instrument and addressing all the practical and engineering obstacles such as noise coupling, materials compatibility, and interface is a very exigent task. To make the task more manageable, our approach is modularization, in which we first design, build, test and debug a miniaturized module for each function independently, and subsequently integrate them all into a single instrument. A system level verification ensures the functionality of the system as a whole. As each module is developed independently it can be replaced by its enhanced version (e.g. a custom microelectronic chip) without other modules being affected. In other words, we use the "one factor at a time" (OFAT) methodology [11] to manage a very complex problem. This method is considered to be the only "scientific" approach by many scientists [11].

2.3 Standard Molecular Diagnostics Procedures

Conventional laboratory medical diagnostic techniques can be primary classified into three categories:

1. Immunoassay based: These tests identify and quantify a specific bio-

chemical substance through the detection and analysis of an antibody's reaction with its specific antigen. The number of immunoassay tests is limited by their seroconversion window, their sensitivity, and limited range of antibodies.

2. Flow-cytometry based: This technique suspends a sample in a stream of fluid, and uses an optical detection system to gather scatter and fluorescence. This information is then processed to identify/quantify the sample. The use of flow-cytometry is hindered by the cost and large size of the equipment coupled to complex data processing algorithms.

3. Nucleic-acid based: These tests use specifically-designed probes for an individual genetic sequence of a desired pathogen. Even though nucleic-acid tests are accurate, sensitive, and quantitative, these tests involve many steps and require expensive and extensive equipment.

Due to the advantages and wide applicability offered by nucleic-acid tests, we have focused our efforts on miniaturizing, integrating, and automating infrastructures required for this category of molecular diagnostics tests. Here, we specifically focus on techniques that use polymerase chain reaction (PCR) for the genetic amplification.

A nucleic-acid based test involves three main steps:

1. Sample preparation: the extraction and segregation of genetic material (e.g. DNA) from a raw sample (e.g. urine).

2. Genetic amplification: selective amplification of a desired genetic sequence (e.g. H1N1 flu virus) using an amplification method (here PCR).

3. Detection and analysis: detection and quantification of the genetic sequence of interest using methods such as capillary electrophoresis (CE) or melting temperature (T_m) analysis.

2.4 Design

Considering the required steps for a nucleic-acid based diagnostics, we designed, built and tested individual modules using off-the-shelf components for each step and integrated them together. As illustrated in Chapter 3, a modular, scalable, and inexpensive instrument combines the genetic amplification and analysis functionalities through a combination of temperature control (for PCR), fluidic handling, high voltage generation/control (for CE), and florescence excitation/detection (for laser induced fluorescence detection). In Chapter 4, the sample preparation functionality is added by introducing a new module to extract the genetic material form a raw sample. The on-chip extraction of DNA is performed using ChargeSwitch magnetic beads. These beads, which attach to DNAs at a low pH (pH$<$6.5), are moved through a wash solution using a miniaturized magnetic X-Y stage. DNAs are subsequently released by the addition of PCR master mix (pH$>$8.5).

Chapters 5 and 6 reflect our methodology of replacing individual components with custom designed microelectronic chips. In Chapter 5, the high voltage generation/control module is replaced by a single microelectronic chip, while in Chapter 6 both high voltage generation/control and florescence excitation/detection are replaced by a microelectronic chip.

Based on our demonstrations we can clearly establish a “Moore’s law” trend for

cost of an instrument as the technology evolves, see Figure 2.1. This trend proves that the cost of a LOC instrument will not longer be the main bottleneck in the widespread use of LOC technology for POC diagnostic tests.

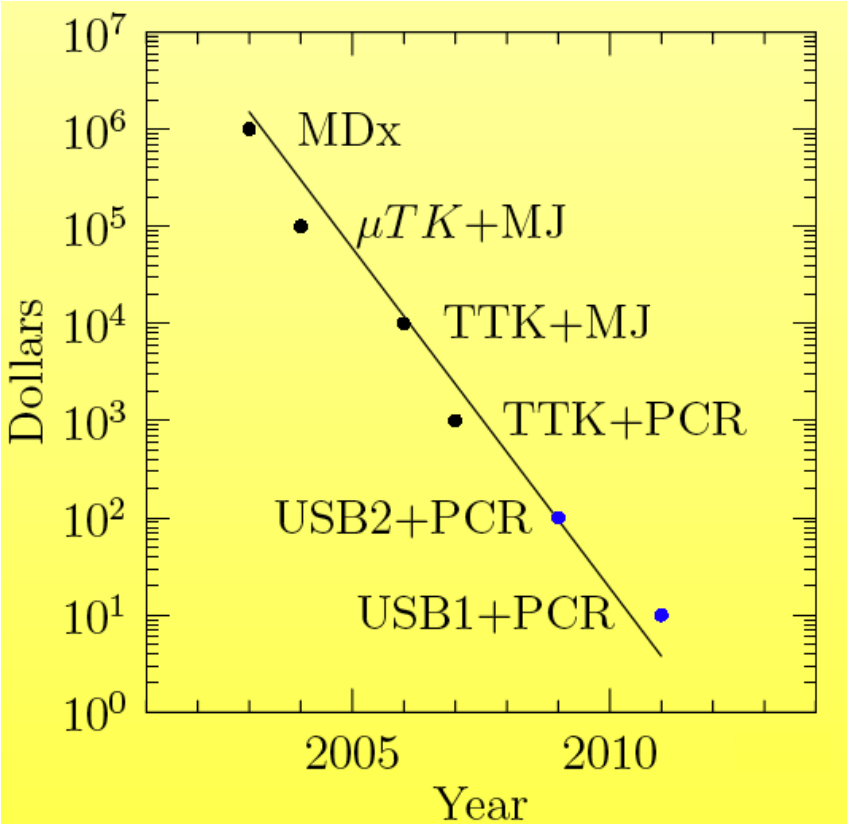

Figure 2.1: Graph of instrument cost reduction as technology progresses. MDx denotes the cost of equipment in conventional molecular diagnostic laboratories which is ≈$1M. μTK+MJ denotes the cost of a conventional microchip based CE system and a conventional thermocycler (used for PCR). TTK+MJ denotes the cost of our first toolkit, which only performed CE, and a conventional thermocycler. TTK+PCR denotes the cost of our instruments based on a modular and scalable architecture presented in Chapters 3 and 4. USB2+PCR denotes the cost of a two-chip (one microfluidic and one microelectronic chip) instrument based on a custom microelectronic chip and a glass microfluidic, similar to what is presented in Chapters 5 and 6. USB1+PCR denotes the cost of a monolithic microelectronic-microfluidic chip fabricated using mass-production equipment. Image courtesy of Dr. C. Backhouse.

2.5 Definition of Commonly Used Terms

- **Capillary electrophoresis:** Capillary electrophoresis (CE) is a technique to separate molecules based on their relative charge and size.

- **Polymerase chain reaction:** Polymerase chain reaction (PCR) is a enzyme-meditated genetic amplification technique that requires repeated heating and cooling (i.e. temperature cycling) of a specific mixture. This technique is used to selectively amplify a known sequence of DNA. A PCR mixture consists of DNA template, primers, deoxynucleoside triphosphates (dNTPS), Taq polymerase, buffer solution, and magnesium or manganese ion.

- **Limit of detection:** As noted in [12], the limit of detection (LOD) of an instrument is the lowest concentration of an analyte that can reliably be detected. For the laser induced fluorescence (LIF) detection based capillary electrophoresis, the limit of detection is defined as the amount of sample required to produce a peak height that is equal to three times the standard deviation (3σ) of the electropherogram's baseline.

- **Signal-to-noise ratio:** For the LIF based capillary electrophoresis, the signal-to-noise ratio (SNR) is defined as the ratio of the peak amplitude to the standard deviation (σ) of the noise in the signal (i.e. baseline).

- **Resolution:** The separation efficiency is commonly presented by resolution. In the capillary electrophoresis technique the resolution is defined as the ratio of the distance between two peaks (Δt) to the average of peak widths (i.e. full width at half maximum, FWHM, W). The resolution is

usually normalized to the natural unit “per base”, hence the resolution per base (R) is defined as equation 2.1, where ΔM is the two peaks’ size difference in base pairs (bps). The resolution, R, equals to unity when the peaks of two DNA fragments with size difference of 1 bp overlap at half of their height (FWHM) [13].

$$R = \frac{\Delta t}{W \Delta M} \tag{2.1}$$

In this dissertation, we report the resolution of a instrument in terms of base pairs (Rbps), i.e. the minimum size difference in base pair required to get two peaks that overlap at half of their height. Hence Rbps is $\frac{1}{R}$ [14].

Bibliography

[1] E. Verpoorte and N. F. D. Rooij, "Microfluidics meets MEMS," *Proceedings of the IEEE*, vol. 91, no. 6, pp. 930–953, 2003.

[2] M. Kopp, H. Crabtree, and A. Manz, "Developments in technology and applications of microsystems," *Current Opinion in Chemical Biology*, vol. 1, no. 3, pp. 410–419, 1997.

[3] V. Srinivasan, V. Pamula, and R. Fair, "An integrated digital microfluidic lab-on-a-chip for clinical diagnostics on human physiological fluids," *Lab on a Chip*, vol. 4, no. 4, pp. 310–315, 2004.

[4] P. Mitchell, "Microfluidics–downsizing large-scale biology," *Nature Biotechnology*, vol. 19, no. 8, pp. 717–721, 2001. [Online]. Available: http://dx.doi.org/10.1038/90754

[5] C. J. Easley, J. M. Karlinsey, J. M. Bienvenue, L. A. Legendre, M. G. Roper, S. H. Feldman, M. A. Hughes, E. L. Hewlett, T. J. Merkel, J. P. Ferrance, and J. P. Landers, "A fully integrated microfluidic genetic analysis system with sample-in-answer-out capability," *Proceedings of the National Academy of Sciences of the United States of America*, vol. 103, no. 51, pp. 19 272–19 277, DEC 19 2006.

[6] R. G. Blazej, P. Kumaresan, and R. A. Mathies, "Microfabricated bioprocessor for integrated nanoliter-scale Sanger DNA sequencing," *Proceedings of the National Academy of Sciences of the United States of America*, vol. 103, no. 19, pp. 7240–7245, MAY 9 2006.

[7] M. Burns, B. Johnson, S. Brahmasandra, K. Handique, J. Webster, M. Kr-

ishnan, T. Sammarco, P. Man, D. Jones, D. Heldsinger, C. Mastrangelo, and D. Burke, "An integrated nanoliter DNA analysis device," *Science*, vol. 282, no. 5388, pp. 484–487, OCT 16 1998.

[8] Z. Hua, J. L. Rouse, A. E. Eckhardt, V. Srinivasan, V. K. Pamula, W. A. Schell, J. L. Benton, T. G. Mitchell, and M. G. Pollack, "Multiplexed Real-Time Polymerase Chain Reaction on a Digital Microfluidic Platform," *Analytical Chemistry*, vol. 82, no. 6, pp. 2310–2316, MAR 15 2010.

[9] E. T. Lagally and R. A. Mathies, "Integrated genetic analysis microsystems," *Journal of Physics D-Applied Physics*, vol. 37, no. 23, pp. R245–R261, 2004.

[10] P. Yager, T. Edwards, E. Fu, K. Helton, K. Nelson, M. R. Tam, and B. H. Weigl, "Microfluidic diagnostic technologies for global public health." *Nature*, vol. 442, no. 7101, p. 412, 2006.

[11] Nist/sematech e-handbook of statistical methods. [Online]. Available: http://itl.nist.gov/div898/handbook/index.htm

[12] D. MacDougall and W. B. Crummett, "Guidelines for data acquisition and data quality evaluation in environmental chemistry," *Analytical Chemistry*, vol. 52 (14), pp. 2242–2249, 1980.

[13] C. Heller, "Principles of DNA separation with capillary electrophoresis," *Electrophoresis*, vol. 22, no. 4, pp. 629–643, 2001.

[14] V. J. Sieben and C. J. Backhouse, "Rapid on-chip postcolumn labeling and high-resolution separations of DNA," *Electrophoresis*, vol. 26, no. 24, pp. 4729–4742, 2005.

Chapter 3

A Scalable and Modular Lab-on-a-Chip Genetic Analysis Instrument

This chapter was published in the Analyst Journal, and it was featured on the front cover page. The instrument demonstrated here is a general-purpose and reconfigurable microfluidic toolkit that performs all the required fluidic manipulation, thermocycling, and optical detection necessary for genetic analysis. This instrument is a self-contained system that has been developed and used in our laboratory as a test-bed to accelerate our new lab-on-a-chip developments. As the lead author, my role in this development was interdisciplinary; I led the instrument design (i.e. hardware including testing and debugging), thermal and optical calibration as well as microfabrication process development/improvement.

Preface

We demonstrate a new and extremely inexpensive, multipurpose desktop system for operating lab-on-a-chip (LOC) devices. The system provides all of the infrastructure necessary for genetic amplification and analysis, with orders of magnitude

---

A version of this chapter has been published. Behnam *et al.* 2010. Analyst. 135. 1606.

improvement in performance over our previous work [1]. A modular design enables high levels of integration while allowing scalability to lower cost and smaller size. The component cost of this system is ≈$600, yet it could support many diagnostic applications. We demonstrate an implementation of genetic amplification via PCR, and analysis using capillary electrophoresis (CE). The PCR is able to amplify from single or several copies of target DNA and the CE performance (e.g. sensitivity) is comparable to that of commercial photomultiplier-based confocal lab-on-chip instrumentation. We believe this demonstrates that the cost of infrastructure need no longer be a barrier to the wide-spread application of LOC technologies in healthcare and beyond.

3.1 Introduction

The lab-on-a-chip (LOC) community has made significant progress in transferring a wide variety of chemical and life-science functionalities onto microfluidic chips, but with limited progress in developing a cost-effective infrastructure for operating them. For LOC technologies to be widely adopted in applications such as point-of-care disease diagnostics, it is essential that an inexpensive, effective and portable instrumental platform be developed [2, 3]. Particularly critical for such diagnostic applications is the implementation of the polymerase chain reaction (PCR) and capillary electrophoresis (CE), and their integration onto microfluidic formats [4]. The combination of PCR/CE forms the basis of many medical diagnostics (e.g. [5, 6, 7]). Our implementation of PCR/CE also demonstrates the functionality (e.g. pumps, valves, temperature control, electrophoresis, detection) needed for a platform capable of implementing a wider range of molecular biology protocols.

Medical diagnostic protocols have been demonstrated on LOC systems, but are generally confined to use within a laboratory setting due to cost and the need for extensive LOC infrastructure. A number of excellent reviews summarise the field in general, as well as PCR and CE in particular [3, 8, 9, 10]. Laser-induced fluorescence (LIF) detection is the method of choice for CE [11], largely because of its excellent sensitivity but also because it is readily transferred to a LOC format. Therefore, in this work we have focused on the development of a system for implementing PCR followed by CE with LIF detection.

Recent reviews (e.g. [10, 8]) have summarised commercial LOC systems and their demonstrations. Existing commercial products are highly focused, with relatively little flexibility and this limits their use as a generic tool for developing and implementing microfluidic applications. For example, there are a number of commercially available bench-top microchip-based CE analysis systems such as the Agilent 2100, BioRad's BioFocus/Experion, Caliper's LabChip 90 system and Hitachi's SV1100. However, while such bench-top CE systems are appropriate for laboratory use, inexpensive and portable diagnostics will require more highly integrated systems. For genetic diagnostic applications, the two main approaches taken commercially are 1) PCR followed by array-based detection and 2) real-time PCR. Although these are useful advances, they are only able to implement a specific technology (typically a specific commercial product rather than being a general purpose platform), and none implement the key PCR/CE functionality. We are aware of only one commercial system capable of PCR/CE, that being from NEC and Arbiotec (Japan) [12] as announced in a recent and preliminary report. That report

suggests a briefcase-sized system capable of PCR/CE within a chip approximately 18×8 cm (no results were presented).

As demonstrated in the academic literature, the wide range of capabilities of the LOC technologies is truly impressive, The early demonstration by Burns *et al.* [13] integrated isothermal amplification, electrophoresis and laser-induced fluorescence detection. Although a remarkable advance, their system was not sufficiently sensitive (with a detection limit of 10 ng/μL of intercalator-labeled DNA), had limited resolution ($\approx$ 50 base pairs (bp)) and was not flexible enough for general application (or for that matter to PCR/CE). This tour-de-force demonstration of a nearly self-contained system showed that it was feasible to develop a true lab-on-a-chip system. As noted in the review by Lagally and Soh [14], Lagally *et al.* [6] were the first to demonstrate a field-portable, fully integrated PCR/CE system. However, as reviewed by Myers and Lee [3], the demonstrations shown to date of integrated PCR/LIF-CE (e.g. [15, 5]) have relied on expensive optical infrastructure (e.g. photomultiplier tubes (PMTs) and confocal optics).

Demonstrations by the Mathies group [6, 16] have shown portable self-contained systems and these, along with the Sandia system [17], represent the state of the art in terms of high performance portable CE systems. However, as pointed out by Myers and Lee [3], even these are relatively expensive PMT-based systems and more effort is needed to miniaturise, automate and to reduce cost. To put this in perspective, the system presented here is already less expensive than a typical small-format PMT that might be used in one of the portable systems noted above. As we and others recently reviewed [1, 3, 9, 10], there have been no demonstrations of inex-

pensive PCR/LIF-CE systems - clearly such an integration is a challenge.

As described by Johnson and Landers [11] in their review of ultrasensitive LIF detection in microsystems, the most sensitive detection mode in microsystems is LIF, and LIF-based CE is the primary detection method in DNA sequencing and sizing. Also as they describe, the standard method of LIF detection is the confocal approach that illuminates and collects fluorescence from a small volume. This elegant method is well-suited for LOC technologies since it allows for the detection spot (often on the scale of micrometres across) to be focused within a microfluidic channel, thereby being relatively insensitive to light (excitation or fluorescence) from the channel wall or the bulk of the microchip. These systems therefore tend to have a very low baselines (i.e. the signal output in the absence of a fluorescent material in the channel). Unfortunately, this requires precision machining of relatively large optical systems in order to maintain such a tight focus within the microchannel. Moreover, the collection of the light from such a small volume requires very high gains so that PMTs or avalanche photodiodes (APDs) are usually used. Finally, the individual components of such systems (such as PMTs, dichroic mirrors, filters, collimation optics) are expensive, with typical costs of several hundreds of dollars or more (e.g. Johnson [11] refers to optical filters costing $1000). As pointed out by Zhang and Xing [10], the detection methods have not developed as rapidly as other LOC technologies, particularly regarding the miniaturisation of LIF detection.

It is far simpler to use a non-confocal approach in which one illuminates the channel while collecting the fluorescence with a lens, passing it through a filter and into a solid-state detector. Such a non-confocal approach also offers considerable

advantages in compactness and cost, but tends to be several orders of magnitude less sensitive [18, 19]. Moreover, non-confocal approaches tend to collect far more scattered excitation light (e.g. from channel walls) and this results in high baselines. Such systems are sensitive to laser power fluctuations since they give rise to variations in the baseline that can be difficult to distinguish from fluorescent signals.

We are exploring what we feel are central questions for the LOC field – how inexpensively one can build the infrastructure needed to support LOC operation, and how well can that infrastructure be integrated with the LOC devices themselves ? We seek to demonstrate systems that are orders of magnitude lower in cost than those presently available, yet that might support entire life-science protocols. Such a "toolkit" for implementing inexpensive and portable LOC PCR/LIF-CE requires an effective integration of such capabilities as a high voltage power supply, LIF detection, thermal control and fluid control. In addition, the development such systems requires the co-adaptation of molecular biology and the LOC technologies.

We present a modular instrument based on photodiode-based detection. We earlier reported on a non-modular PCR/CE instrument based on a charge coupled device (CCD) for optical detection [1]. We now present a photodiode-based system with greatly increased sensitivity and speed. In addition, without the CCD, the cost of the optical detection system has been decreased by two orders of magnitude, halving the system cost. To demonstrate the instrument, we chose to work with a microfluidic chip design we previously reported on [1]. Our modular approach has enabled a rapid evolution of system performance, particularly in terms of thermal control and detection. Our LIF detection is readily able to sample data two orders

of magnitude faster than previously [1] and now has a sensitivity comparable to those of commercial CE systems. Similarly, our present thermal control is now far faster than that we previously reported [1]. As noted by Johnson and Landers [11], the majority of the reports in the literature do not provide enough detail to allow others to construct the LIF systems used. With this in mind, we provide a detailed description of our system and its performance.

We believe that to use LOC technologies in applications such as healthcare, an inexpensive yet reconfigurable platform is needed, i.e. a toolkit that can implement a wide range of life-science procedures. The present PCR/CE implementation of such a toolkit (Figure 3.1) has a component cost of ≈$600 and sensitivities adequate for medical diagnostic applications. This portable and modular instrument is suitable for single patient testing using a PCR/CE diagnostic format. We believe that systems such as this will enable the cost-effective deployment of the wealth of LOC technologies developed by the wider LOC community.

3.2 Instrumental Architecture

The system is composed of hardware modules linked by a microcontroller running firmware that enables basic molecular biology procedures under the control (via a USB serial link) of a graphical user interface (GUI) located on an external laptop computer. Each of these components is described below and further details can be found in past work [1].

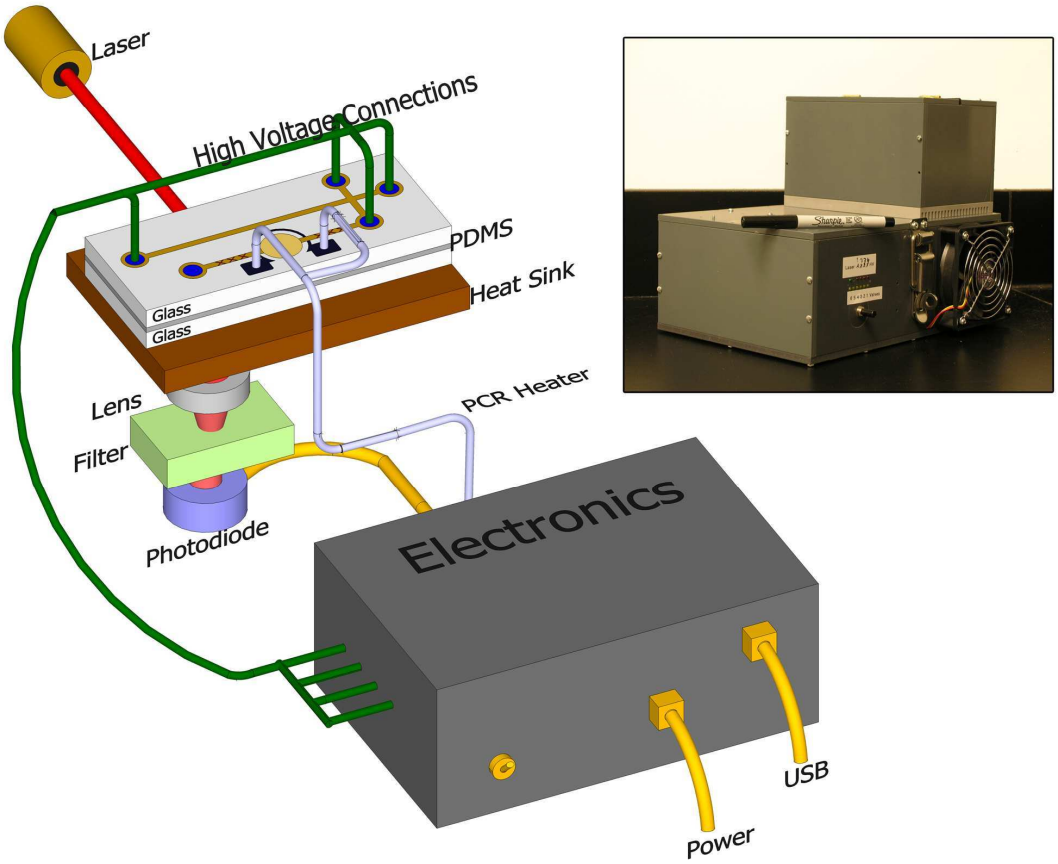

Figure 3.1: Block diagram of the LOC toolkit as a PCR/CE instrument. Inset: Image of the toolkit (30×20×11 cm for the main box), with the top box containing the PCR/CE chip.

Hardware: Each of the electronics modules are present in the form of a printed circuit board (PCB) that communicates to a microcontroller on a shared communication bus with an industry standard serial peripheral interface (SPI) protocol and using a set of standardised commands, as demonstrated in Figure 3.2. Each PCB module performs a dedicated function (as outlined below) and is individually addressable on the SPI bus. To perform a function (e.g. electrophoresis), the control commands are issued to the appropriate board by the microcontroller. Once the user-specified run parameters are entered into the GUI, the tasks are transmitted to

the microcontroller, allowing control of the hardware while the external computer records the generated data.

a) Microprocessor control unit (MCU): This module is based on a PIC micro-

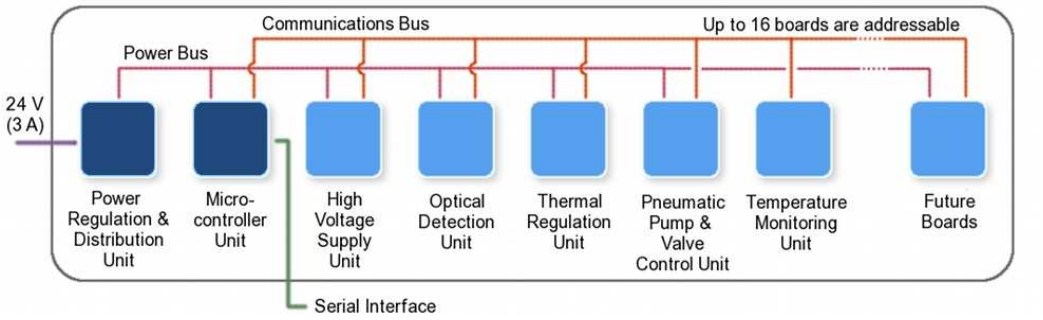

Figure 3.2: The modular architecture of the PCR/CE instrument is based on multiple single-function printed circuit boards on common power and communication buses. The 'future boards' can readily be added as the system design evolves.

controller (PIC 18F4550, Microchip Technology Inc., Chandler, AZ, USA) and is responsible for control of, and communication with, all other modules (via SPI).

b) Thermal regulation unit: This module controls the current through the thin-film heater on the PCR/CE chip and simultaneously measures the voltage across the heater. The MCU uses this information to calculate the temperature of the heater, thereby enabling this unit to be both an actuator and a sensor (thermal control is discussed in depth below).

c) Temperature monitoring unit: The operation of the system is affected by shifts in room or component temperature. This board monitors the heatsink temperature and the ambient temperature.

d) Optical detection unit: This unit consists of a laser, a lens, an interference filter, a photodiode, an amplifier, and a 16-bit analog to digital converter. The collected fluorescence is converted to a current by the photodiode and digitised, with the data transferred over the SPI bus (further details in Sections 3.3.7 and 3.3.8). In related

work, we are transferring this functionality onto a single microelectronic (CMOS) chip.

e) High voltage supply unit: This board uses an EMCO DC-DC converter (C60, Sutter Creek, CA, USA) to generate up to 6000 V. In total, four relays are used to control the state for the electrodes interfacing with the microchip, to either apply a fixed voltage, electrically disconnect the electrode, or ground the electrode. We recently reported on a low-voltage version of this power supply on a single CMOS chip [20].

f) Pneumatic pump and valve control unit: The valve board offers valving (and pumping) functionality necessary for fluid handling within the microchip. Each valve board consists of up to seven three-way valves (six were used here) that can be addressed individually and that can switch up to 30 psi differential pressures provided either from external sources or from on-board minipumps (as in [1]). We have recently demonstrated an on-chip version of these micropumps and microvalves in conjunction with an implementation of PCR [21].

g) Power regulation and distribution unit: The input to this unit is a laptop power supply at 24 V, 3A and the unit regulates and distributes "clean power" within the toolkit at +24 V, $\pm$14V and 7 V. This approach limits the amount of electrical noise that is distributed within the unit. To further suppress noise picked up by the power lines within the unit, the $\pm$14V and 7V supplies are regulated to $\pm$12V, and 5V respectively on each board.

Modules that use the same SPI commands can be upgraded without affecting system operation. Although successive versions of the hardware may be significantly improved, this approach makes most hardware changes invisible to the higher

levels of the system (i.e. firmware, software and user, as described below).

Firmware: All time-critical functions, such as thermal control and optical data collection, are handled by the microcontroller executing firmware (programmed in the C language) that provides a simple real-time operating system. The microcontroller communicates with the external computer via a USB serial link and follows a standardised set of commands (referred to as the interface protocol). To increase the versatility of the toolkit (particularly for debugging operations), a user can also communicate with the microcontroller using a terminal program on an external computer (using the USB link as a serial port). The initialization of each module, communication, control, and data acquisition is also programmed in the firmware. Although successive versions of the firmware may see significant improvement, this approach makes any firmware changes invisible to the higher levels of the system (i.e software and user, as described below).

Software: The use of an embedded microcontroller for time-critical functions allows us to use conventional consumer-grade external computers (e.g. a Windows-based laptop) for data acquisition without concern for the erratic timing characteristic of multi-tasking operating systems or overwhelming the bandwidth of the serial link. To enable platform independence, the GUI was written in Python (a language that is a standard component of many operating systems). In addition to logging the raw data as a time-stamped text file with the run information and the user-entered information, the plotted raw and processed data are also saved by the GUI as images (png format). After the completion of each run, the GUI combines the run-specific information, user notes, and images into a report in a standard HTML format.

3.3 Methods & Materials

3.3.1 Microchip Fabrication

Our PCR/CE microfluidic chips consist of two layers (top and bottom) of 1.1 mm Borofloat glass (Schott AG, Germany) and a PDMS membrane between them (Figure 3.3) based on the approach taken by [22, 23]. This structure enables the integration of microvalves and pumps within the microfluidic chip while requiring a relatively simple chip fabrication technology. The PCR reaction chamber has a volume of 600 nL and is 90 μm deep, while the fluidic channels are 45 μm deep. The detailed fabrication procedure is much as described in our earlier report [1] and only variations will be discussed here.

The substrates were diced with the resulting edges showing a slightly frosted appearance with a root-mean-square roughness of 80 nm. Partway through this work, a number of changes were made due to equipment failure and component replacement (notably the interim use of another dicing saw), and subsequently the diced edges were significantly poorer - i.e. rougher, leading to a highly frosted appearance and sometimes showing chipping.

The sensitivity of the CE detection was very dependent on how well the channel could be illuminated by the laser and we believe that this was due to some form of shadowing, possibly from chipped edges from the dicing process or non-uniformity of the PDMS-glass interface. Within chips without such shadowing, the laser illumination could readily be focused to a spot of less than $\approx$200 μm. By contrast, in

chips with such shadowing, the laser illumination was scattered across the channel and could not be focused - such chips were not used for CE.

For optimal control of membrane properties (i.e. thickness and uniformity), we fabricated PDMS membranes with the monomer and curing agent mixed in a 10:1 weight ratio (Sylgard 184, Dow Corning). The PDMS was then poured onto a Cr/Au substrate, followed by a 15 s spreading cycle at 100 rpm and then 300 s at 140 rpm. The substrate was then placed in a pre-heated oven at 80 °C for 2 hours and this resulted in a PDMS membrane with a thickness of 254 μm ($\pm$ 10% variation). The PDMS membrane was irreversibly bonded to the upper and lower etched glass plates (referred to as the fluidic and control layer respectively, Figure 3.3). Bonding was performed with a protocol based on that of [24], using an oxygen plasma exposure within a reactive ion etch chamber (MicroEtch RIE). We exposed the control layer and the PDMS film to oxygen plasma for 30 s (25% O_2 flow, 500 mTorr, 40 W (13.3%) RF power). The exposed face of PDMS was then placed on the glass surface. The fluidic layer glass plate and the bonded control layer-PDMS plate were bonded by the same procedure and left untouched for 8 hours to ensure irreversible bonding. For the first 2 hours after bonding, nitrogen was blown through the fluidic channels intermittently to ensure that the valves did not inadvertently bond permanently in the closed position.

To access the control layer and metal layers through the drill holes, the PDMS layer was cut (after bonding) by using a 2 mm diameter acrylic tube that had been sharpened at one end to a knife-edge. This was hard enough to cut the PDMS, but soft enough not to damage the platinum electrodes. As a verification that no damage

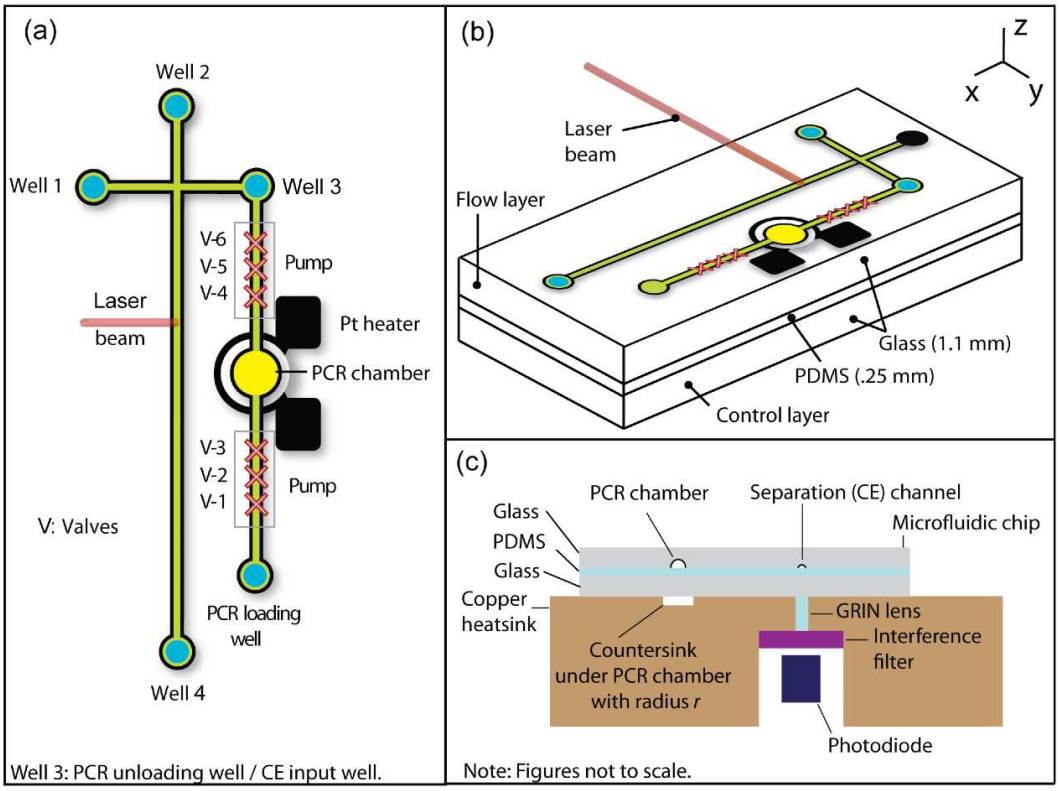

Figure 3.3: a) Schematic representation of the components within the chip – PCR chamber, valves (3 in a row forming peristaltic pumps), electrophoresis channels, fluidic wells and platinum heating/sensing elements. b) Perspective view of the glass/PDMS/glass chip with orthogonal laser beam. c) A depiction of the chip atop heat-sink and LIF detector. Chip dimensions: $95 \times 19 \times 2.5$ mm.

to the electrodes occurred, the chip was turned upside down and inspected under a microscope with illumination from below. Damage, such as a scratch, was readily apparent as a patch of light in a dark field.

3.3.2 PCR Protocol

Although our PCR protocol is essentially as in our past work, [7] for completeness we briefly describe the protocol here. A 25 μL PCR mixture con-

sists of 2.5 μL of 10X PCR buffer (containing 200 mM Tris-HCl and 500 mM KCl, pH 8.4), 2 μL of 50 mM $MgCl_2$ (final concentration of 4 mM), 5U Platinum®Taq polymerase, 0.5 μL of 10 mM dNTPs, 0.5 μL of 1% BSA (Sigma-Aldrich, Oakville ON, Canada), 1 μL of 99.7% DMSO (final concentration of 4%) (Fisher Scientific, Ottawa, Canada), 0.5 μL of forward primer (5'-GTGACCAACACAGCTACCACAGTGT-3', 10 μM), 0.75 μL of reverse Cy5-labelled primer (Cy5-5'-TCAAACACCCTAACCTCTTCTACCTG-3',10 μM, Integrated DNA Technologies, Coralville, IA, USA), 0.5 μL of sample standard, and 15.75 μL of PCR grade water (nuclease-free, MP Biomedicals Inc. OH, USA). Platinum®Taq DNA polymerase kits (including Platinum®Taq polymerase, 10X PCR buffer and $MgCl_2$) and dNTPs were purchased from Invitrogen Canada Inc. (Burlington, ON, Canada). The sample was a reference standard graciously provided by Dr. Xiao-Li Pang (of the Provincial Laboratory for Public Health (Microbiology) [PLPHM], Edmonton, Canada) and consists of BK virus DNA at a concentration of $\approx 10^7$ copies/mL. The thermal conditions were: pre-denaturation temperature of 94 °C for 120 s, 35 cycles of 94 °C for 10 s, 56 °C for 20 s, and 70 °C for 20 s, and a post-extension temperature of 70 °C for 120 s. As described in our earlier work [7], the BK virus can be a threat to individuals with compromised immune systems, such as immunosuppressed organ-transplant recipients where an increased viral load can lead to organ failure. The reference standard was purified and quantitated (by the PLPHM) from human urine using a Qiagen DNA mini-kit (Qiagen Inc., Mississauga, Canada) following the manufacturer-recommended procedure, resuspending in the elution buffer of the kit. Following resuspension it was quantitated by RT-PCR. Although we have previously demonstrated analysis directly from urine, this purified standard is less infectious.

3.3.3 Operational Procedures for Microchip PCR

As a standard procedure, 50 μL PCR mixtures were prepared, and simultaneous on-chip and conventional thermal cycler runs were performed. An aliquot of 10 μL of each mixture was run as the positive control on the thermal cycler (GeneAmp PCR System 9700, Applied Biosystems, Foster City, CA, USA), while the remaining 40 μL (stored on ice for the period between PCR runs) was used to perform multiple on-chip PCR/CE experiments. This positive control was electrophoretically analysed, and if the product peak intensity was less than 0.2 times the usual intensity, or if anomalous peaks were evident, then the PCR mixture was considered to have been contaminated and further analysis was not performed. Negative controls (PCR mix with PCR-grade water in the place of the sample) were performed to ensure that the processing and the PCR reagents did not introduce contamination.

Loading PCR Mixture: After 5 μL of the PCR mixture was pipetted into the PCR sample well, the on-chip pump was actuated to fill the PCR chamber (Figure 3.3a). Typically, 3-4 pump cycles (sequential action of 3 consecutive valves with a time period of 500 ms between each individual valve) on a PCR/CE chip was found sufficient to fill the PCR chamber. If a larger number of pump cycles was required then this was an indication that the on-chip valves were not operating effectively, and further testing was not performed on that chip. Once the PCR chamber was filled, the valves were closed, and any remaining PCR mixture was extracted from the PCR sample well with a micropipetter. Thermal cycling was then performed based on the parameters (above) set in the GUI.

Unloading: After thermal cycling, 5 μL of 0.01xTTE (see Section 3.3.4) was

pumped through the PCR chamber by actuating the valves for 8 pump cycles. This mixed 0.01xTTE and the PCR product, and moved the mixture into the CE sample well (see Figure 3.3a). Approximately 5 μL of thermo-cycled PCR product in buffer was present in the CE sample well post-cycling. However, if less than 4 μL was recovered, then this was taken to indicate a failure of containment due to valve failure, and further analysis was not performed. In total, two chips had valve-failures, both at the PCR loading stage when the valves were found to be stuck in the closed state. This was likely due to an error in microfabrication.

In order to assess the relative strengths of on-chip and conventional PCRs, we performed consecutive on-chip PCR and conventional thermal cycling PCRs as follows: One 50 μL PCR mix was made (as per the above procedures), 10 μL of which was run on the conventional thermocycler, and 20 μL of which went to 4 on-chip products, all run on the same day. The resulting product from both on-chip, and tube-based PCR were electrophoretically analyzed (with the our system, as described below). To ensure analysis of similar DNA concentrations (and similar ionic strengths) between the on-chip PCR, and the tube-based PCR, 4 μL of the on-chip PCR (0.6 μL of on-chip PCR product diluted with about 4.5 μL of 0.01xTTE as it was flushed out from the PCR chamber, a dilution of 12 times $\pm$20%) was compared with 0.5 μL of tube-based PCR (mixed with 3.5 μL of 0.01xTTE in the CE input well, a dilution of 12.5 times). The means of the PCR product peak heights on the electropherograms were compared between the on-chip PCR and tube-based PCR to estimate the relative PCR yields.

3.3.4 Capillary Electrophoresis Protocol

As in past work [7], we used 4% linear polyacrylamide (LPA) as the separation matrix in order to discriminate between the PCR product peak and the PCR primer peak (the BKV primers were 25 or 26 bp in length and the resulting PCR product was expected to be 299 bp in length). The LPA and chip were prepared as described in [1, 6] with a 10X TTE buffer that was 500 mM tris-base, 500 mM TAPS and 10 mM Na_2EDTA. Since we are seeking to show scalability of the instrument to smaller distance separations (without changing the microfluidic chip) we have chosen here to use a separation distance of 13 mm even though the chip is significantly longer. Again, as in past work [1], prior to first filling the sieving matrix in the PCR/CE chip, the CE channels were coated to minimize analyte adsorption and electro-osmotic flows. The channels were then filled with LPA, and 4 μL of 1x TTE buffer was pipetted into each of the wells except the CE sample well. Once the sample was loaded (as described below), DNA was electrokinetically injected into the shorter channel using 200 V ($\approx$222 V/cm) for 80 s, followed by a separation voltage of 600 V (electric field of $\approx$67 V/cm) for 250 s. Likely due to variability in the unloading process, the samples gave rise to injection currents that also showed run-to-run variability. If the injection current exceeded 40 μA then the injection voltage was reduced to 150 V for the remainder of the injection period. In either case, the injection time was sufficient to have the primer and product DNA reliably reach the intersection. The typical maxima of the currents during injection and separation were about 30 and 4 μA respectively. Following injections were for 20 s under the same field as used in the first injection. Detection was performed at 13 mm from the CE channel intersection, along the longer section of the channel. Due to evaporative losses, the wells would dry out in approximately 15 minutes

(depending on airflow and humidity). The runs were performed in duplicate or, if there was enough time before the wells dried out, in triplicate.

We performed CE using the PCR/CE chip in both our custom-built instrument and, as a reference, in a commercial PMT-based confocal instrument (the μTK, Micralyne, Edmonton, Canada). Unless otherwise indicated, the electrophoresis conditions were identical for the two systems, a gain of 0.8 was used for the μTK PMT, and the laser of our system was turned on for 10 minutes prior to use. From the 5 μL that was moved through the PCR chamber into the CE sample well, 1 μL of this was used to perform control runs using the PCR/CE chip with the μTK and the remaining 4 μL was used for the on-chip CE within our instrument. To run the on-chip PCR sample on the μTK, 1 μL was loaded with 3 μL of 0.01xTTE in the CE sample well (further diluting the on-chip PCR sample), with the rest of the chip prepared in the same manner as above.

As a control, the CE of the conventionally thermal-cycled PCR product was run on our system or the μTK. In either case, 0.5 μL of the PCR product was pipetted with 3.5 μL of 0.01xTTE into the CE injection well and all other conditions were as above. In this manner, the dilution of the conventionally thermal-cycled product was comparable to the dilution of the on-chip product.

In order to size the amplified PCR product, we performed an injection and separation of 1 μL of DNA ladder (ALFExpress, Amersham Biosciences, NJ, USA) along with 3 μL of 0.01xTTE in the CE sample well. We noted the peak arrival times of the DNA ladder, and interpolated to estimate the size corresponding to that

of the arrival time of the PCR product peak as obtained in a separate analysis under the same electrophoretic conditions of injection and separation. Separate runs were required because our signal processing is tailored for isolated peaks. Signal processing of the size standard data with its closely spaced peaks led to distortion but the peak arrival times could be extracted readily.

3.3.5 Operational Procedure: Microchip Alignment

In order to ensure that the laser beam was focused above the CE channel, a one-time laser focus adjustment was necessary when the system was first assembled. To do so, we placed a black background (e.g. black vinyl electrical tape) above the centre of the lens and we adjusted the focus of the laser to observe the smallest laser spot size ($\approx$100 μm) on the black background. The focus of the beam was not greatly affected by subsequently putting the chip in place.

Prior to performing the CE run, the PCR/CE chip was aligned on the instrument to ensure optimal light coupling into the CE channel. This procedure was done with an empty PCR/CE chip. In the x-y plane, first the PCR/CE chip was placed to ensure the CE channel lay over the middle of the lens, 13 mm from the CE channel intersection. This alignment was guided via alignment marks on the heat sink. The laser was then adjusted along the z-axis (z-axis is the height of the chip) to position it at the same height as the CE channel, as was evident by a bright laser scatter on the channel wall (within a $\approx$200 μm spot). Laser adjustment along the z-axis was necessary as materials thicknesses varied slightly from chip to chip. However, after this alignment process, the chip could be removed and replaced without align-

ment (with accurate dicing and precise thickness control there would be no need for alignment).

3.3.6 Thermal Control

A central appeal of the LOC technologies is that the low thermal inertias within a LOC allow rapid changes in temperature, thereby enabling PCR within a matter of minutes rather than the hour or so required by typical multi-well thermocyclers. As pointed out in a recent review [9], the continuous-flow PCR devices avoid these issues of thermal inertia simply by moving the reaction mixture between temperature zones. As a result, the flow-devices have amplification times on the order of 10 minutes for 40 cycles. Other approaches such as IR-mediated heating (e.g. [25, 26]) allow the rapid thermal cycling of small volumes (e.g. 9 min for [26]), but this may not be amenable to extremely low-cost approaches. Our approach is to scale the resistive heating to very small volumes that equilibrate very rapidly. For brevity, the recent improvements to the thermal control (beyond those described in [1]) will be outlined here, and a more detailed exploration of this topic will be presented elsewhere.

The yield of PCR depends on the temperature at each of the three stages of annealing (56 °C), extension (70 °C) and denaturation (94 °C) during the thermal cycling. A customized proportional integral controller, similar to that of past work [27], was programmed into the firmware, and this ensured rapid and stable thermal transitions. As described in [28], the PCR chamber temperature acts much as the voltage across a capacitor connected to resistive divider, i.e. the PCR chamber tem-

perature will take some time to stabilize (about 10 s) at a value between the heater temperature and the room temperature. The exact relationship between the heater, room and chamber temperatures was established by simulation (finite element analysis in COMSOL Multiphysics 3.5a) and by calibration with thermochromic liquid crystals (TLCs) [29].

Since the temperature sensing was accomplished by measuring the resistance of the heater, the relationship of the resistance to the temperature must be accurately established. We have improved the microfabrication compared to our earlier report [1] by reducing the variability of the platinum thickness during deposition, and by using an improved thermal calibration procedure to establish the resistance vs. temperature. This relation was determined by least-squares fitting of the resistance of the chip as it was swept through several temperatures within a temperature-stabilised waterbath, Hakke C25P Circulator (Thermo Fisher Scientific Inc., Waltham, MA, USA). We now estimate that we can predict the temperature of the chamber from the heater resistance to within about 1 °C once these calibrations are made. Although we do not account for ambient temperature variations during the run, these variations were monitored to ensure that they were less than 1 °C. (No variations larger than 1 °C were found.)

A significant improvement in our system was the use of a heat-sink to more rapidly and reliably control the PCR chamber temperature. In our previous work [28], we showed that the equilibration time of the heat-sunk region scaled with the inverse square of the radius of the heat sink, enabling far faster operation with smaller chips. The copper heat-sink contacts the bottom of the chip (Figure 3.3c)

beyond a radius of 3.5 mm from the centre of the PCR chamber. As in our previous work [28], the equilibration time of such a heat-sunk region was predicted to be about 10 s. (Although the system could operate even faster, this would require a new chip design.)

In order to calibrate our thermal control, we produced calibration chips by filling PCR/CE chips with TLCs within the PCR reaction chamber. As described in more detail in previous work [28, 29], the TLCs were custom-synthesized (Hallcrest, Glenview, IL, USA) to change reflected colour with a bandwidth of 3 °C centred around one of several temperatures chosen to be typical of those for PCR (i.e. 58, 70 or 94 °C). As the temperature was increased, each TLC went through a red, green and then blue colour phase, with the start of the green phase coinciding with 58, 70 or 94 °C. To assemble a calibration standard, the TLC slurry was applied and spread onto the PCR chamber within the fluidic layer of the chip (prior to the assembly of the PCR/CE chip) using a pipette tip. The chip and TLC slurry was then allowed to dry for 15 minutes. The PCR/CE chip was then assembled by applying the PDMS membrane atop the fluidic substrate (without an oxygen plasma activation step), and bonding to the control layer. Although the TLCs are calibrated by the manufacturer [30], their characteristics can vary with time (personal communication with company engineers). Therefore, we further verified the temperature dependence of the TLCs by placing the calibration chips into a watertight bag placed within a temperature-controlled water bath (Haake C25P, Thermo Fisher Scientific Inc., Waltham, MA, USA). The temperature of the water bath was set to the start of the green band of the TLC and it was verified that the colour changed to green at this temperature.

To verify the thermal control of the system, calibration chips were loaded into the system as if a normal PCR run were being executed. Thermal cycling was started while visually monitoring (either by eye or with a camera) to verify colour change at the appropriate temperature, depending on the TLC chosen. The temperature control was verified at 58, 70 and 94 °C. To test variability, we removed and replaced calibration chips several times. After each such replacement, we thermally cycled the chip and observed the colour changes. The colour appeared to be the same each time, demonstrating that electrical contact, and thermal contact contribute minimally to variations from run-to-run.

3.3.7 Optical Detection

We make use of a non-confocal configuration of an interference filter (HQ669LP, Chroma Technology Corp., Rockingham, VT, USA), a gradient index (GRIN) lens (LGI630-6, Newport, Irvine, CA, USA) and a photodiode (NT57-506, Edmund Optical, Barrington, NJ, USA), (Figure 3.3c) and as detailed in [31]. As compared with light-emitting diodes (LEDs), diode lasers are advantageous because of their collimated light and spectral purity. Photodiodes are inexpensive, compact and easily incorporated into microelectronic chip designs (e.g. CMOS). The photodiode enables signal acquisition with good sensitivity and high speed. However, as expected with such a non-confocal system, we have a high baseline (about 2 V, or 50 times the signal from a typical PCR product).

As noted by Johnson and Landers [11], diode lasers usually need to be tem-

perature controlled and filtered for acceptable beam quality. For instance, both the laser wavelength and intensity can be nonlinear functions of the operating temperature of the laser [32]. As a result of such phenomena, fluctuations in the operating temperature can affect the intensity and wavelength. Any variation in intensity can lead to a variation in power consumption in a feedback situation that can lead to instabilities. While it was feasible to use a commercially available cooled laser with built-in temperature controller to stabilize the laser temperature (e.g. within $\pm$ 0.01 °C, with intensity stabilities of less than 1% in the TECRL laser series, World Star Tech., Toronto, Canada), such lasers are far more expensive than our entire system, and hence unsuitable for our goals. We chose instead to use an inexpensive and miniaturized red (635 nm) laser module (M635-5; US Lasers, Hazlehurst, GA, USA) that contains a simple laser diode with a driver circuit. The laser manufacturer states that the optical intensity for this laser varies by $\approx$5% when operated at room temperature (i.e. 21-24 °C). Based on our experimental measurements, using both our optical module and Keithley 6487 picoammeter (Keithley Instruments, Inc. OH, USA), the intensity of this laser varies by $\approx$1.5%. (We evaluated several such lasers and the characteristics given here are representative.) This laser intensity varies with a time scale (seconds) and magnitude comparable to those from the passage of a DNA peak.

This would seem to preclude effective operation of the system - the spurious signals from the variation of the baseline as the laser varies are indistinguishable from the real DNA signals (i.e. 1.5% gives an apparent signal of 30 mV, comparable to typical product peaks). However, by using both a heat-sink (of about 80 g of metal), we increased the thermal mass of the laser package, thereby increasing the

time constant of any instabilities. We also added a pre-run warm-up period of 10 minutes to bring the laser to equilibrium. With these, the laser intensity variation was reduced to less than 0.5%, comparable to the stability of expensive laser modules. Most importantly, the time constant of the instabilities was greatly increased - the variations were then very slow, typically lasting tens of seconds, and were easily dealt with by signal processing (see Section 3.3.8).

Using these methods we were able to utilise an inexpensive laser to develop a simple and compact non-confocal LIF detection method. The signal-to-noise ratio for the optical module was found to be sufficient for medical diagnostics (discussed in detail below). Moreover, this approach lends itself to being scaled to smaller systems. We have built far smaller (though less sensitive) prototypes of LIF detection systems consisting of as little as a laser and a microelectronic chip [31].

3.3.8 Signal Processing

The LIF amplifier is a standard transimpedance amplifier configuration based on a single op-amp (OPA129U, Texas Instruments) in a high-gain (10^9 V/A) and low bandwidth configuration that suppressed frequency components higher than about 1.5 Hz (further detail is provided elsewhere [31]). An analysis of the signal found that it was remarkably clear of the 60 and 120 Hz pickup noise often generated from power supplies. The main sources of noise were from a slow baseline drift and from white noise. The white noise (i.e. no spectral peaks were apparent in the analysis of the data), was likely from the electronics. The slow baseline drift arose from the system electronics as it warmed up and from instabilities in the laser (described

above). The amplifier bandwidth could readily be adjusted for higher speed, but the present amplifier is well-suited for these electrophoretic conditions.

The raw data from the optical module was saved and processed within the GUI. The GUI output the processed and raw data in a report format, as detailed in the software section. For DNA electrophoresis and detection through LIF, we chose a sampling rate of 100 Hz. This sampling rate was sufficient as the data of interest was slowly-varying (the passage of the DNA peaks are several seconds in duration). In order to obtain a smooth electropherogram, the raw data underwent a low-pass filtering and then a median subtraction (described below).

The low pass filter, implemented in software, suppresses the white noise above 1.5 Hz and results in a smooth electropherogram. This filter, which was designed using MATLAB's filter design and analysis tool (FDATOOL), was a standard low-pass finite impulse response (FIR) equiripple filter with attenuation initiated at 1.2 Hz and a cut-off frequency of 1.5 Hz.

Median subtraction is a standard method for removing slowly varying baselines. Such variations can be caused by increases in the photodiode temperature and electronic circuitry, or by the laser itself. The length of the moving median subtraction used here was 400 points (corresponding to 4 s). This window was sufficiently wide to not affect the data of interest (i.e. DNA peaks).

We use the signal to noise ratio (SNR) as a metric to evaluate the signal quality. The SNR was calculated using data that underwent processing as detailed above.

The first 50 s of the data of the separation phase of CE were used to determine the standard deviation of the noise. The SNR of the product was then determined using the ratio of PCR product peak height to the calculated standard deviation of the noise in the signal.

The above signal processing method reliably leads to electropherograms with isolated peaks corresponding to the primer and product peaks. On occasion, just prior to the arrival of a peak, a brief decrease in the processed signal strength (i.e. a dip) can be seen. Such dips are artifacts of the signal processing, and are attributable to the sinc-like impulse response of our filter. These dips do not affect the peak height and are proportional to the peak height. As such, they cannot generate or suppress a peak and therefore the dips do not affect our SNR or detection limits. These artefacts are more evident when (in the raw data) the product peak is preceded by a slowly decreasing baseline.

3.3.9 Limit of Detection

To characterise the optical sub-system, we established the limit of detection (LOD) using known concentrations of end-labeled DNA (Cy5 labeled primers, as detailed in the Section 3.3.2). In order to avoid sample-stacking effects that would lead to overly-optimistic LOD estimates, the LOD was established using DNA at various concentrations within a sample that had essentially the same ionic concentrations as for the PCR product from a PCR/CE run. We used an LOD standard composed of a mock PCR mixture, i.e. a PCR mixture without the unlabelled forward primers, BKV template and Taq polymerase. The ionic concentrations were dominated by

the other components, notably the PCR buffer, and these were kept constant. The Cy5 labeled primer was diluted using PCR grade water from a stock solution to an initial concentration of 2.49 ng/μL (or 0.3 pmol/μL). This mixture was then diluted with PCR grade water to concentrations of 0.749 ng/μL, 0.498 ng/μL and 0.249 ng/μL, and these were subsequently mixed with the other PCR components as per the PCR protocol. This spans the concentration range of interest for PCR products expected from the present protocol.

CE was performed in triplicate or duplicate on each concentration of primer using the CE protocol, i.e. 1 μL of this PCR mix and 3 μL of 0.01xTTE was put into the sample well. For all the electrophoresis runs, identical chips, reagents and electrophoretic conditions were employed. The data were then processed and the peak heights of the three different concentrations of DNA were plotted versus concentration. We then made use of a standard procedure [33] to use a linear regression on that plotted data to extrapolate the fitted line to a value of 3 times the average noise level from the first 50 s of all runs (see Section 3.3.8).

3.3.10 Instrumental, Microchip and Molecular Variabilities

Our signal strengths varied slightly from one run to the next, and we sought to identify the source of these variabilities - i.e. how much variation originated with the instrument, how much from the microchip, and, in the case of the PCR, how much was intrinsic to the molecular biology itself.

3.3.10.1 Variabilities in CE

In order to establish the variability associated with microchip-based CE on our system, we compared the results of running a reference sample of DNA on a commercial CE system (the μTK), and on our system. For each case, the chip was loaded with a sample as per the CE and LOD protocol, and duplicate runs were made (reloading and replacing the chip each time). In all, five samples were run twice each to determine both mix-to-mix, conventional PCR variability and CE variability at the same time. In this way, we achieved an estimate of the uncertainties in the CE signal amplitude that arose from variations in optical alignment or other errors (We believe that optical alignment was the dominant source of variation in each case).

3.3.10.2 Variabilities in PCR and PCR/CE

To establish the variability inherent to the molecular biology of conventional PCR (due to thermal cycling, pipetting etc.) we compared the results of 5 PCR runs on a conventional thermal cycler (PCR as detailed above). The 5 runs were made on 5 different days and their product was stored at 4 $^{\circ}$C after thermal cycling. Once all 5 samples had been collected the results were analysed on the μTK under identical conditions (as above).

In assessing the variability of LOC PCR, a 50 μL PCR mixture was kept on ice and 4 PCR/CE runs were made over the course of several hours. In this way we assessed the variability in combined PCR/CE either with commercial equipment or with our system. With knowledge of the variabilities due to the CE component we

could estimate the contribution from the PCR component.

3.4 Results and Discussion

3.4.1 Thermal Stability and Reproducibility

All calibration standards (Section 3.3.6) were found to give temperature transitions that were reproducible to within about 1 °C, indicating that placement, alignment, and thermal contact issues were reproducible. The TLCs indicated that the thermal equilibration times were approximately 10 s, as expected from simulation and calculation.

3.4.2 Limit of Detection

As is common with LOC analyses, the chip has far more sample in the sample well than is used in the analysis. As such, it is more appropriate to consider the concentration of the sample than the volume of sample used. Therefore, the above LODs are given as the minimum detectable concentration of DNA in the sample as loaded in the chip. The units ng/μL are appropriate for the analysis of PCR product where the product concentrations are often known in such units. (A very strong PCR product might contain 1000 $ng/\mu L$).

Since our signal is measured in units of millivolts (mV), we therefore estimate the sensitivity of the system in terms of signal strength per unit concentration, i.e. $\frac{mV-\mu L}{ng}$.

Following the procedures of Section 3.3.9, two consecutive sets of two runs each were performed at each concentration, resulting in average SNRs of 363, 229, and 194 (with standard deviations of 91, 60 and 51 respectively) for the concentrations of 0.749, 0.498, and 0.249 ng/ μL of end-labeled DNA, respectively (Figure 3.4).

The LOD was estimated to be 6 pg/μL of end-labeled primer DNA, corresponding to 700 pM (i.e. 7.0×10^{-16} mol/μL) of fluorophores. This in turn corresponds to a LOD of 60 pg/μL (also 700 pM since equal molarities give equal numbers of fluorophores) for detecting end-labeled double-stranded PCR product of $\approx$250 base pairs (with both primers labeled). If intercalators were used, we might expect labeling as high as 1 fluorophore per 3 bases, i.e. about 100 fluorophores per molecule and thus 50 times more heavily labeled. In this case, we might expect a LOD of 1.2 pg/μL or about 4 million molecules per μL. Whatever the labeling technique, the system is orders of magnitude more sensitive than required to detect a standard PCR product.

The well-known agarose gel and ethidium bromide combination is the conventional analysis method for PCR products. As described by Pelt-Verkuil *et al.* (page 142) [34], this remarkable combination has a lower limit of detection and quantitation of about 20 pg/μL and is linear for several orders of magnitude above that. Our LOD result indicates that our system is comparably sensitive.

In part because this type of information is dependent upon the procedure, we were not able to locate references to the LODs for any of the commercial systems

we discussed above. However, applying the above procedures (Section 3.3.9) to the μTK, we obtained a LOD of 2.3 pg/μL or 2.8x10^{-16} mol/μL of end-labelled primer DNA, i.e. this commercial product based on a confocal approach with a PMT detector was only approximately 3 times more sensitive than our system.

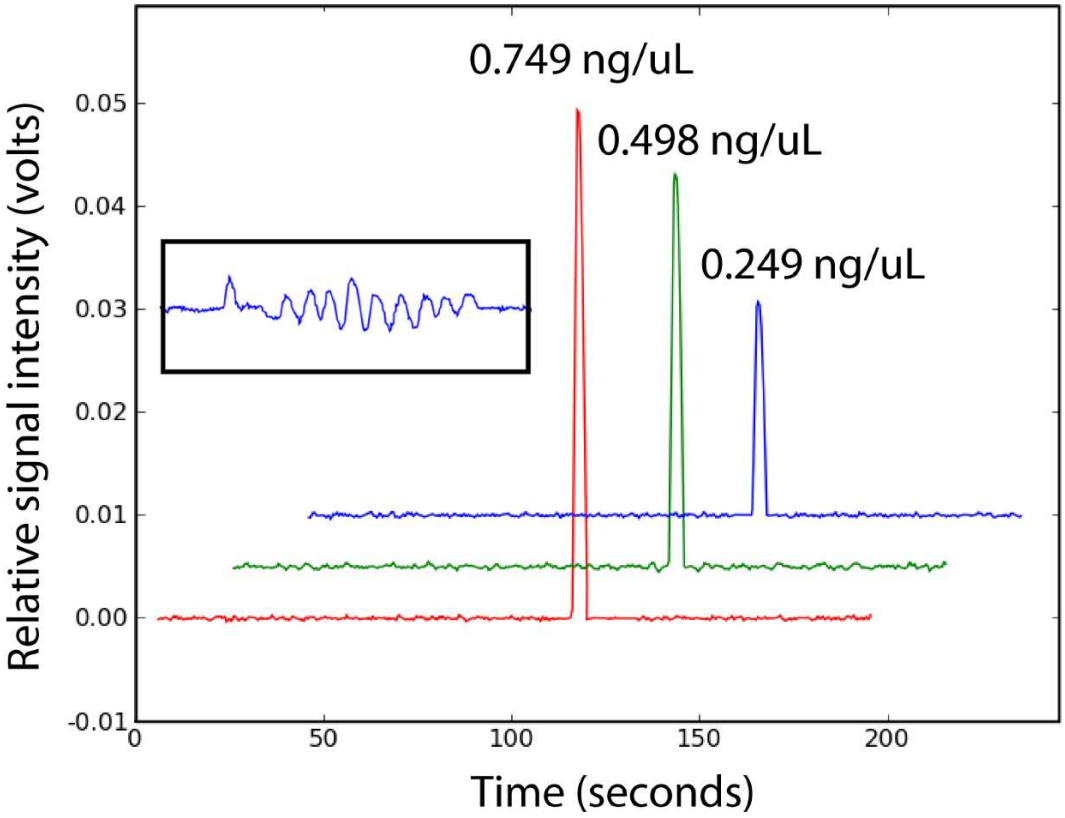

Figure 3.4: Limit of detection electropherograms for 0.749, 0.498, and 0.249 ng/μL of DNA. The inset shows the separation of primers and the AlfExpress size standard (50-500 bp) over a range of 0.01V and from 100 to 250s. As described in Section 3.4.4, the peaks are distorted by signal processing that has been optimised for the detection of isolated peaks rather than a regularly spaced DNA ladder. (An improved estimate of the resolution is given in Section 3.4.4)

From Figure 3.4, we arrive at a sensitivity of 67 $\frac{mV-\mu L}{ng}$ for primers, 13 $\frac{mV-\mu L}{ng}$ for doubly-labeled product DNA (of about 250 bp in length) and 7 $\frac{mV-\mu L}{ng}$ for singly-

labeled product DNA (of the same length). (We estimate the uncertainties in these numbers as about 10%).

The inset of Figure 3.4 shows the results of running the size standard and primers. For isolated peaks (e.g. primer and product), the median subtraction method was very effective as a baseline removal method. However, as is apparent from the inset, the peaks were distorted and suppressed by the median subtraction. The median subtraction associated with the primer peak has suppressed the 50 base peak of the sizer, with the following peaks at intervals of 50 bases up to 500 bases. A more effective estimate of the resolution is made in Section 3.4.4.

3.4.3 CE and PCR Variabilities

As described above (Section 3.3.10.1), we determined the μTK to have a run-to-run standard deviation of about 16%. We found our CE system to have a standard deviation of about 24%. The conventional PCR products (as analysed by the μTK) had a standard deviation of approximately 25%.

Even in a set of on-chip PCR/CE runs performed at much the same time from the same PCR mixture, we found that the intensities varied by a factor of about 2 from the mean of the set. In other words, the variability of the on-chip PCR was the dominant source of variability. Similar variability was found by Legendre *et al.* [26] - this is not surprising given that we based our passivation approach on theirs. We found that the on-chip PCR product concentration was typically about 17% of that of the conventional thermal-cycler (data not shown). In work such as that of Kim *et al.* [35], such low levels of on-chip PCR yield are characteristic of inade-

quate passivation. This is intriguing since work by others (e.g. [36, 37]) suggested that the effects of the PDMS were small or negligible relative to the effects of the glass. As a result, (and as described previously [1]) we had coated only the glass of our PCR chamber with SigmaCote (rather than the entire chamber as done by Legendre *et al.*). We note that with a surface area to volume ratio (SVR) of 0.16 $mm^2/\mu L$, Kolari *et al.* found that neither glass nor PDMS suppressed PCR significantly. However, in our system the SVR is approximately 70 times larger than in the work of Kolari *et al.*, and the surface effects should be far more pronounced. As Zhang *et al.* [9] concluded in their PCR review, more work is required to assess the biocompatibility of microfluidic materials. Our results show that the further work suggested by Zhang *et al.* will need to be undertaken at lab-on-chip scales of SVR. Clearly there is room for improvement in our chip passivation methods.

3.4.4 System Level PCR/CE Results

Following the procedures described above (Section 3.3.10.2), all but one of the positive control runs were of normal intensity, the exception showed no detectable product and this was attributed to operator error. As shown in Figure 3.5, the resulting electropherograms are similar to those obtained with commercial equipment (not shown), have good SNR and clearly resolve the product peaks. The primer peak arrives at approximately 130 s of separation (26 bases in length), and the product arrives at approximately 180 s, corresponding to a size of 300 bp ($\pm$ 20 bp as estimated from interpolation with a size standard, not shown). This is in good agreement with the expected size of 299 bp (as expected from a BLAST prediction (www.ncbi.nlm.nih.gov/BLAST/ as described by [38]).

The system has been in successful operation for several months without a failure (i.e. no false positive or false negative results). As the system was tested and improved, and in addition to the runs described above (with exactly the protocols given), another 22 PCR/CE runs were made with minor variations in the protocols (e.g. 2 °C shifts in annealing or denaturation temperature). Since our goal was to compare system performance (especially LOD etc.) we performed only 2 negative control runs on chip in order to demonstrate that our procedures were not susceptible to contamination.

With the sample concentration of 10^7 copies/mL, we expect ≈100 copies in the PCR chamber. With the same protocols as described above, we also tested several dilutions and found the expected statistical behaviour when working with dilutions of 10^5 copies/mL - arising from having either 0, 1 or several copies in the PCR chamber (data not shown). This indicates, as in previous work [21], that the system is able to detect at or near the single copy level.

We occasionally observed a third broad peak at approximately 250s (Figure 3.5), corresponding to a size of approximately 700 bp (for our size standard, the 500 bp peak arrives at 201.5s). This peak was attributed to non-specific amplification, and was low in intensity (≈8 times weaker than the PCR product peak in both on-chip and thermal cycler runs), was significantly broader than the other peaks, and as a result was greatly attenuated by the signal processing. A BLAST search of all known viral genomes found matches for our primers only for BK virus variants, all with the expected product length of 299 bp. A wider BLAST search of all avail-

able sequences (the non-redundant database) found potential matches in the human genome. This non-specific peak was observed in about half of the on-chip PCR runs, but was always seen in our control runs performed using the conventional thermal cycler and analysed by the μTK. This behaviour may be due to variations in the injection characteristics (Section 3.3.4), or may have been due to statistical effects that can be expected at low concentrations of human target DNA. Apart from the non-specific peak, the conventional and on-chip runs showed the same peaks. As expected, negative controls showed only a primer peak (not shown).

Using the sensitivity estimated above (Section 3.4.2), this system can also be used to quantitate the PCR product. Using the sensitivity for singly-labeled product DNA, the middle peak of Figure 3.5 has a signal strength of about 17 mV which corresponds to about 2.6 ng/μL. As a consistency check, if we assume that the peak intensities in the electropherogram are proportional to the corresponding DNA concentrations in the sample well then we can estimate the product DNA concentration from the known primer concentration (300 nM). From Figure 3.5 (middle trace), and taking into account the dilution by a factor of about 5 as part of the unloading process, we would predict a total concentration of 1.9 ng/μL. Given the uncertainties (in the unloading) and the assumption made, this is consistent. (Better estimates could likely be made by using the area of each peak rather than the peak height.)

The primary uncertainty in these estimates of sensitivity and LOD originates from the variation in laser intensity. However, occasional instabilities in laser intensity (even after stabilisation) can lead to bursts of noise (e.g. Run 1 in Figure 3.5, near 220 s) that are of significant magnitude, though rare. For this reason, it

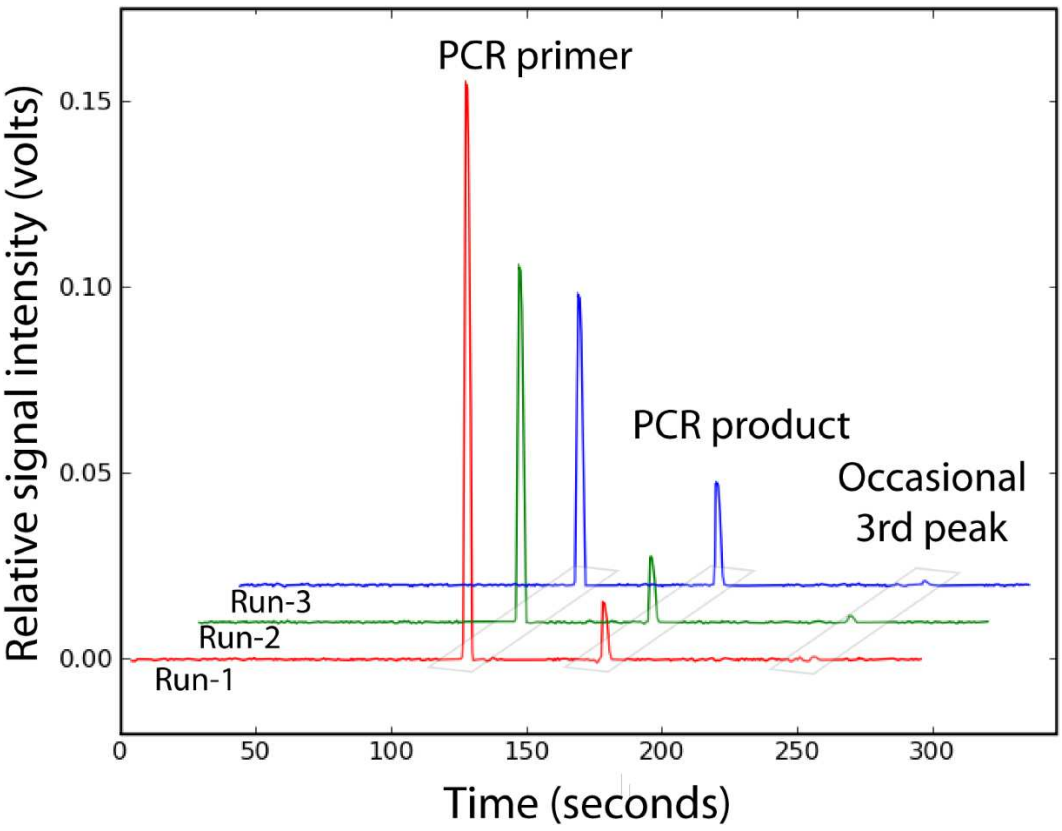

Figure 3.5: Three consecutive microchip-based PCR/CE results are plotted (as per given protocols). For each of the runs (1, 2, & 3) the peak on the left is the PCR primer peak, and the peak on the right is the PCR product peak (299 bps) representing the presence of BK virus in the sample being tested.

is important to perform all electrophoretic runs in duplicate or triplicate in order to identify and discard runs containing such bursts of noise (i.e. ignoring sporadic peaks). During such bursts of noise, the system sensitivity is reduced to about 120 pg/μL.

Using the approach detailed in [39], the resolution in CE separation was calculated to be $\approx$12 bps. This was comparable to the resolution obtained using the PCR/CE chip with a DNA sizing ladder (inset of Figure 3.4), whether on the μTK

or our system. As we noted before, [1], this suggests that the resolution was determined by a combination of the microchip and electrophoretic conditions, and that our system does not cause any loss of resolution.

The peak arrival times varied by about ≈2%, and we speculate that this variation in peak arrival time was due to variations in buffer concentration, electro-osmotic flow, and perhaps pressure-driven flows. The source of this variation is under investigation. However, given that this variation in timing corresponds to about 5 bps, it does not seem to significantly contribute to the uncertainty in the sizing of the PCR product. For some applications it might be desirable to achieve higher resolutions, and this might be achieved by the use of either longer distance separations or another separation medium - we note various reports of microfluidic CE with single bp (e.g. [40]) resolutions.

3.5 Concluding Remarks

The entire system in its current form is 'shoebox-sized', with a component cost of ≈ $600, yet it still demonstrates a performance comparable to commercial systems that are more that 100 fold more expensive. The modularity of the platform allows individual modules to rapidly evolve without redesign of the overall system. Our primary intent here is to demonstrate the functionality of a general purpose and inexpensive LOC platform that could be used to implement portable applications. However, a secondary goal is to develop a platform that can be used to develop progressively less expensive systems. Both the instrument and microfluidic chip we present are modular and scalable to far smaller sizes and lower costs. Our sys-

tem could demonstrate significantly higher performance with a revised design of microfluidic chip. For instance, with the scaling behaviours described above, a chip half the size could perform electrophoresis twice as fast and PCR four fold faster. Similarly, much of the electronics and optics is readily integrated into CMOS microelectronic chips.

In terms of PCR, this inexpensive system has been demonstrated to perform reproducibly, with single or several molecule sensitivity. Although there is some variability in PCR product intensity, this appears comparable to those levels reported elsewhere (e.g. [26]), although it is significantly higher than we found for conventional PCR. On average, we found that the LOC PCR product peak was about 17% the strength of that from a thermal cycler. We attribute this to inadequate surface passivation, and this is a focus of ongoing investigation.

In terms of CE, this system is comparable in sensitivity to commercial laser and PMT-based confocal systems, as well as to the standard intercalator-agarose gel combination commonly used to assess PCR products. The LOD of the present system is orders of magnitude better than is needed to detect a PCR product in a typical diagnostic application.

The performance of this system, along with its high level of integration, has led to it being a standard tool in our laboratory. We intend to explore higher levels of integration as we continue to lower the system cost. At the same time, we believe that this work clearly demonstrates that the cost of the LOC infrastructure need not be a barrier to future LOC applications. We hope that such a fully re-configurable,

portable and cost-effective LOC toolkit will catalyze the use of LOC technology for a wide range of applications.

Bibliography

[1] G. V. Kaigala, V. N. Hoang, A. Stickel, J. Lauzon, D. Manage, L. M. Pilarski, and C. J. Backhouse, "An inexpensive and portable microchip-based platform for integrated RT-PCR and capillary electrophoresis," *Analyst*, vol. 133, no. 3, pp. 331–338, 2008.

[2] P. Yager, T. Edwards, E. Fu, K. Helton, K. Nelson, M. R. Tam, and B. H. Weigl, "Microfluidic diagnostic technologies for global public health." *Nature*, vol. 442, no. 7101, p. 412, 2006.

[3] F. B. Myers and L. P. Lee, "Innovations in optical microfluidic technologies for point-of-care diagnostics," *Lab on a Chip*, vol. 8, no. 12, pp. 2015–2031, 2008.

[4] E. T. Lagally and R. A. Mathies, "Integrated genetic analysis microsystems," *Journal of Physics D-Applied Physics*, vol. 37, no. 23, pp. R245–R261, 2004.

[5] C. Koh, W. Tan, M. Zhao, A. Ricco, and Z. Fan, "Integrating polymerase chain reaction, valving, and electrophoresis in a plastic device for bacterial detection," *Analytical Chemistry*, vol. 75, no. 17, pp. 4591–4598, SEP 1 2003.

[6] E. Lagally, J. Scherer, R. Blazej, N. Toriello, B. Diep, M. Ramchandani, G. Sensabaugh, L. Riley, and R. Mathies, "Integrated portable genetic analysis microsystem for pathogen/infectious disease detection," *Analytical Chemistry*, vol. 76, no. 11, pp. 3162–3170, JUN 1 2004.

[7] G. V. Kaigala, R. J. Huskins, J. Preiksaitis, X.-L. Pang, L. M. Pilarski, and C. J. Backhouse, "Automated screening using microfluidic chip-based PCR and product detection to assess risk of BK virus-associated nephropathy in

renal transplant recipients," *Electrophoresis*, vol. 27, no. 19, pp. 3753–3763, 2006.

[8] Y. Sun and Y. C. Kwok, "Polymeric microfluidic system for DNA analysis," *Analytica Chimica Acta*, vol. 556, no. 1, pp. 80–96, 2006.

[9] Y. H. Zhang and P. Ozdemir, "Microfluidic DNA amplification - a review," *Analytica Chimica Acta*, vol. 638, no. 2, pp. 115–125, 2009.

[10] C. Zhang and D. Xing, "Miniaturized PCR chips for nucleic acid amplification and analysis: latest advances and future trends," *Nucleic Acids Research*, vol. 35, no. 13, pp. 4223–4237, 2007.

[11] M. E. Johnson and J. P. Landers, "Fundamentals and practice for ultrasensitive laser-induced fluorescence detection in microanalytical systems," *Electrophoresis*, vol. 25, no. 21-22, pp. 3513–3527, 2004.

[12] M. Asogawa, M. Sugisawa, K. Aoki, H. Hagiwara, and Y. Mishina, "Development of portable and rapid human dna analysis system aiming on-site screening," in *Twelfth International Conference on Miniaturized Systems for Chemistry and Life Sciences*, vol. 1, October 2008, pp. 1072–1074.

[13] M. Burns, B. Johnson, S. Brahmasandra, K. Handique, J. Webster, M. Krishnan, T. Sammarco, P. Man, D. Jones, D. Heldsinger, C. Mastrangelo, and D. Burke, "An integrated nanoliter DNA analysis device," *Science*, vol. 282, no. 5388, pp. 484–487, OCT 16 1998.

[14] E. Lagally and H. Soh, "Integrated genetic analysis microsystems," *Critical Reviews in Solid State and Materials Sciences*, vol. 30, no. 4, pp. 207–233, OCT-DEC 2005.

[15] C. J. Easley, J. M. Karlinsey, J. M. Bienvenue, L. A. Legendre, M. G. Roper, S. H. Feldman, M. A. Hughes, E. L. Hewlett, T. J. Merkel, J. P. Ferrance, and J. P. Landers, "A fully integrated microfluidic genetic analysis system with sample-in-answer-out capability," *Proceedings of the National Academy of Sciences of the United States of America*, vol. 103, no. 51, pp. 19 272–19 277, DEC 19 2006.

[16] P. Liu, T. S. Seo, N. Beyor, K.-J. Shin, J. R. Scherer, and R. A. Mathies, "Integrated portable polymerase chain reaction-capillary electrophoresis microsystem for rapid forensic short tandem repeat typing," *Analytical Chemistry*, vol. 79, no. 5, pp. 1881–1889, MAR 1 2007.

[17] R. J. Meagher, A. V. Hatch, R. F. Renzi, and A. K. Singh, "An integrated microfluidic platform for sensitive and rapid detection of biological toxins," *Lab on a Chip*, vol. 8, no. 12, pp. 2046–2053, 2008.

[18] J. L. Fu, Q. Fang, T. Zhang, X. H. Jin, and Z. L. Fang, "Laser-induced fluorescence detection system for microfluidic chips based on an orthogonal optical arrangement," *Analytical Chemistry*, vol. 78, no. 11, pp. 3827–3834, 2006.

[19] T. Kamei, N. M. Toriello, E. T. Lagally, R. G. Blazej, J. R. Scherer, R. A. Street, and R. A. Mathies, "Microfluidic genetic analysis with an integrated a-Si:H detector," *Biomedical Microdevices*, vol. 7, no. 2, pp. 147–152, 2005.

[20] M. Behnam, G. V. Kaigala, M. Khorasani, P. Marshall, C. J. Backhouse, and D. G. Elliott, "An integrated CMOS high voltage supply for lab-on-a-chip systems," *Lab on a Chip*, vol. 8, no. 9, pp. 1524–1529, SEP 2008.

[21] G. V. Kaigala, V. N. Hoang, and C. J. Backhouse, "Electrically controlled microvalves to integrate microchip polymerase chain reaction and capillary electrophoresis," *Lab on a Chip*, vol. 8, no. 7, pp. 1071–1078, 2008.

[22] W. H. Grover, A. M. Skelley, C. N. Liu, E. T. Lagally, and R. A. Mathies, "Monolithic membrane valves and diaphragm pumps for practical large-scale integration into glass microfluidic devices," *Sensors and Actuators B-Chemical*, vol. 89, no. 3, pp. 315–323, 2003.

[23] N. M. Toriello, C. N. Liu, and R. A. Mathies, "Multichannel reverse transcription-polymerase chain reaction microdevice for rapid gene expression and biomarker analysis," *Analytical Chemistry*, vol. 78, no. 23, pp. 7997–8003, 2006.

[24] S. Bhattacharya, A. Datta, J. M. Berg, and S. Gangopadhyay, "Studies on surface wettability of poly(dimethyl) siloxane (PDMS) and glass under oxygen-

plasma treatment and correlation with bond strength," *Journal Of Microelectromechanical Systems*, vol. 14, no. 3, pp. 590–597, 2005.

[25] H. Kim, S. Vishniakou, and G. W. Faris, "Petri dish PCR: laser-heated reactions in nanoliter droplet arrays," *Lab on a Chip*, vol. 9, no. 9, pp. 1230–1235, 2009.

[26] L. A. Legendre, J. M. Bienvenue, M. G. Roper, J. P. Ferrance, and J. P. Landers, "A simple, valveless microfluidic sample preparation device for extraction and amplification of DNA from nanoliter-volume samples," *Analytical Chemistry*, vol. 78, no. 5, pp. 1444–1451, 2006.

[27] G. Kaigala, J. Jiang, C. Backhouse, and H. Marquez, "System design and modeling of a time-varying nonlinear temperature controller for microfluidics," *IEEE Trans. on Control Systems Technology*, vol. DOI: 10.1109/TCST.2009.2015937, p. 6, 2009.

[28] V. N. Hoang, G. V. Kaigala, A. Atrazhev, L. M. Pilarski, and C. J. Backhouse, "Strategies for enhancing the speed and integration of microchip genetic amplification," *Electrophoresis*, vol. 29, no. 23, pp. 4684 – 4694, 2008.

[29] V. N. Hoang, G. V. Kaigala, and C. J. Backhouse, "Dynamic temperature measurement in microfluidic devices using thermochromic liquid crystals," *Lab on a Chip*, vol. 8, pp. 484–487, 2008.

[30] Hallcrest, "Handbook of thermochromatic liquid crystal technology." Hallcrest Inc., Glenview, IL, USA, Tech. Rep., 1991.

[31] G. V. Kaigala, M. Behnam, C. Bliss, M. Khorasani, S. Ho, J. N. McMullin, D. G. Elliott, and C. J. Backhouse, "Inexpensive, universal serial bus-powered and fully portable lab-on-a-chip-based capillary electrophoresis instrument," *IET Nanobiotechnology*, vol. 3, no. 1, pp. 1–7, MAR 2009.

[32] G. W. Kamin, "Laser diode intensity and wavelength control," Litton Systems Inc., Beverly Hills, CA, USA, US Patent 4,792,956, 1988.

[33] D. MacDougall and W. B. Crummett, "Guidelines for data acquisition and data

quality evaluation in environmental chemistry," *Analytical Chemistry*, vol. 52 (14), pp. 2242–2249, 1980.

[34] E. v. Pelt-Verkuil, A. v. Belkum, and J. P. Hays, *Principles and Technical Aspects of PCR Amplification*. Springer Netherlands, 2008.

[35] J. A. Kim, J. Y. Lee, S. Seong, S. H. Cha, S. H. Lee, J. J. Kim, and T. H. Park, "Fabrication and characterization of a PDMS-glass hybrid continuous-flow PCR chip," *Biochemical Engineering Journal*, vol. 29, no. 1-2, pp. 91–97, 2006.

[36] K. Kolari, R. Satokari, K. Kataja, J. Stenman, and A. Hokkanen, "Real-time analysis of PCR inhibition on microfluidic materials," *Sensors And Actuators B-Chemical*, vol. 128, no. 2, pp. 442–449, 2008.

[37] A. R. Prakash, M. Amrein, and K. V. I. S. Kaler, "Characteristics and impact of Taq enzyme adsorption on surfaces in microfluidic devices," *Microfluidics And Nanofluidics*, vol. 4, no. 4, pp. 295–305, 2008.

[38] S. Karlin and S. F. Altschul, "Applications and statistics for multiple high-scoring segments in molecular sequences." *Proceedings of the National Academy of Sciences of the USA*, vol. 90, pp. 5873–7, 1993.

[39] V. J. Sieben and C. J. Backhouse, "Rapid on-chip postcolumn labeling and high-resolution separations of DNA," *Electrophoresis*, vol. 26, no. 24, pp. 4729–4742, 2005.

[40] R. G. Blazej, P. Kumaresan, and R. A. Mathies, "Microfabricated bioprocessor for integrated nanoliter-scale Sanger DNA sequencing," *Proceedings of the National Academy of Sciences of the United States of America*, vol. 103, no. 19, pp. 7240–7245, MAY 9 2006.

Chapter 4

Sample Preparation, PCR Amplification and Analysis in a Low-Cost Portable Platform

This chapter is based on a manuscript submitted for publication to the journal of Microfluidics and Nanofluidics. As more functionalities are integrated into microfluidic chips, manual sample manipulations get more challenging. To realize a complete lab-on-a-chip based diagnostic, it is necessary to build a self-sufficient instrument that accepts raw sample from a patient and performs all the steps to generate the test result. To do this, we enhanced our microfluidic toolkit with an automated sample preparation module. We demonstrate the functionality of this module by extracting genetic material from a raw patient sample and performing genetic amplification and analysis all in a single microfluidic chip that is operated on a single bench-top instrument. As the lead author, I led the instrument design (i.e. hardware including testing and debugging), thermal and optical calibration, as well as biological protocol adaptation.

A version of this chapter has been submitted for publication. Behnam *et al.* 2010.

Preface

We present a low-cost lab-on-a-chip (LOC) instrument that performs polymerase chain reaction (PCR)-based diagnostic testing, starting from a raw sample, in a single microfluidic chip. Without the requirement for any specialized equipment other than this inexpensive LOC system, nucleic acids (NAs) are extracted from an unprocessed sample (sample preparation, SP), amplified via PCR, and analysed by capillary electrophoresis (CE) with laser-induced fluorescence detection. The system integrates a stage to manipulate a permanent magnet beneath the chip in either 1 or 2 dimensions, thereby moving magnetic beads with bound NAs within microchannels directly above the magnet, which allows for separation of DNA from cellular debris. Although this is a general purpose platform, we demonstrate it here with human buccal cells, performing DNA purification and PCR-CE on a single microchip. The SP-PCR-CE system is fully integrated into a low-cost (approximately $1000 in component cost), shoe-box sized instrument. To the best of our knowledge this is the first fully integrated LOC-based SP-PCR/CE instrument capable of performing sample-in-answer-out analysis in an inexpensive portable format. We amplify and detect the β2 microglobulin gene from buccal cells as a prototype for a wide range of diagnostic applications.

4.1 Introduction

The implementation of molecular medicine on portable and inexpensive systems has the potential to improve healthcare, particularly in low resource settings [1]. While major strides have been made in medical diagnostics implemented on LOC devices, one limiting factor in the application of these technologies outside the lab-

oratory is the need for considerable operating infrastructure, most of which is required for the processing of raw samples [2]. While a large number of diagnostic techniques have now been demonstrated on microfluidic chips [3], these typically require substantial manual, off-chip SP steps in a well-equipped facility with trained operators. The current state-of-the-art for commercial systems consists of assays that require many steps (e.g. 15 steps) that can take several hours, while requiring expensive equipment, and dedicated space for separated (offline) SP and amplification [4]. In addition, most systems also require reagent kits that cost $50 - $100/test in addition to transport and storage below room temperature. There is therefore a great need for simple and generic SP technologies that circumvent challenges in PCR efficiency or versatility [4]. In this respect, current microfluidic technology remains tied to the conventional infrastructure it is intended to replace.

4.1.1 Sample Preparation

The sensitive molecular diagnostic testing of complex biological samples (blood, tissue, buccal cells) requires the separation of nucleic acids (DNA/RNA) from cell components that may otherwise inhibit downstream processes such as PCR [5]. Well-characterized conventional techniques exist to extract NAs from samples at the macroscale (e.g. [6, 7]), but, as pointed out by [8], it can only be with an increased development of SP capabilities that truly automated LOC platforms will be enabled. As this is a critical area of development for the field, the level of activity is such that it is no longer possible to refer to all the work in the field, although there are a number of excellent recent reviews (discussed below).

Bao and Lu [9] reviewed the microfluidic state of the art for SP of bacteria via chemical, optical, thermal and electrical means (with and without beads). In another review, Brennan *et al.* [10] described the ideal specifications for point of care (POC) applications: a sample to answer capability in less than 60 minutes, a cost per test of less than $10 and a capital cost of less than $2000 – and the capability of simultaneous testing for 100 polymorphisms! Although these criteria are far more challenging than those required in many applications, and clearly beyond the present state-of-the-art in the LOC field, they would be in keeping with the overall goal of the LOC field– i.e. "true" LOC systems consisting of little more than the chip itself. However, such integrated nucleic acid-based assays remain an unresolved challenge due to SP-related issues [11]. Dobson *et al.* [12] concluded that there are no currently available SP systems suited for POC applications.

Progress in the area of nucleic acid extraction techniques has achieved on-chip extraction efficiencies comparable to those using conventional methods (Kim *et al.* [13]). While solid phase extraction (SPE) (e.g. silica with chaotropic salts) gives the best efficiency in DNA recovery, it is difficult to implement on chip [4]. Successful demonstrations of SPE SP have analyzed human cells in an automated platform that used an isothermal method for genetic amplification and detection [14]. SP was carried out on a credit card-sized platform with sample collection on a filter, followed by SPE and washing to remove cell debris. Although a powerful demonstration, this is a relatively complex system with attached pre-concentration and consisting of silica filters, membranes, 2 syringe pumps, multiport valves, heaters and chips that are not scalable. The chip itself was assembled by hand from various components (such as valves and filters) and stored all the needed reagents. In another

state-of-the-art demonstration, cell lysis and DNA extraction from bacteria within samples of whole blood using a disposable microfluidic chip was presented [15], with an on-chip performance comparable to that of standard kits. The sample was first mixed off-chip and 450 μL was placed on-chip with a syringe. Multiple rinses were required in applying a microscale SPE process that was optimised to enhance lysis, by using detergents, repeated freeze-thaw cycles, or boiling.

As described in the review by Kim *et al.* [13], although magnetic beads are the most difficult SP technology to integrate on-chip, they do have compelling advantages. Magnetic particles confer both high speed (eg. 10 min) and high efficiency, are commercially-available (ChargeSwitch™), circumvent the use of chaotropic salts and solvents, and are inherently less inhibitory to subsequent PCR. Beads facilitate both the initial reduction of sample volume from the mL scale and the concentration of the sample (e.g. from several copies/mL to a level of ng/μL). Duarte *et al.* [16] characterized the SPE extraction of DNA from blood with magnetically controlled silica beads, finding that dynamic methods are more effective than packed beads and produce more concentrated solutions too. In related work with real-time and Taqman-based PCR (without CE), we note the significant advancements in integrations of magnetic beads and RT-PCR by Lien *et al.* [17], and Hua *et al.* [18]. Although all of these demonstrations required substantial instrumentation, we also note the exploration by House *et al.* [19] of reliable minimalist SP methods (e.g. boiling) followed by a Taqman assay for pathogen detection.

4.1.2 SP Integrations with PCR and CE

Although the SP-PCR-CE combination has seen less development than SP-real time PCR/Taqman, the addition of CE gives this system the advantage of providing the product size, corroborating the diagnosis by determining if non-specific amplification occurs. SP-PCR-CE also provides a general platform for many applications as it is the basis of many medical diagnostics.

The LOC community has sought to develop fully integrated systems with a sample-in to answer-out capability, but the challenges of SP have led to "surprisingly few" complete systems [13]. As noted by these authors, a versatile SP technology is critical and the reduction of SP complexity will be required for effective and reliable systems. They put forward the work of the Landers group [20] as representing the state-of-the-art in SP integration. That work was a powerful demonstration, presenting a 24 minute SP-PCR/CE assay that includes SP of raw bodily fluids via SPE in a silica bed. However, the system requires extensive supporting infrastructure, including an Ar ion laser, IR thermal cycling apparatus and a syringe pump. More recent work from that group describes a microdevice with on-chip silica bead-based SP from blood using commercial kits, followed by on-chip PCR using a conventional thermal cycler and then external CE [21]. This approach requires no complex controls (eg. valves), and represents a powerful simplification of previous approaches for SP, despite requiring considerable external infrastructure (syringe pump, thermal cycler, CE system).

Lui *et al.* [22] recently presented a review of the state-of-the-art in nucleic acid-based detection of pathogens in integrated LOC systems, with a focus on strate-

gies and challenges for portable platforms. They note the commercial developments by ACLARA Biosciences, Fluidigm, Affymetrix, Agilent Tech., Alderon, Roche Molecular Diagnostics, Motorola and others, and give particular mention to Cepheids GeneXpert (GX) system for single use cartridge-based SP, amplification and detection. They presented the work of the Mathies group [23] as being the state-of-the-art in portable implementations of PCR/CE. Demonstrations of microfluidic implementations of PCR/CE and SP-PCR/CE by that group have shown systems of great functionality ([23, 24, 25]), albeit with relatively expensive instrumentation.

In spite of many recent advances, a portable, self-contained and inexpensive (i.e. less than $2000) system capable of SP-PCR-CE has yet to be demonstrated. We are developing such highly integrated, low-cost and portable PCR/CE-based LOC systems. To this end, we earlier demonstrated a shoebox-sized, charge-coupled device (CCD)-based PCR/CE instrument [26] for applications such as pathogen detection [27], cancer biomarker detection [28], and genotyping [29]; and more recently, the highly modular and scalable architecture of a LOC toolkit with photodiode-based detection [30].

In the present work, we significantly increase the versatility and functionality of our PCR/CE toolkit/instrument by integrating a SP unit to process raw samples, making nearly handling-free diagnostic testing possible with essentially no additional equipment required. In terms of SP, the ideal SP technology would be one that was simply a miniaturized version of a widely-used conventional method. With this in mind, we have chosen to use a paramagnetic bead-based approach, a miniaturization of the widely-used conventional method. Within a single integrated mi-

crofluidic chip, we perform cell lysis, magnetic particle transport and delivery, particle trapping for nucleic acid purification, fluidic movement, mixing, confinement of the fluid, and thermal cycling with on-chip microvalves and a patterned platinum heater/sensing element. We demonstrate the versatility of our instrument (shown in Figure 4.1A) in the processing of samples by detecting the β2-microglobulin gene using magnetic bead-based purification of nucleic acids from buccal cells, followed by amplification via PCR and analysis by CE. To the best of our knowledge, this is the first demonstration of such a portable instrument with SP-PCR/CE functionality within a single microchip.

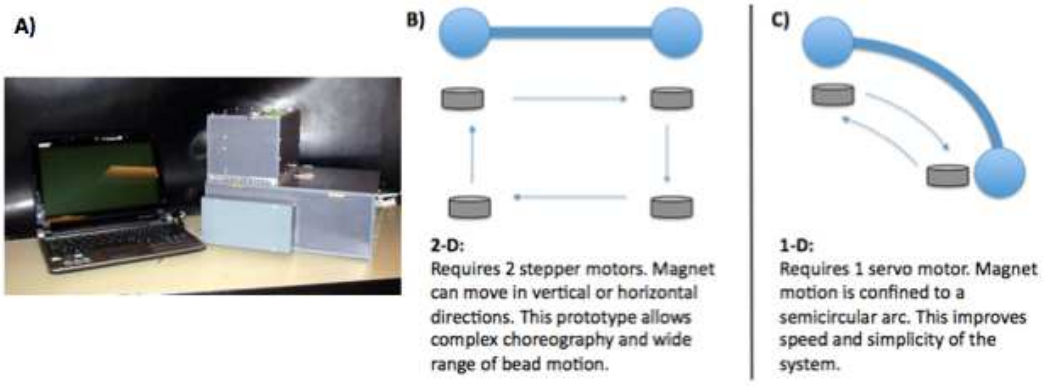

Figure 4.1: (A) Photograph of our shoebox sized lab-on-a-chip toolkit ($30\times20\times11$ cm for the main box) (B) The two-dimension sample preparation module consists of a miniaturized motorized X-Y stage and drive electronics. This module controls the magnet movement along predefined paths, manipulating the magnetic beads within the SP-PCR-CE chip as specified via a graphical user interface. (C) We further constructed a simplified servomotor driven stage capable of motion in only a single dimension.

4.2 Materials and Methods

4.2.1 Microfluidic Chip

Here we briefly describe the architecture of our tri-layer SP-PCR/CE microfluidic chip (further fabrication details are presented elsewhere [30]). The chip (Figure 4.2) consists of two layers (top and bottom) of 1.1 mm Borofloat glass (Schott AG, Germany) and a 254 μm thick polydimethylsiloxane (PDMS) membrane between them. Such an architecture enables the integration of microvalves and pumps within the chip using standard microfabrication technologies. The PCR reaction chamber is etched 90 μm deep, allowing for a volume of 600 nL, the CE microfluidic channels are 45 μm deep and 100 μm wide, and the SP channel is 100 μm deep and 500 μm wide.

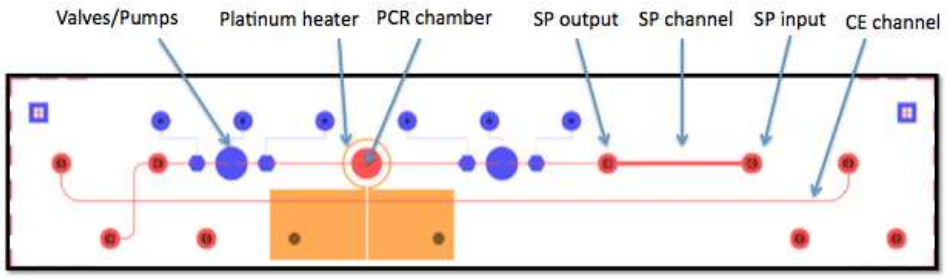

Figure 4.2: Design of the integrated SP-PCR/CE chip showing the sample preparation (SP) input and output wells, SP separation channel, micropumps, valves, CE channels, PCR chamber and platinum thin-film heating element. The pumps and valves are etched into the upper face of the bottom layer of the tri-layer stack designated as the control layer. The CE, PCR and SP channels are etched into the bottom face of the top layer of the tri-layer stack. The platinum element is patterned onto the bottom layer of the tri-layer chip.

4.2.2 Instrument Architecture

The instrument (shown in Figure 4.1A) consists of several modules, including thermal regulation, temperature monitoring, optics, high voltage generation and switching, pumping and valving, power, and SP. Each module has been previously described [30], except the SP module which enables a sample-in-answer-out functionality (detailed in 4.2.3). The supporting electronics are controlled via a microcontroller regulated by resident firmware (written in the C language). This firmware also performs data collection and interacts via a USB interface with a graphical user interface (GUI, written in python) running on a laptop computer. During CE, the fluorescence signal (from the diode) is sampled at 100 Hz. To remove electronic noise, we process the raw data using a low-pass filter to suppress white noise above 1.5 Hz and perform median subtraction to remove slowly varying baselines. The GUI logs the data collected by the firmware, interfaces with the user for the collection of run parameters and generates run reports. Further details of signal processing can be found elsewhere [30].

4.2.3 Sample Preparation Module

We have developed both a two dimensional (2D) and a one dimensional (1D) SP module, shown in Figure 4.1B and Figure 4.1C respectively. The 2D module consists of two computer-controlled stepper motors that allow arbitrary movements of a neodymium-iron permanent magnet in the horizontal plane (range of 25 mm $\times$ 25 mm), with encoders for position sensing, and infrared transceivers for auto-zeroing. The permanent magnet is machined to a 2 mm tip to localize the magnetic field for the migration of beads within the SP microchannel (Figure 4.3).

The 1D module is composed of a simple servomotor connected via a standard 3-wire pulse-width modulated (PWM) interface to a microcontroller. In such compact (thumb-sized) motors, the duty cycle of the PWM control line is used to control the degree of rotation of the servomotor shaft. By attaching an arm to the servomotor shaft, the degree of rotation is translated to a position along an arc of rotation. Since the PWM signal is controlled by software, the position of a permanent magnet (attached to the arm) can readily be determined with nothing more than a motor, 3 wires and an arm.

For the chip shown in Figure 4.2, with its straight SP channel, the 2D module is most appropriate. For simplicity we will describe the application of the 2D module. The only change required to use the 1D module would be to use a chip having a circular arc for a SP channel. We have found both the 1D and 2D modules to work equally well for the relatively simple bead movements described here. Further details are provided in the supplementary data section.

4.2.4 Bead-based Nucleic Acid Purification

Our approach to NA extraction using beads is to take the simplest possible approach while performing what is essentially a miniaturized version of the conventional processing, yet using no additional instrumentation such as a centrifuge. To do this, we have developed an approach that involves the use of a micropipetter, a swab and reagents from a standard SP kit (ChargeSwitch™gDNA Blood Kit, Cat. # CS11000, Invitrogen, Carlsbad, CA). The development of that protocol, its appli-

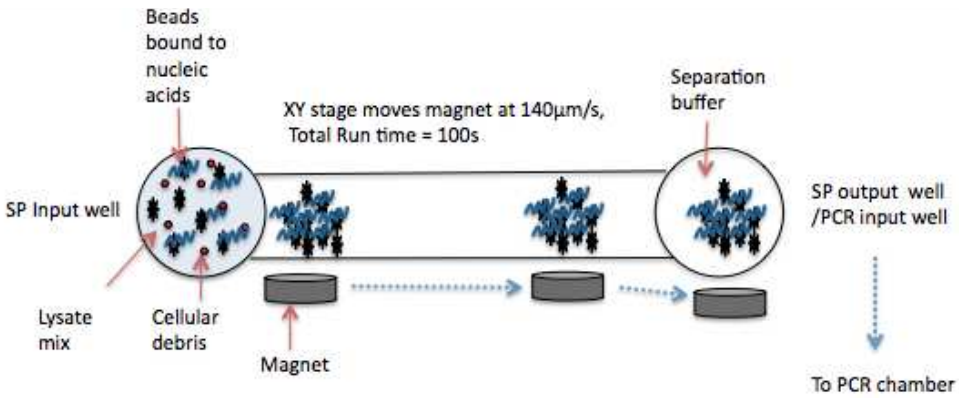

Figure 4.3: Manipulation of the beads in two dimensions (X-Y) within the SP channel from the SP input well into the SP output by a computer-controlled magnet beneath the chip stage. This entire process of bead migration is completed within ≈100 seconds.

cation to extraction of parasite DNA from blood, and a quantitative comparison of its performance to that of conventional methods, will be presented elsewhere [31]. The present work is focused upon the on-chip integration of SP with PCR-CE.

Nucleic acids are purified using ChargeSwitch™magnetic beads by controlling their surface charge with the pH of the surrounding liquid. In low pH conditions ($<$ 6.5 pH), the beads are positively charged and bind to the negatively charged backbone of nucleic acids. The bead/NA conjugate is separated from the surrounding solution by the application of a magnetic field and the NAs are subsequently eluted by raising the pH above 8.5, by virtue of simply mixing the beads with PCR reagents (Figure 4.4).

Before each on-chip DNA extraction, we perform an off-chip (i.e. tube-based) extraction as a reference experiment to test the ChargeSwitch™magnetic bead kit and to compare on-chip performance with the conventional methods. Our protocol

for tube-based purifications replaces the ChargeSwitch™wash buffer and elution buffer with our SP separation matrix (25% sucrose, 1%Tween20, in ChargeSwitch™wash buffer) and PCR master mix, respectively, for compatibility with on-chip extraction (Section 4.2.6).

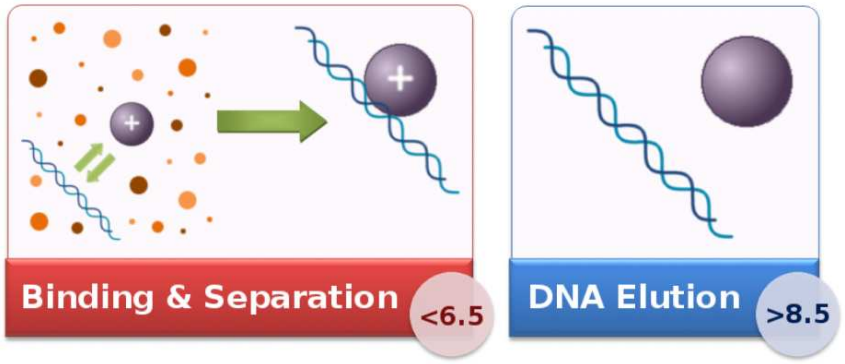

(a)

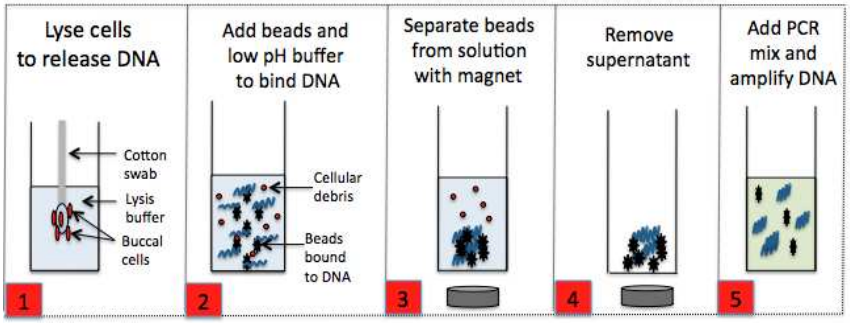

(b)

Figure 4.4: (A) Working principle of magnetic beads. The surface charge on the magnetic beads is controlled by the pH of the surrounding fluid. In low pH conditions ($<$ 6.5 pH), the magnetic beads are positively charged and bind to the negatively charged nucleic acids. Nucleic acids are eluted by raising the pH $>$8.5. (B) Illustration of multiple step processes performed using conventional tube-based DNA purification (adapted from Invitrogen Product Manual).

4.2.5 Off-chip Bead-based Nucleic Acid Extraction (Reference Method)

Buccal swabs were obtained from healthy volunteers with informed consent using a 15 cm sterile swab (AMG Medical, Montreal, QC) applied to the left and right buccal surfaces for 30 sec each. The swabs are incubated for 15 min in 500 μL lysis buffer to lyse the epithelial cells, followed by a 10 min incubation with 5 μL of Proteinase K to digest the histones and improve primer access during PCR. Subsequently, the addition of 25 μL of purification buffer, 5 μL of the ChargeSwitch™beads (stored in 10 mM MES (2-(N-morpholino)ethanesulfonic acid), pH 5.0, 10 mM NaCl, 0.1% Tween20) and 12 μL of 10% Tween20 (Sigma Aldrich, USA) results in a mixture we refer to as the SP lysate mixture. 5 μL of SP lysate mixture is added to a tube containing 5 μL of SP separation matrix (25% sucrose, 1% Tween20 in ChargeSwitch™wash buffer). The use of Tween20 and sucrose is used to enhance washing effects and to increase the density and viscosity. However, the increased viscosity aids in allowing the beads to move through a stationary fluid (i.e. the viscosity holds the separation matrix fixed) while tending to break up the bead pellet for better sample washing [31, 32]. The magnetic beads are then collected into a pellet at the bottom of the tube by an external magnet, following which, 1 μL of the bead suspension is removed using a micropipettor. Instead of then adding the entire 1 μL volume of beads and SP separation matrix present in the pipette tip to the PCR mix (24.2 μL, see Section 4.2.7 for description of PCR protocol), we transfer the magnetic beads by placing a permanent magnet directly under the PCR tube. This transfers the beads to the PCR mixture while leaving behind the SP separation matrix in the pipette tip, which ensures that the beads are transferred into the PCR reaction with minimal SP separation matrix contribution (experiments

with the SP separation matrix added to the PCR mix showed poor efficiency). After adding magnetic beads from the off-chip SP to the PCR mixture, PCR is performed in a commercial thermocycler (PTC-200, MJ Research, MA, USA).

4.2.6 On-chip Nucleic Acid Extraction

To perform on-chip SP, the swabs are obtained and incubated (as in the off-chip method) to produce the SP lysate mixture. The SP output well and SP channel (see Figure 4.3) are filled with SP separation matrix. After the channel is filled completely, any excess separation matrix in the SP input well is removed using a micropipetter. The magnet is then positioned beneath the SP input well and 4 μL of SP lysate mixture is added to the SP input well. The X-Y stage then moves linearly at 140 μm/s, beneath the SP output well (this takes $\approx$100 sec), which drags the beads through the separation matrix. We believe that the density and viscosity of the separation matrix enhances the washing effect, with the net effect being the separation of the beads from the cellular debris. The beads are then positioned/immobilized in the center of the output well by the magnet so the content of both SP input and SP output wells can be emptied by a micropipetter without removing the beads. Subsequently, 4.8 μL of PCR mix (see Section 4.2.7) is added to the SP output well in preparation for on-chip PCR. The pH of the PCR mix (pH of 8.8) releases the DNA from the magnetic beads and this PCR mix is then pumped into the PCR chamber.

4.2.7 PCR Protocol

As a standard procedure, a 24 μL mixture is prepared with all PCR reagents except DNA template. This mixture is used for both on- and off-chip reactions. The PCR reaction contains: 20 mM Tris pH 8.4, 50 mM KCl, 4 mM MgCl2, 200 μM dNTPs (Invitrogen, Burlington, Ontario) 0.02% BSA (New England Biolabs, Ipswich, MA) 4% DMSO (Fisher Scientific, Ottawa, Ontario), 200 nM of each β2M specific primer (forward 5'-GTACTCCAAAGATTCAGGTTTACT-3'; reverse Alexa647-5-ACGGCAGGCATACTCATCTTTTTCAG-3'; Integrated DNA Technologies, Coralville, IA) and 0.2 U/μL Platinum®Taq polymerase (Invitrogen, Burlington, Ontario). The primers are designed to amplify a 236 bp segment of the β2 microglobulin gene.

As a positive control for amplification (off-chip), purified human gDNA (purified from whole blood; FlexiGene DNA kit, Qiagen, Mississauga, Ontario) is used as a template. An aliquot of 19.2 μL of the above 24 μL PCR mixture is used as a PCR control reaction on the commercial thermocycler, while 4.8 μL of the remaining PCR mixture volume is used for the on-chip SP-PCR/CE experiment. This 4.8 μL of PCR mixture is pipetted into the PCR sample well in the chip containing the bead/DNA conjugate. The magnet is moved away from the well while the PCR solution is mixed with the beads by pipetting in/out the PCR solution. Subsequently the on-chip pump is actuated to fill the PCR chamber. Typically, 3-4 pump-cycles (sequential action of 3 consecutive valves with a time period of 500 ms between each individual valve) on a PCR/CE chip is sufficient. Once the chamber is filled, the valves are closed, and any remaining PCR mixture is removed from the PCR sample well with a micropipetter. The well is then washed with water to remove

any residual content of the PCR mixture.

On-chip thermal cycling is performed by setting parameters within the GUI. The thermal conditions are: pre-denaturation temperature of 94°C for 120 s, 35 cycles of 94°C for 30 s, 60°C for 30 s, and 72°C for 30 s, and a post-extension temperature of 72°C for 120 s. Positive and negative controls (i.e. PCR reactions with and without beads, with and without gDNA) are performed on a conventional thermocycler using identical PCR conditions in order to ensure the PCR reagents are not contaminated. For each chip run, the 19.2 μL aliquot of the PCR mixture was combined with an estimated 76 ng of purified human gDNA to form a positive control. On-chip negative controls (SP-PCR) were performed to ensure that no contamination from the chip was introduced prior to or during PCR (details in Section 4.3).

4.2.8 Unloading Thermally Cycled Mixture and Capillary Electrophoresis

After on-chip thermal cycling, 5 μL of 0.01$\times$TTE (1xTTE; 50 mM Tris pH 8.2, 50 mM TAPS, 1 mM EDTA) buffer is pipetted into the PCR input well and then pumped into the chamber by actuating the on-chip pumps. This mixes the buffer with the PCR product and moves it into the CE sample well. For analysis, approximately 4 μL of diluted product is present in the well after thermocycling. Analysis of the on-chip thermocycled product is performed using capillary electrophoresis and laser induced fluorescence (LIF) detection. As in past work [26], for microchip CE we use 4% linear polyacrylamide (LPA) as the CE separation matrix. The LPA

and chip are prepared as described in [23] with a 1×TTE buffer. Prior to loading the CE separation matrix, the CE channel surfaces on the microchip are coated to minimize electroosmotic flow [26]. The channels are then filled with LPA and 4 μL of 1×TTE buffer is pipetted into all CE wells except the sample well.

DNA from the thermocycled product present in the CE sample well is electrokinetically injected into the shorter channel (see Figure 4.2) using 200 V (≈222 V/cm) for 80 s, followed by a separation voltage of 600 V (≈67 V/cm) for 250 s. Detection is performed at 13 mm from the CE channel intersection, along the longer section of the channel. As our goal is to miniaturize this instrument even more, we chose to perform CE separation at distance of 13 mm even though the chip is significantly longer.

4.3 Results and Discussion

With our custom-built instrument (Figure 4.1A) and integrated microfluidic chip (Figure 4.2), we amplify and detect the β2-microglobulin (β2M) gene from buccal cells collected from cheek swabs. Buccal swabs are a convenient source of genomic DNA for non-invasive genotyping, as they are safer and easier to obtain than blood, and human saliva is generally less pathogenic than human blood. Thus, chip-based genotyping of buccal cells enables cost-effective diagnostic testing and population screening. β2 microglobulin is a housekeeping gene expressed in all mammalian white blood cells. Amplification of this gene on-chip using the integrated instrument provides a proof-of-concept for a wide range of applications, including the pathogen detection. With a simple change in the primer sequences we can detect a

wide range of targets, thus demonstrating the broad applicability of this system.

Successful SP and amplification in quadruplate (runs 1–4) is demonstrated and shown in Figure 4.5. The PCR primer and product peaks are observed at $\approx$100 s and $\approx$140 s respectively. Each sample was analysed electrophoretically at least twice and we found the second run to slightly more consistent in arrival times. By comparing the electrophoretic mobilities extracted from the second run of each product with those of the size standard (data not shown), we obtained a size of 230 ± 20 bp. We would have been able to make more accurate measurements of the size if we had performed an electrophoretic analysis of a sample of the size standard mixed with the PCR product, especially if separated over a longer distance. However, in the present work we have attempted to size from timing alone, thereby simplifying the analysis. We suspect that most of the uncertainty arises from variations in reagent concentration from the manual loading of the chip.

The results obtained by the on-chip SP-PCR/CE were successfully verified with tube-based SP, followed by PCR amplification on a bench-top PCR system, and analysis on a commercial microchip CE instrument (the μTK, Micralyne, Edmonton, Alberta) using a similar microfluidic chip under the same electrophoretic conditions. This inidcates that on-chip processing results are comparable to those obtained with conventional bench-top systems. A third weak peak is typically seen at approximately 180 s, likely indicating non-specific amplification – i.e. that the PCR could be optimised further. Since the third peak was also seen in the off-chip reference runs this is not a chip-related issue.

We performed several negative control runs to confirm an absence of contamination from the chips, reagents and laboratory environment. For the first control, we skipped the SP step and performed on-chip PCR/CE, replacing the sample/beads in the PCR mix with PCR-grade water. This control ensures that no contamination was introduced during microchip fabrication or reagent pipetting, and was found to be negative (Figure 4.5). As a second set of control runs, we performed the entire on-chip SP, amplification and analysis process without including buccal cells in the SP lysate mix (water replaces the lysate buffer and buccal cell volume as detailed in Section 4.2.7). As seen in Figure 4.5, no PCR product was generated in the absence of buccal cells, indicating our on-chip SP-PCR/CE technique and its associated reagents, including the magnetic beads, do not introduce contamination.

4.3.1 Variability and Limit of Detection

The PCR/CE component of this system is detailed in our earlier report [30] and the CE component of that system was found to have a limit of detection of 6 pg/μL of end-labelled primer DNA. As a first-order approximation, we would expect to see the same total fluorescence signal split between the primer peak and the product peak. In practice, the total fluorescence signal in that work varied by a factor of 1.5 from minimum to maximum (this variation was attributed to slight variations in operator handling of the reagents). After normalization of the product peak by the primer peak (to account for handling variations), the PCR yield varied by as much as a factor of 3 from minimum to maximum. This variation was attributed to variations in surface passivation in the high surface area to volume devices (this phenomenon is under investigation).

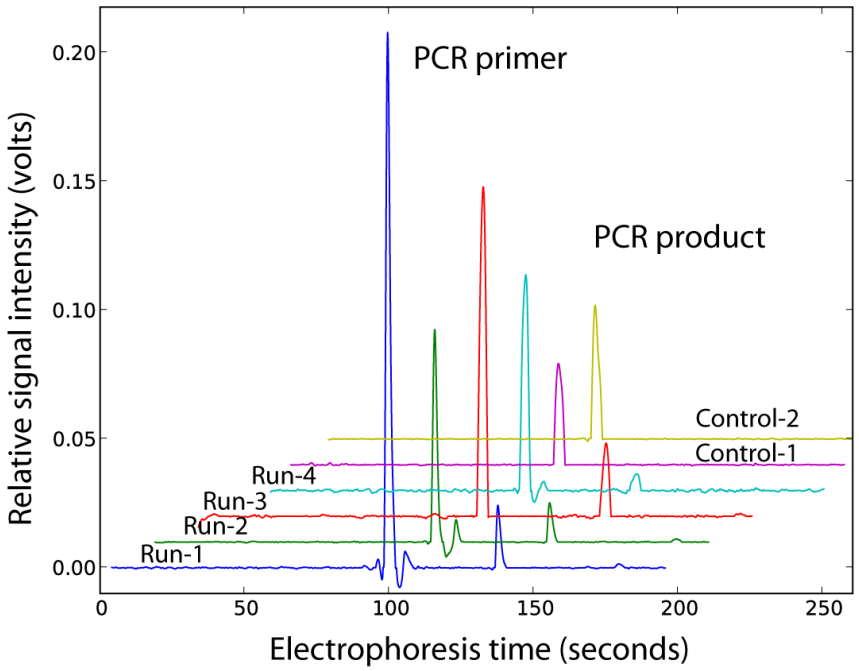

Figure 4.5: In a single microchip we isolate genomic DNA from buccal cells using magnetic beads, perform PCR, and visualize the β2M product using LIF based capillary electrophoresis. This electropherogram (time vs. fluorescence signal in volts) demonstrates the successful result of this process. Four consecutive SP-PCR-CE runs are performed to demonstrate repeatability. Representative traces from our negative controls are included to demonstrate the PCR product peak signal is from the buccal cells and not contamination. On occasion, a brief decrease in the processed signal intensity (i.e. a dip) is seen just after the arrival of the primer peak. These are artifacts of the signal processing and do not affect the limit of detection.

The present system has the same detection system and hence the same limit of detection. The PCR product peak intensities (Figure 4.5) for the SP-PCR/CE runs are 0.024 V, 0.015 V, 0.028 V, and 0.016 V, with signal-to-noise ratios (SNR) of 154, 152, 56, and 53, respectively. The SNR is defined here as the ratio of the peak amplitude to the standard deviation of the noise in the signal (calculated using the first 50 s of the processed data from the CE separation phase).

However, the total fluorescence signal varies by a factor of 2.5 from minimum to maximum – a variation that is significantly larger than in previous work, likely reflecting a combination of there being more operator handling in the additional SP. However, we cannot, at present, rule out a chip-to-chip variability in the amount of collected light coupled into the CE microchannel. Given that the PCR yield varied by as much as a factor of 3 after normalization, similar to that seen in previous work, the PCR yield does not appear to have been adversely affected by the addition of the SP stage.

The focus of this demonstration is the integration of several processes onto a single microchip and instrument, in a manner that allows for both integration and flexibility in the choice of the protocol used. Future work will explore techniques to improve run-to-run and chip-to-chip variability through improved surface passivation and chip design. Our present chip is the size of a microscope slide for convenient handling. Except for the volume of the PCR chamber, the chip could readily be scaled to far smaller sizes or have many more tests on board. In past work, the 600 nL PCR volume was chosen to be large enough so that statistical effects do not play a role for typical concentrations of viruses in PCR-CE done without SP (e.g. [27]). Past work with this design (without SP) would have been problematic with low-concentration samples. However, one of the most powerful features of bead-based SP is that the beads can convey large amounts of DNA (well beyond statistical levels) even from dilute samples. As a result, PCR volumes are no longer constrained so that this integrated SP-PCR-CE chip design can now be greatly reduced in size.

4.4 Conclusion

Challenges associated with the processing of raw samples have limited the use of LOC systems in molecular diagnostic settings. To analyze samples, we demonstrate a magnetic bead-based nucleic acid purification technique requiring simple and inexpensive instrumentation, and its integration with PCR amplification and analysis/detection via capillary electrophoresis using a compact photodiode-based optical detection module. The SP module is integrated in our shoe-box size instrument and performs bead manipulation without the need for complex fluid manipulation, reducing the potential for sample handling errors.

The SP module can be used for a wide range of applications. Although we have purified nucleic acids from buccal cell swabs, there are commercially available beads for isolating DNA and RNA from a wide range of biological sources, including yeast, bacteria, human tissues, plants, and forensic samples. In addition to nucleic acid isolation, magnetic bead-based collection can be used to concentrate DNA and RNA in nanoliter volumes for subsequent transfer to microscale reservoirs within the microchip for molecular testing. This strategy can enable the analysis of large sample volumes with analytes or cells at low concentration, a situation that is otherwise incompatible with microscale testing.

We believe that such an automated LOC approach for raw sample analysis would reduce the variability associated with inter-run and inter-patient analysis inherent to manual processing of samples. We are also exploring various surface passivation techniques on glass (or an alternate reduced-charge surfaces) to reduce

the interactions of the nucleic acids with the microfabricated surfaces of the chip.

This integration of sample purification, PCR, and CE allows for direct molecular analysis of a patient sample within a single LOC microfluidic device. The present system was designed for modularity such that SP, PCR and CE can be optimised and run separately, or operated in an integrated fashion with limited manual support (i.e. the use of a micropipetter). Having established the optimal protocol for the integrated system, we are developing a more complex microvalving system for performing the same operations in a manner that requires minimal operator intervention. Moreover, since the present system is scalable to smaller sizes (or larger numbers of samples), and since it is readily adapted to a wide range of molecular biology protocols, we believe that it could form the basis for many LOC applications. We believe that this low-cost ($\approx$\$1000), integrated and portable LOC toolkit may facilitate high-throughput diagnostic testing, and represents a significant advancement in the use of LOC for diagnostics.

Bibliography

[1] P. Yager, T. Edwards, E. Fu, K. Helton, K. Nelson, M. R. Tam, and B. H. Weigl, "Microfluidic diagnostic technologies for global public health." *Nature*, vol. 442, no. 7101, p. 412, 2006.

[2] R. Mariella, "Sample preparation: the weak link in microfluidics-based biodetection," *Biomedical Microdevices*, vol. 10, no. 6, pp. 777–784, 2008.

[3] M. G. Roper, C. J. Easley, and J. P. Landers, "Advances in polymerase chain reaction on microfludic chips," *Analytical Chemistry*, vol. 77, pp. 3887–3894, 2005.

[4] M. A. Dineva, L. Mahilum-Tapay, and H. Lee, "Sample preparation: a challenge in the development of point-of-care nucleic acid-based assays for resource-limited settings," *The Analyst*, vol. 132, no. 12, pp. 1193–1199, 2007. [Online]. Available: http://dx.doi.org/10.1039/b705672a

[5] A. Akane, K. Matsubara, H. Nakamura, S. Takahashi, and K. Kimura, "Identification of the Heme Compound copurified with Deoxyribonucleic-Acid (DNA) from Bloodstains, a Major Inhibitor of Polymerase Chain-Reaction (PCR) Amplification," *Journal of Forensic Sciences*, vol. 39, no. 2, pp. 362–372, MAR 1994.

[6] J. Sambrook, E. Fritsch, and T. Maniatis, *Molecular cloning: a laboratory manual*. New York, USA: Cold Spring Harbor Laboratory Press, 1989.

[7] S. C. Tan and B. C. Yiap, "DNA, RNA, and Protein Extraction: The Past and The Present," *Journal of Biomedicine and Biotechnology*, 2009.

[8] E. Verpoorte, "Microfluidic chips for clinical and forensic analysis," *Elec-*

trophoresis, vol. 23, no. 5, pp. 677–712, 2002.

[9] M. Zourob, S. Elwary, and A. P. F. Turner, Eds., *Principles of Bacterial Detection: Biosensors, Recognition Receptors and Microsystems*. Springer, 2008, ch. 30.

[10] D. Brennan, J. Justice, B. Corbett, T. McCarthy, and P. Galvin, "Emerging optofluidic technologies for point-of-care genetic analysis systems: a review," *Analytical and Bioanalytical Chemistry*, vol. 395, no. 3, pp. 621–636, OCT 2009.

[11] L. Chen, A. Manz, and P. J. R. Day, "Total nucleic acid analysis integrated on microfluidic devices," *Lab on a Chip*, vol. 7, no. 11, pp. 1413–1423, 2007.

[12] M. G. Dobson, P. Galvin, and D. E. Barton, "Emerging technologies for point-of-care genetic testing," *Expert Review of Molecular Diagnostics*, vol. 7, no. 4, pp. 359–370, JUL 2007.

[13] J. Kim, M. Johnson, P. Hill, and B. K. Gale, "Microfluidic sample preparation: cell lysis and nucleic acid purification," *Integrative Biology*, vol. 1, no. 10, pp. 574–586, 2009.

[14] T. Baier, T. E. Hansen-Hagge, R. Gransee, A. Crombe, S. Schmahl, C. Paulus, K. S. Drese, H. Keegan, C. Martin, J. J. O'Leary, L. Furuberg, L. Solli, P. Gronn, I. M. Falang, A. Karlgard, A. Gulliksen, and F. Karlsen, "Hands-free sample preparation platform for nucleic acid analysis," *Lab on a Chip*, vol. 9, no. 23, pp. 3399–3405, 2009.

[15] M. Mahalanabis, H. Al-Muayad, M. D. Kulinski, D. Altman, and C. M. Klapperich, "Cell lysis and DNA extraction of gram-positive and gram-negative bacteria from whole blood in a disposable microfluidic chip," *Lab on a Chip*, vol. 9, no. 19, pp. 2811–2817, 2009.

[16] G. R. M. Duarte, C. W. Price, J. L. Littlewood, D. M. Haverstick, J. P. Ferrance, E. Carrilho, and J. P. Landers, "Characterization of dynamic solid phase DNA extraction from blood with magnetically controlled silica beads," *Analyst*, vol. 135, no. 3, pp. 531–537, 2010.

[17] K.-Y. Lien, C.-J. Liu, P.-L. Kuo, and G.-B. Lee, "Microfluidic System for Detection of alpha-Thalassemia-1 Deletion Using Saliva Samples," *Analytical Chemistry*, vol. 81, no. 11, pp. 4502–4509, JUN 1 2009.

[18] Z. Hua, J. L. Rouse, A. E. Eckhardt, V. Srinivasan, V. K. Pamula, W. A. Schell, J. L. Benton, T. G. Mitchell, and M. G. Pollack, "Multiplexed Real-Time Polymerase Chain Reaction on a Digital Microfluidic Platform," *Analytical Chemistry*, vol. 82, no. 6, pp. 2310–2316, MAR 15 2010.

[19] D. L. House, C. H. Chon, C. B. Creech, E. P. Skaar, and D. Li, "Miniature on-chip detection of unpurified methicillin-resistant Staphylococcus aureus (MRSA) DNA using real-time PCR," *Journal of Biotechnology*, vol. 146, no. 3, pp. 93–99, APR 1 2010.

[20] C. J. Easley, J. M. Karlinsey, J. M. Bienvenue, L. A. Legendre, M. G. Roper, S. H. Feldman, M. A. Hughes, E. L. Hewlett, T. J. Merkel, J. P. Ferrance, and J. P. Landers, "A fully integrated microfluidic genetic analysis system with sample-in-answer-out capability," *Proceedings of the National Academy of Sciences of the United States of America*, vol. 103, no. 51, pp. 19 272–19 277, DEC 19 2006.

[21] J. M. Bienvenue, L. A. Legendre, J. P. Ferrance, and J. P. Landers, "An integrated microfluidic device for DNA purification and PCR amplification of STR fragments," *Forensic Science International: Genetics*, vol. 4, no. 3, pp. 178–186, APR 2010.

[22] C. Lui, N. C. Cady, and C. A. Batt, "Nucleic Acid-based Detection of Bacterial Pathogens Using Integrated Microfluidic Platform Systems," *Sensors*, vol. 9, no. 5, pp. 3713–3744, MAY 2009.

[23] E. Lagally, J. Scherer, R. Blazej, N. Toriello, B. Diep, M. Ramchandani, G. Sensabaugh, L. Riley, and R. Mathies, "Integrated portable genetic analysis microsystem for pathogen/infectious disease detection," *Analytical Chemistry*, vol. 76, no. 11, pp. 3162–3170, JUN 1 2004.

[24] P. Liu, T. S. Seo, N. Beyor, K.-J. Shin, J. R. Scherer, and R. A. Mathies,

"Integrated portable polymerase chain reaction-capillary electrophoresis microsystem for rapid forensic short tandem repeat typing," *Analytical Chemistry*, vol. 79, no. 5, pp. 1881–1889, MAR 1 2007.

[25] N. M. Toriello, E. S. Douglas, N. Thaitrong, S. C. Hsiao, M. B. Francis, C. R. Bertozzi, and R. A. Mathies, "Integrated microfluidic bioprocessor for single-cell gene expression analysis," *Proceedings of the National Academy of Sciences of the United States of America*, vol. 105, no. 51, pp. 20 173–20 178, 2008.

[26] G. V. Kaigala, V. N. Hoang, A. Stickel, J. Lauzon, D. Manage, L. M. Pilarski, and C. J. Backhouse, "An inexpensive and portable microchip-based platform for integrated RT-PCR and capillary electrophoresis," *Analyst*, vol. 133, no. 3, pp. 331–338, 2008.

[27] G. V. Kaigala, R. J. Huskins, J. Preiksaitis, X.-L. Pang, L. M. Pilarski, and C. J. Backhouse, "Automated screening using microfluidic chip-based PCR and product detection to assess risk of BK virus-associated nephropathy in renal transplant recipients," *Electrophoresis*, vol. 27, no. 19, pp. 3753–3763, 2006.

[28] J. VanDijken, G. V. Kaigala, J. Lauzon, A. Atrazhev, S. Adamia, B. J. Taylor, T. Reiman, A. R. Belch, C. J. Backhouse, and L. M. Pilarski, "Microfiuidic chips for detecting the t(4;14) translocation and monitoring disease during treatment using reverse transcriptase-polymerase chain reaction analysis of IgH-MMSET hybrid transcripts," *Journal of Molecular Diagnostics*, vol. 9, no. 3, pp. 358–367, JUL 2007.

[29] J. Chowdhury, G. V. Kagiala, S. Pushpakom, J. Lauzon, A. Makin, A. Atrazhev, A. Stickel, W. G. Newman, C. J. Backhouse, and L. M. Pilarski, "Microfluidic platform for single nucleotide polymorphism genotyping of the thiopurine S-methyltransferase gene to evaluate risk for adverse drug events," *Journal of Molecular Diagnostics*, vol. 9, no. 4, pp. 521–529, SEP 2007.

[30] G. V. Kaigala, M. Behnam, A. C. E. Bidulock, C. Bargen, R. W. Johnstone, D. G. Elliott, and C. J. Backhouse, "A scalable and modular lab-on-a-chip

genetic analysis instrument," *The Analyst*, vol. 135, no. 7, pp. 1606–1617, 2010. [Online]. Available: {http://dx.doi.org/10.1039/b925111a}

[31] B. J. Taylor, K. A. Martin, R. Samuel, M. Nielsen, H. J. Crabtree, M. Behnam, C. J. Backhouse, L. M. Pilarski, and S. K. Yanow, "Extraction of Plasmodium falciparum DNA using magnetic beads and a simple lab-on-a-chip sample preparation module," *BioTechnique*, vol. Submitted, 2010.

[32] C. Jegat, A. Bois, and M. Camps, "Continuous phase viscosity influence on maximum diameters of poly(styrene-divinylbenzene) beads prepared by suspension polymerization," *Journal of Polymer Science, Part B: Polymer Physics*, vol. 39, no. 2, pp. 201–210, JAN 15 2001.

Chapter 5

An Integrated CMOS High Voltage Supply for Lab-on-a-Chip Systems

This chapter is based on a manuscript published in the Lab on a Chip Journal. The dramatic development of the computer and consumer electronics field has been attributed to the ability to mass produce integrated circuits by means of microfabrication technologies. This integrated circuit fabrication technology offers advantages such as high reproducibility, small size, low power, and extremely low fabrication cost in mass production, all of which are well-suited for inexpensive and miniaturized lab-on-a-chip instruments. In this demonstration, we illustrate the possibility of using this technology for miniaturizing one of the main components for capillary electrophoresis (i.e. high voltage generation and switching). As the lead author, in addition to being part of the microelectronic chip design group, my roles in this demonstration were: designing and building the instrument (i.e. hardware including testing and debugging), calibration, and experiment design and execution.

Preface

Electrophoresis is a mainstay of lab-on-a-chip (LOC) implementations of molecular biology procedures and is the basis of many medical diagnostics. High voltage

---

A version of this chapter has been published. Behnam *et al.* 2008. Lab on a Chip. 8. 524-1529.

(HV) power supplies are necessary in electrophoresis instruments and are a significant part of the overall system cost. This cost of instrumentation is a significant impediment to making LOC technologies more widely available. We believe one approach to overcoming this problem is to use microelectronic technology (complementary metal-oxide semiconductor, CMOS) to generate and control the HV. We present a CMOS-based chip (3 mm $\times$ 2.9 mm) that generates high voltages (hundreds of volts), switches HV outputs, and is powered by a 5 V input supply (total power of 28 mW) while being controlled using a standard computer serial interface. Microchip electrophoresis with laser induced fluorescence (LIF) detection is implemented using this HV CMOS chip. With the other advancements made in the LOC community (e.g. micro-fluidic and optical devices), these CMOS chips may ultimately enable true LOC solutions where essentially all the microfluidics, photonics and electronics are on a single chip.

5.1 Introduction

Despite progress in lab on a chip (LOC) systems, the cost effectiveness, ease of manufacturability and portability of the external instrumentation remains largely unaddressed [1]. Microfluidic chips have been demonstrated in a wide range of medical diagnostic applications, from genetic profiling and diagnosis [2] to disease monitoring [3], but this has been done in conjunction with expensive and large instruments. To realize a truly portable LOC system it is necessary to replace this external infrastructure while simultaneously reducing cost, size and power consumption. Capillary electrophoresis (CE), a key LOC technology, has important medical applications but typically requires high voltage (HV) power supplies, optics, and

interface circuits that limit portability and hinder the development of a LOC-based point-of-care tool. Several advancements in the integration and cost-effectiveness of optical detection on microfluidic chips [4, 5] have been made and many photonic components have been ported to microelectronic chips [6], yet so far, little has been achieved in miniaturizing HV components. Much of the infrastructure needed for CE is for the high voltage sub-system, consisting of high voltage generation and control, switching and interfacing. We recently demonstrated [4] a $1000 genetic analysis tool that implements CE and is an advancement in portability and cost-effectiveness. In that system, the HV subsystem accounts for almost 50% of the system cost and most of its size. In a more general context, HV components are central to the operation of many micro-electro-mechanical system (MEMS) devices in addition to CE systems, yet there are no demonstrations of truly miniaturized HV sub-systems.

In terms of electrophoresis, there are presently several benchtop electrophoresis platforms such as the ABI PRISM 3100 (Applied Biosystems, Foster City, CA, USA), Agilent 2100 Bioanalyzer (Agilent Technologies, SantaClara,CA, USA), and the Microfluidic Tool Kit (μTK, Micralyne Inc., Edmonton, AB, Canada). These systems are based on relatively large external high-voltage power supplies (and relays) requiring complex control/interface hardware and software, thus are not suitable as portable systems. In recent reports relating to HV subsystems for CE [7, 8, 9, 10], the required HV is generated using either one or multiple off-the-shelf DC–DC converters (e.g. a widely used commercial component made by EMCO, Sutter Creek, CA), and switching is performed either by manual switches or electro-mechanical relays assembled on printed circuit boards (PCBs). Often,

to also ensure electrical isolation, multiple circuit boards are used, one for the HV components, and the other for the control circuitry – this further increases size. Additionally, the interface and communication with these components adds to complexity and cost. Recent developments involving HV sub-systems include: Jackson *et al.* [7] incorporated a DC–DC converter into a CE system with electrochemical detection. In another demonstration, Kappes *et al.* [10], presented a battery powered CE system that could generate up to 30 kV with amperometric, potentiometric and conductiometric detection. Similarly, Garcia *et al.* [9] built a battery operated 3-channel HV supply (with 3 DC–DC converters). Erickson *et al.* [11] introduced a single HV module that generates up to 700 V, but provides only a single channel (i.e. a single DC–DC converter) with manual switching. In a related demonstration, to achieve HV precisely, Collins *et al.* [12] presented a resistor divider network to vary the generated voltages, based on the use of a DC–DC converter. One of the first demonstrations of a portable CE system was by Sandia laboratories [8], in work that miniaturized the entire CE system (with DC–DC supplies and relays) and is directed towards protein separations. A particularly impressive and optimized HV module reported recently by Jiang *et al.* [13] demonstrated a HV sub-system that is powered froma universal serial bus (USB) port. In that work multiple DC–DC converters with multiple control circuit boards were used.

Although the development of the LOC technologies, including the above work in HV sub-systems, has been impressive, there have been no reports to date of a HV sub-system that is compatible with a very inexpensive, portable and highly integrated diagnostic. Our goal is ultimately to build true LOC diagnostic instruments consisting, almost entirely, of a single (or several) chips. In order to do this, there

is a need to realize an integrated HV sub-system (i.e. a single module that could generate and control high voltages) that is inexpensive and highly compact – to our knowledge there have been no prior demonstrations of such sub-systems.

In the present work, we demonstrate a single-chip HV subsystem that generates, controls, and distributes HV potentials, and interfaces with an external controlling device (a laptop computer). This chip is designed and fabricated with a mixed high/low voltage microfabrication process. Because of the mixed high/low voltage devices, both low voltage and high voltage components are integrated in a single chip. The low voltage (high density) electronics provides an interface capability over a serial link to a personal computer, while the high voltage (lower density) electronics interfaces directly to the microfluidic chip. As a result, one serial link (with power delivery capability, such as USB) can be used to power and control this chip. Eight independent HV outputs are provided in the design, which facilitates the implementation of wide range of CE protocols. Rapid switching capability (in the range of several kHz), coupled with longevity, is achieved by replacing the commonly used mechanical relays with solid-state HV switched-output circuits, integrated on the complementary metal-oxide semiconductor (CMOS) chip. In addition to the CMOS chip, only a few external discrete components such as capacitors and a single inductor and diode are required to perform a complete CE functionality (Figure 5.2b). Thus, the small footprint ($\approx$ 3mm $\times$ 2.9 mm) of the chip itself and its low power consumption (28 mW) make this module highly suitable for portable and manufacturable LOC solutions. To the best of our knowledge, this is the first demonstration of a microelectronic chip-based LOC HV subsystem.

5.2 System Description

To demonstrate the functionality of the HV CMOS chip for CE we replace the HV module in our earlier demonstration [4] with the present microelectronic chip. As shown in Figure 5.1, the system uses a CCD camera, a filter (not shown), a lens and a solid state laser for fluorescence detection. Although the HV CMOS chip could be interfaced through any serial interface, it was convenient to use a microcontroller (PIC 16F877, MicrochipTechnology Inc., Chandler, AZ, USA) to perform the USB to serial peripheral interface, SPI (a standardized communication protocol) conversion. Although both SPI and USB interfaces are serial in nature, the latter is far more complex and would require a very considerable amount of additional CMOS design. Such USB interfaces are commonly implemented in silicon and are not the focus of this work.

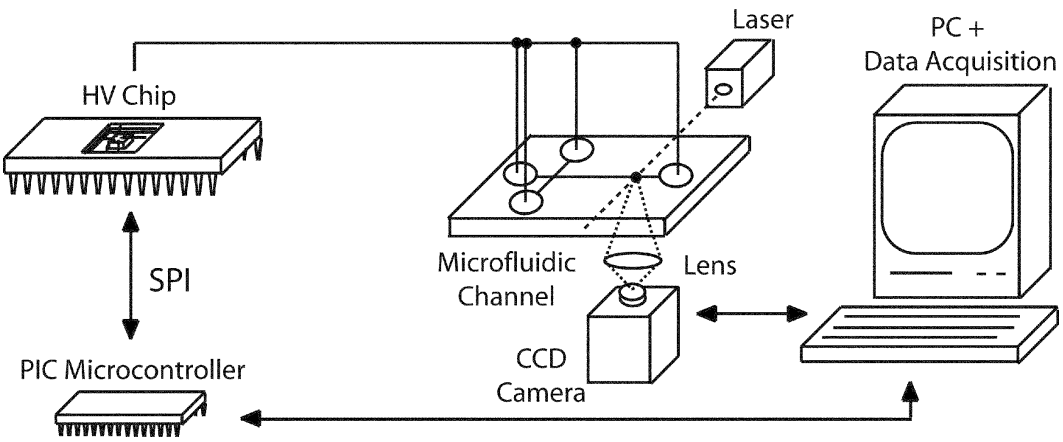

Figure 5.1: System level block diagram of the set-up to perform microchip electrophoresis.

5.2.1 CMOS Chip

This HV chip (Figure 5.2a) was designed with the Cadence integrated circuit design tools (Cadence Design Systems Inc., CA, USA) and fabrication was performed using DALSA Semiconductors (Bromont, QC, Canada) three metal layer, triple well, dual gate oxide 0.8 μm 5 V HV CMOS/DMOS (double diffused MOS) process. This process supports both the HV circuitry, along with the low-voltage circuitry (5 V) for digital logic control and communication. From a functionality standpoint, this chip consists of three main units (Figure 5.2c): (a) DC–DC boost converter that generates the required voltage, (b) eight independently controlled HV switched-outputs that are coupled to the microfluidic chip and, (c) communication and control interface (CCI) that controls and monitors the operation of the chip.

5.2.1.1 DC–DC Boost Converter

A common non-isolated inductive DC–DC boost converter is implemented in CMOS to generate up to 150 V using a 5 V input supply. The operating principle of this is detailed in [14, 15]. Briefly, the implementation involves storing energy on an inductor from the 5 V supply and periodically breaking the current flow. By doing so, the inductor opposes any changes (a decrease in this case) in current by reversing its potential and inducing high electric potential across its terminals, briefly supplying current at high voltage through a diode to the HV supply capacitor. This HV supply is programmable via the serial interface, with an internal voltage comparator shutting down the boost converter when the supply reaches the set point specified by a digital to analog converter (DAC) (all of these function integrated on chip). This closed loop control mechanism has a resolution of less than 2 V at the output.

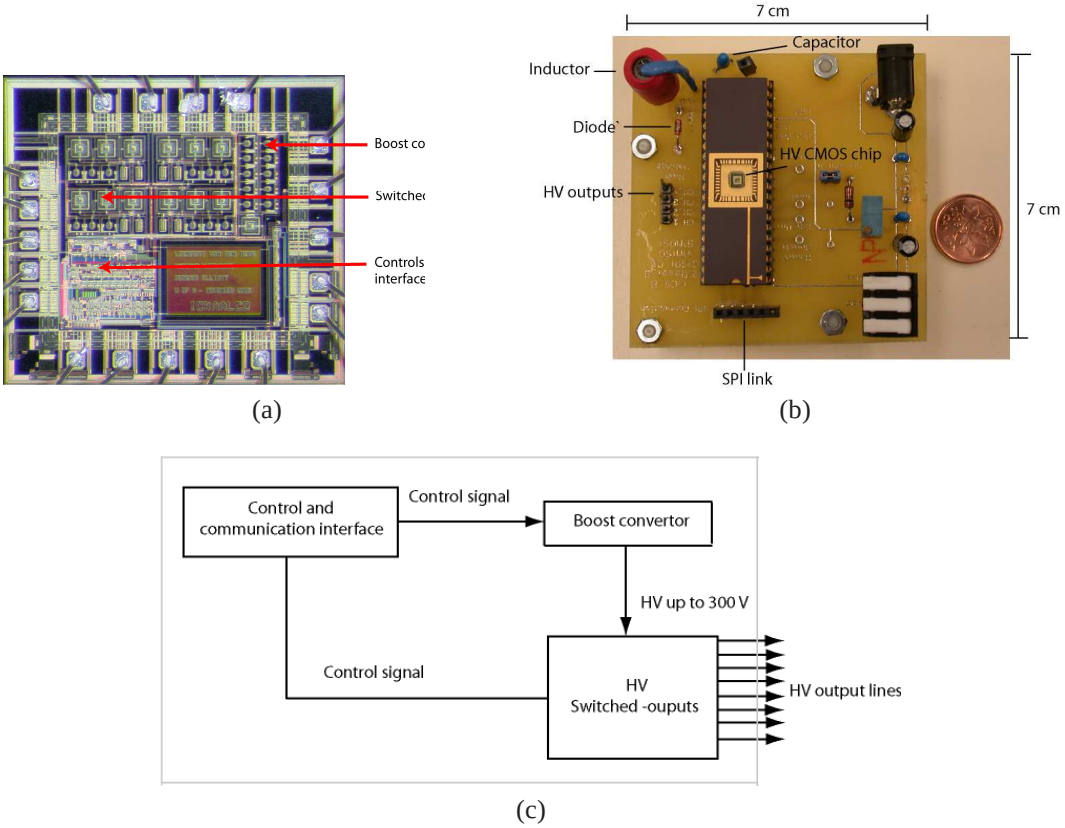

Figure 5.2: (a) Photograph one of our HV CMOS CE chips – we are developing several variations of this HV microelectronic chip. (b) The printed circuit board (7 cm $\times$ 7 cm) for hosting the HV CMOS chip. This board can readily be shrunk by compact placement of components and smaller footprint components. To operate this HV CMOS chip, in addition to the CMOS chip an inductor, a capacitor and a diode is used. (c) High voltage switched-output design, providing 8 HV outputs.

Further details can be found in [16, 17].

5.2.1.2 HV Switched-output Circuit

The CCI circuitry controls the HV transistors, which drive the eight HV 300 V tolerant outputs, with each output separately controlled. Five of these outputs can be driven to the positive supply voltage (e.g. 150 or 300 V), ground (0 V) or discon-

nected (alternatively described as open circuit, float, high impedance or tri-state). To reduce the number of HV-transistors, three of the outputs can only be driven to ground or disconnected. The HV outputs are coupled to the microfluidic chip wells by platinum electrodes (Figure 5.1).

5.2.1.3 Communication and control

Communication between the HV CMOS chip and a microcontroller (or any other control system such as a computer) is via a standard serial interface protocol (SPI). The communication and control interface decodes the SPI commands sent by the microcontroller using standard logic. These commands set and control the on-chip high-voltage supply output, as well as the state of the HV outputs.

5.3 Electrophoresis

5.3.1 Electrophoresis System

The optical set-up is based on a CCD camera detection much as described in [4]. A 5 mW commercial red laser (635 nm, M635-5, U.S. Lasers Inc., Baldwin Park, CA, USA) is used for excitation of the fluorophores. The emitted fluorescence is focused on a CCD detector (Meade Instrument Corporation, Irvine, CA, USA) by a 15 mm lens (MGF2TS, Edmund Optics Inc., Barrington, NJ, USA) through an interference filter (D750/100 m, Chroma Technology Corp., Rockingham, VT, USA) that prevents the excitation light (from the laser) from reaching the detector. Data acquisition software (running on a computer) captures and stores a sequential set of images taken during the electrophoresis run. This set of images is processed

by custom-developed software to determine the intensity of the fluorescence. The analysed data is then plotted against time, producing an electropherogram (graph of fluorescence intensity vs. time) as shown in Figure 5.4a.

5.3.2 Electrophoresis Protocol

Prior to the usage of the microfluidic chip (Figure 5.3a), pre-treatment of the channel surface is performed using a commercial dynamic coating (Gel Co., San Francisco, CA, USA) solution. The channel is then filled with 4% linear polyacrylamide (LPA) that is prepared by mixing 900 μL of water with 100 μL 10$\times$TTE [18] (Tris TAPS EDTA) and 400 mg of 10% LPA (Polysciences, Inc, Warington, PA (Cat # 19901, MW 600 000–1 000 000). TTE buffer was prepared from 0.01 mM EDTA (ethylenediaminetetraacetic acid, Sigma, USA), 0.5 mM TAPS ([(2-hydroxy-1,1-bis(hydroxymethyl)ethyl)amino]-1-propanesulfonic acid, N-[tris(hydroxymethyl)methyl]-3-aminopropanesulfonic acid, Sigma, USA) and 0.5 mMTris (tris(hydroxymethyl) aminomethane, Fisher Scientific, Canada). The buffer well, sample waste well, and buffer waste well are then filled with 3.0 μL 1$\times$TTE buffer solution while the sample inlet well (where the DNA to be separated is included) is filled with 0.3 μL of 1$\times$TTE, 1 μL sample (ALFExpress™Sizer™, 50-500 base pair sizer, Amersham Bioscience, Piscataway, NJ, USA and labelled with DyeAmidite 667 (Cy-5) dye that has a maximum excitation wavelength of 646 nm and maximum emission wavelength of 664 nm) and 1 μL distilled water. We adapted and optimized the CE protocols for adequate performance at short distance detection (e.g. 13 mm from the intersection). The protocol is detailed elsewhere [4].

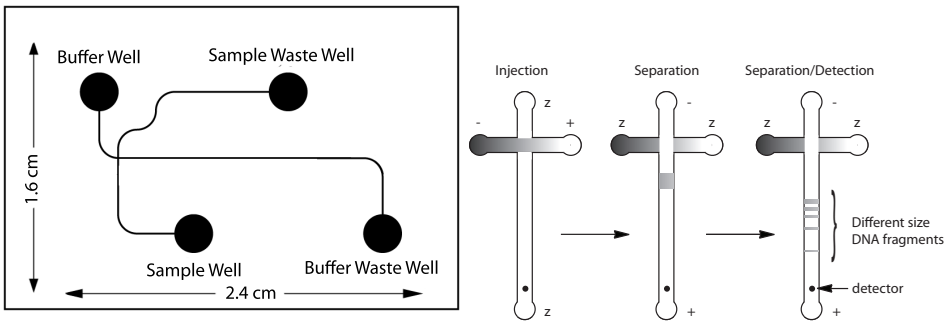

(a) (b)

Figure 5.3: (a) Glass–glass CE chip with separation channel length of 21mm and optical detection performed at 13 mm from the intersection of the two channels (b) During the injection stage of CE, positive HV is applied to the sample waste well, with a ground state applied to the sample well and a floating state (high impedance) to both buffer well and buffer waste well. Injection is performed for 120 s. During separation, positive HV is applied to the buffer waste well for 180 s while the buffer well is set to ground and the sample well and sample waste well are set to a floating state – thus producing electrophoretic migration of DNA.

5.4 Results and Discussion

5.4.1 Electrical Characterisation

The integrated DC–DC boost converter supplies 150 V to the outputs at up to 15 μA. A leakage path in an internal rectifier diode limits the HV supply to 150 V. This limitation has been corrected in the next integrated circuit design, now being manufactured. The remaining functionality of the HV chip, including the switched output, internal comparator, and control circuitries were all demonstrated successfully up to 300 V (using an external power supply). In the present work, we perform electrophoresis with 150 V applied, corresponding to electric fields of 71.4 V/cm. The output voltage ripple is measured to be $\approx$ 0.8 V using a digital oscilloscope (MSO6034 A, Agilent Technologies, Santa Clara, CA, USA) for a 10MΩ load (further details can be found in Table 5.1). The electrical resistance of the CE channel

filled with 4% LPA is approximately 100 MΩ, and hence, the output voltage ripple in practice will be lower than 0.1 V, since the output voltage ripple is inversely proportional to the load.

Table 5.1: Switched-output circuit measurements for up to 300V (driving a 52 pF || 10 MΩ load).

Parameter	*Measured*	*Unit*
Rise time (10%–90%)	9.99	μs
Fall time (10%–90%)	5.82	μs
Slew rate (rising)	24.00	V/μs
Slew rate (falling)	42.00	V/μs
Min operating voltage	5.0	V
Source current (@VOH = 299 V)	149.9	μA
Sink current (@VOL = 1 V)	-387.6	μA

For certain applications, such as field inversion electrophoresis [19], switching of the HV outputs at up to 1 kHz is necessary. Commonly used mechanical relays have an operation life on the order of 10^6 switching cycles. Therefore, when they are rapidly switched the mean time to failure as per the lifetime specification is about 20 minutes. Hence, for such applications, solid-state switches are necessary–such as the ones integrated in our HV CMOS chip. The measured HV output combined rise time plus fall time is 16.45 μs, far exceeding the requirements for 1 kHz switching, thus demonstrating the applicability of this HV CMOS chip for CE variants such as field inversion.

5.4.2 CE Experiment

The HV CMOS chip is used to perform CE with the set-up in Figure 5.1 with a standard injection–separation electrophoresis procedure to analyse fragments of end-labelled DNA. Using the same microfluidic chip, comparable performance (peak arrival times of the DNA fragments) was the present chip-based CE system (Figure 5.1) as with a commercial confocal-based CE system, the μTK (manufactured by Micralyne, Edmonton, Canada). Additionally, we adapted our CE protocols to achieve short distance electrophoresis (21 mm long channel and 150 V) to realize comparable performance (resolution in separation of the DNA fragments) to our earlier demonstrations using a 95 mm long chip and 6 kV [20]. In our earlier CE-based diagnostics we typically detected the presence or absence of a fragment of DNA (signifying the presence or absence of the genetic sequence or pathogen) in the size range of 200 bps to 300 bps [20], hence, here we evaluate the fragment resolution of the electropherograms in this particular range. Using the approach in [21], the resolution in DNA separation for this prototype system was evaluated and found to be 15 bps, which is comparable to the 12.6 bps on the commercial μTK system [4].

The signal to noise ratio (SNR) of the present system is somewhat lower than that of the commercial system and this is due to the simplified optics and CCD camera in our set-up (Figure 5.1) as compared to the expensive confocal optics in the commercial system (μTK). Although we are in the process of improving the performance of the optical detection, the present system is adequate for performing genetic analysis. Hence, the present chip enables the simple system shown in Figure 5.1, along with a CCD, a solid state laser, a lens and filter, to provide comparable

capabilities to more conventional electrophoresis instruments (Figure 5.4).

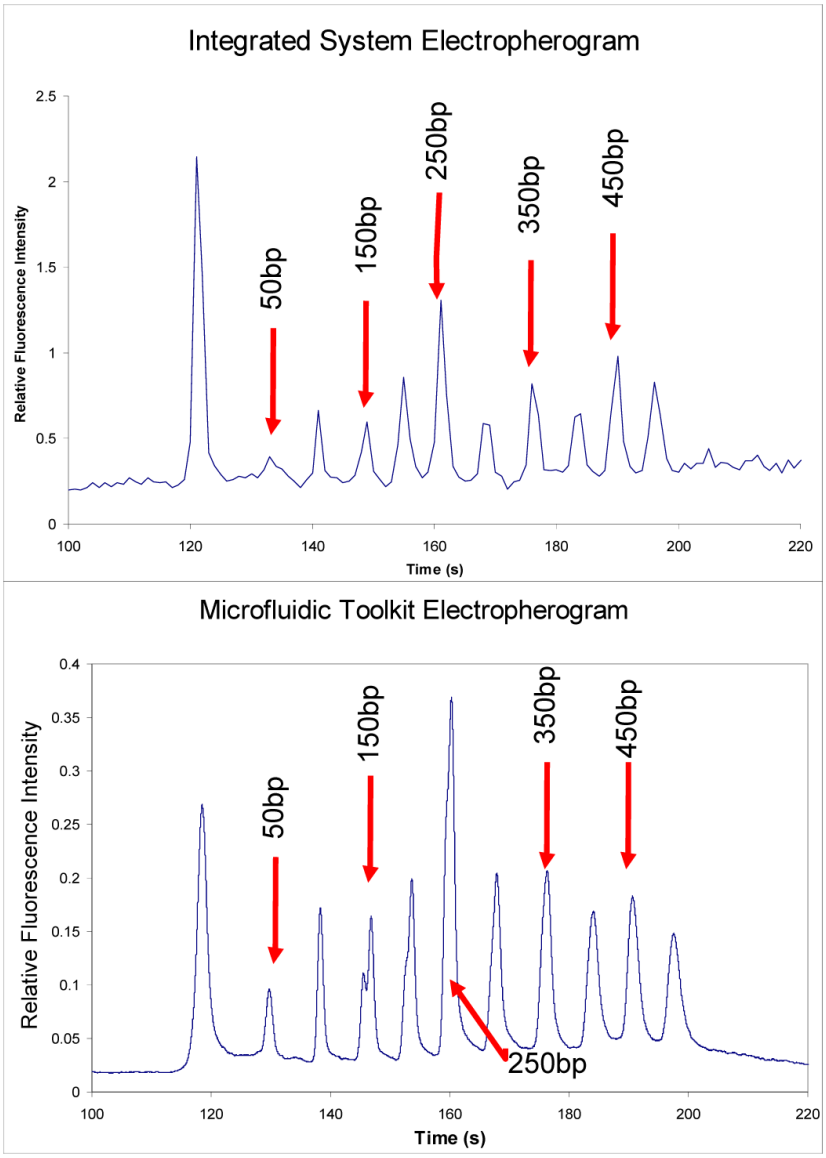

Figure 5.4: Comparison of electropherogram results between the presented design and the commercial electrophoresis equipment (μTK).

Here, we demonstrate HV generation, switching and low voltage control and interfacing using a single microelectronic chip. With this demonstration of a CMOS-

based HV sub-system, we replace the widely used DC–DC converters, relays, control and interface circuits on multiple boards with a 3 mm $\times$ 2.9 mm HV microelectronic chip. We demonstrate separation of a DNA sizer by combining this HV microelectronic chip with a microfluidic chip, and have found comparable performance with a commercial bench-top system, yet the HV chip could cost as little as $10 in mass production.

With this technology and with minimal additional cost, we expect to integrate other functionality on the CMOS chip to realize a complete CMOS-based LOC CE system. The present HV chip halves the cost of our earlier $1000 (component cost) genetic analysis system demonstration [4] by eliminating all other HV components. In the future, with the integration of other sensing technologies on CMOS silicon wafers, the cost of the entire system is expected to be below $100. We expect such manufacturable CMOS technology will greatly simplify the CE infrastructure while having a major impact on the development of LOC technologies.

Bibliography

[1] G. M. Whitesides, "The origins and the future of microfluidics," *Nature*, vol. 442, no. 7101, pp. 368–373, 2006. [Online]. Available: http://dx.doi.org/10.1038/nature05058

[2] P. Yager, T. Edwards, E. Fu, K. Helton, K. Nelson, M. R. Tam, and B. H. Weigl, "Microfluidic diagnostic technologies for global public health." *Nature*, vol. 442, no. 7101, p. 412, 2006.

[3] J. VanDijken, G. V. Kaigala, J. Lauzon, A. Atrazhev, S. Adamia, B. J. Taylor, T. Reiman, A. R. Belch, C. J. Backhouse, and L. M. Pilarski, "Microfiuidic chips for detecting the t(4;14) translocation and monitoring disease during treatment using reverse transcriptase-polymerase chain reaction analysis of IgH-MMSET hybrid transcripts," *Journal of Molecular Diagnostics*, vol. 9, no. 3, pp. 358–367, JUL 2007.

[4] G. V. Kaigala, V. N. Hoang, A. Stickel, J. Lauzon, D. Manage, L. M. Pilarski, and C. J. Backhouse, "An inexpensive and portable microchip-based platform for integrated RT-PCR and capillary electrophoresis," *Analyst*, vol. 133, no. 3, pp. 331–338, 2008.

[5] C. L. Bliss, J. N. McMullin, and C. J. Backhouse, "Rapid fabrication of a microfluidic device with integrated optical waveguides for dna fragment analysis," *Lab on a Chip*, vol. 7, no. 10, pp. 1280–1287, 2007.

[6] G. T. Roman and R. T. Kennedy, "Fully integrated microfluidic separations systems for biochemical analysis," *Journal of Chromatography A*, vol. 1168, no. 1-2, pp. 170–188, OCT 19 2007.

[7] D. Jackson, J. Naber, T. Roussel, M. Crain, K. Walsh, R. Keynton, and R. Baldwin, "Portable high-voltage power supply and electrochemical detection circuits for microchip capillary electrophoresis," *Analytical Chemistry*, vol. 75, no. 14, pp. 3643–3649, 2003.

[8] R. Renzi, J. Stamps, B. Horn, S. Ferko, V. VanderNoot, J. West, R. Crocker, B. Wiedenman, D. Yee, and J. Fruetel, "Hand-held microanalytical instrument for chip-based electrophoretic separations of proteins," *Analytical Chemistry*, vol. 77, no. 2, pp. 435–441, JAN 15 2005.

[9] C. D. García, Y. Liu, P. Anderson, and C. S. Henry, "Versatile 3-channel high-voltage power supply for microchip capillary electrophoresis," *Lab on a Chip*, vol. 3, no. 4, pp. 324–328, October 2003.

[10] T. Kappes, B. Galliker, M. Schwarz, and P. Hauser, "Portable capillary electrophoresis instrument with amperometric, potentiometric and conductometric detection," *TrAC Trends in Analytical Chemistry*, vol. 20, no. 3, pp. 133–139, MAR 2001.

[11] D. Erickson, D. Sinton, and D. Li, "A miniaturized high-voltage integrated power supply for portable microfluidic applications," *Lab on a Chip*, vol. 4, no. 2, pp. 87–90, April 2004.

[12] G. E. Collins, P. Wu, Q. Lu, J. D. Ramsey, and R. H. Bromund, "Compact, high voltage power supply for the lab-on-a-chip," *Lab on a Chip*, vol. 4, pp. 408–411, March 2004.

[13] L. Jiang, X. Jiang, Y. Lu, Z. Dai, M. Xie, J. Qin, and B. Lin, "Development of a universal serial bus-powered mini-high-voltage power supply for microchip electrophoresis," *Electrophoresis*, vol. 28, no. 8, pp. 1259–1264, 2007.

[14] N. Mohan, T. M. Undeland, and W. P. Robbins, *Power electronics converters, applications, and design*, 3rd ed. John Wiley and Sons, Inc., 2003.

[15] F. L. Luo and H. Ye, *Essential DC/DC Converters*. Boca Raton: Taylor and Francis Group, 2006.

[16] M. Behnam, “Integration of high voltage cmos and microfluidic technologies for genetic analysis systems,” Master’s thesis, University of Alberta, 2007.

[17] M. Khorasani, L. van den Berg, P. Marshall, M. Zargham, V. C. Gaudet, D. G. Elliott, and S. Martel, “Low-power static and dynamic high-voltage cmos level-shifter circuits,” in *International Symposium on Circuits and Systems (ISCAS 2008), 18-21 May 2008, Sheraton Seattle Hotel, Seattle, Washington, USA*. IEEE, 2008, pp. 1946–1949.

[18] N. M. Toriello, C. N. Liu, and R. A. Mathies, “Multichannel reverse transcription-polymerase chain reaction microdevice for rapid gene expression and biomarker analysis,” *Analytical Chemistry*, vol. 78, no. 23, pp. 7997–8003, 2006.

[19] C. J. Backhouse, A. Gajdal, L. M. Pilarski, and H. J. Crabtree, “Improved resolution with microchip-based enhanced field inversion electrophoresis,” *Electrophoresis*, vol. 24, no. 11, pp. 1777–1786, 2003.

[20] G. V. Kaigala, R. J. Huskins, J. Preiksaitis, X.-L. Pang, L. M. Pilarski, and C. J. Backhouse, “Automated screening using microfluidic chip-based PCR and product detection to assess risk of BK virus-associated nephropathy in renal transplant recipients,” *Electrophoresis*, vol. 27, no. 19, pp. 3753–3763, 2006.

[21] V. J. Sieben and C. J. Backhouse, “Rapid on-chip postcolumn labeling and high-resolution separations of DNA,” *Electrophoresis*, vol. 26, no. 24, pp. 4729–4742, 2005.

Chapter 6

Integrated Circuit-Based Instrumentation for Microchip Capillary Electrophoresis

This chapter is based on the manuscript accepted for publication in the IET Nanobiotechnology journal. This chapter illustrates integration of all the required instrumentations for capillary electrophoresis into a single microelectronic chip. This demonstration paves the way for a *true* lab-on-a-chip i.e. one, in which fluidic manipulation is done on a single microfluidic chip and all the instrumentation is integrated into a single microelectronic chip. In addition to being part of the microelectronic chip design group, my roles in this demonstration were: designing/building the instrument (hardware), debugging, calibration, experiment design and execution.

Preface

Although electrophoresis with laser induced fluorescence (LIF) detection has tremendous potential in lab on chip-based point-of-care disease diagnostics, the wider use of microchip electrophoresis has been limited by the size and cost of the instrumentation. To address this challenge, we designed an integrated circuit (IC, i.e. a

A version of this chapter has been published. Behnam *et al.* 2010. IET Nanobiotechnology. 4. 91-101.

microelectronic chip, with total silicon area of <0.25 cm^2, less than 5 mm $\times$ 5 mm, and power consumption of 28 mW), which, with a minimal additional infrastructure, can perform microchip electrophoresis with LIF detection. The present work enables extremely compact and inexpensive portable systems consisting of one or more CMOS chips and several other low-cost components. There are, to our knowledge, no other reports of a CMOS-based LIF capillary electrophoresis instrument (i.e. high voltage generation, switching, control and interface circuit combined with LIF detection). This instrument is powered and controlled using a USB interface to a laptop computer. We demonstrate this IC in various configurations and can readily analyse the DNA produced by a standard medical diagnostic protocol (end-labelled PCR product) with a limit of detection of $\approx$1 ng/μL ($\approx$1 ng of total DNA). We believe that this approach may ultimately enable lab-on-a-chip based electrophoretic instruments that cost on the order of several dollars.

6.1 Introduction

In order for lab-on-a-chip (LOC) technologies to be more widely adopted in applications such as point-of-care (POC) disease diagnostics, inexpensive and portable instruments are essential [1]. One key microfluidic/LOC technology is electrophoresis, the basis of analysis/detection for a large number of molecular biology protocols for disease diagnostics (e.g. [2]). While there have been significant advances in LOC technologies, the limiting factor in employing these technologies in a POC setting is the need for considerable support/operating infrastructure. Hence, there is a pressing need for LOC instruments that can perform molecular biology protocols and yet be inexpensive and compact. Although LOC systems have demonstrated

extensive functionality (e.g. representative demonstrations by Easely [3], Blazej [4] and Hupert [5]), LOC systems largely rely on substantial external infrastructure (e.g. high voltage power supplies and switches, detection systems, valves/pumps, and thermal cyclers). In essence, microfluidic devices are often demonstrated in what might be called "chip-in-a-lab" approaches (i.e. requiring significant support infrastructure) rather than "lab on a chip" approaches. Although the "chip-in-a-lab" approach is an effective way to develop and demonstrate new microfluidic technologies, and is suitable for use in centralised laboratories, it is unsuitable for POC applications. We focus on one widely used LOC technique, capillary electrophoresis (CE). Laser-induced fluorescence (LIF) is one of the most commonly used detection methods in CE, due to high sensitivity and an abundance of well-characterised protocols that have been developed in the life-sciences [6]. In this chapter, we present an integration of most subsystems needed to perform electrophoresis, onto an integrated circuit (IC). We believe that this demonstration lays the groundwork for an ultra-portable LOC electrophoresis system.

Electrophoresis-based LOC commercial instruments include the Agilent 2100 BioAnalyser, BioFocus/Experion™from BioRad and the LabChip®90 system from Caliper. More recently NEC [7] and Sandia [8, 9] demonstrated electrophoretically-based genetic analysis tools. This progression in the development of the LOC infrastructure will continue, but is limited by the challenge of integrating the microfluidics with an optical subsystem, a high-voltage subsystem and an interface subsystem, all composed of discrete components. We believe that such system integration is of central importance to the LOC community since, for simple medical diagnostics based on genetic amplification and analysis (e.g. PCR and electrophore-

sis), much of the costly infrastructure is for the analysis component.

A LIF-CE system is typically built around four subsystems: (a) a high voltage (HV) subsystem to generate and switch (i.e. distribute, typically with mechanical relays) the HV for electrophoresis, (b) an optical subsystem consisting of an excitation source (i.e. laser), optical lens and filters that excites the fluorophores, filters out the excitation light and collects the fluorescence, (c) a detection subsystem consisting of a photodetector, amplifier, and an analogue to digital converter (ADC), and (d) an interface/control subsystem. The size, cost and complexity of these building blocks has hindered the development of LOC applications [10]. Challenges in terms of both design and integration prevent more effective implementations of the CE infrastructure. In this work we address these challenges by integrating the most costly subsystems onto a single IC.

Design: In recent reports, the HV subsystem design for CE [8, 11, 12, 13] has been based on HV generation using either one or multiple off-the-shelf DC-DC converters with switching performed using manual switches or electro-mechanical relays on printed circuit boards [8, 12, 13, 14, 15, 16]. As a result of these many components, HV subsystems are a significant part of the cost and size of any CE instrument. To minimise electrical interference, separate circuit boards are usually used for the HV components and for the control and interface circuitry – further adding to the cost and the size of an instrument.

Photomultiplier tubes (PMTs) are the most commonly used optical detection transducers for LOC fluorescence measurements [17]. While PMTs are highly sen-

sitive, they are costly and delicate. Charged coupled device (CCD) imagers have also been demonstrated in the context of a portable system [18], but they tend to be slower and less sensitive than PMTs. There has been significant interest in photodiodes [19, 20] as they are suitable for compact instrumentation and can be built using standard microelectronic fabrication processes. Although photodiodes are less sensitive than PMTs, with appropriate circuitry and signal processing they can be applied in very cost-effective implementations.

Optical subsystems are commonly based on a confocal optics design – as seen in most LOC based LIF-CE instruments. The confocal design allows LIF detection that has low baseline signal – allowing more sensitive detection. The Mathies group has made impressive advancements in building portable PMT-based confocal CE instruments [17, 21] that are both versatile and highly sensitive. However, this design results in systems that tend to be expensive and delicate which arises from the complexity of the optics system assembly, and also because of the costs of the detection system (typically PMT-based).

Integration: Clearly, it is a challenging task to integrate the wider range of the subsystems and technologies required for a microfluidic LOC-instrument. The LOC community has been moving to progressively more integrated solutions. Integrated LIF detection systems for CE have been well reviewed in [10, 22, 23, 24]. Broadly speaking, these integration efforts for LIF systems can be characterised as either 1) better integrations of the optical subsystem or 2) integration of the detection subsystem (optical electronics).

The optical integration efforts have been well reviewed in the above review papers, these efforts have mainly been to combine the excitation light sources, lenses, filters and detectors that are needed to excite fluorescence, collect the fluorescence and then detect it. As one such example, Hofmann *et al.* [25] combined wavelength-selective waveguides with their microfluidic systems. Similarly, Thrush *et al.* [26] combined laser, lenses, and filters on a GaAs wafer while Balslev *et al.* [27] combined a laser, detectors, waveguides and filters integrated directly with microchannels. Although these integrations are impressive, for our system-level application we find it suffices to use an inexpensive assembly of off-chip components (lens, filter and laser) coupled with integrated optical electronics.

The detection integrations have investigated how to combine the detector and associated electronics. Detection systems for LIF-CE have been well reviewed in [10, 22], and the authors note that there have been limited demonstrations of integrated detection subsystems (i.e. photodiodes, amplifiers and ADCs). It is difficult to do justice to the many advances made; however, the Burns group is of particular note. They used a silicon-based microfluidic chip to demonstrate the integration of optical transducers, heaters/temperature sensors and fluidics [28]. This was a landmark in LOC integration; however, this system still required considerable external infrastructure (e.g. high voltage, optical electronics and control/interface subsystems). More recently [29] they showed an integration of a microfluidic system with a 40-layer interference filter and photodiodes with a limit of detection (with intercalators) of 0.9 ng/μL of DNA. Similarly, Kamei *et al.* [30] demonstrated a multi-chip system consisting of a glass chip with an integrated photodiode. Webster *et al.* [20] demonstrated an integrated photodiode connected to external instrumentation for

measurements. As an extension to single-point detection mode, multiple photodiodes [31] and a photodiode array [32] were used, but both with external detection electronics (i.e. amplifiers and ADCs). Subsequently, Manaresi *et al.* [33] integrated both a photodiode and an amplifier on a single chip, but used an external ADC. More recently Minas *et al.* [34] demonstrated an elegant combination of optical filters, photodiodes and a "light to frequency" converter (albeit for colorimetric use). In the present demonstration we demonstrate a fully integrated detection subsystem comprised of detection, amplification and an ADC.

As described in our recent paper [35], several groups have miniaturised and integrated HV circuits for CE but these systems were based on discrete components (as an example [14]). We recently demonstrated [35], a fully integrated HV subsystem – i.e. generation and switches, along with control and interface, all on a single CMOS IC.

In general, the integration of more functionality onto a single IC (as opposed to having discrete components on a printed circuit board) can lead to lower noise. However, the integration of the sensitive detection electronics of the optical subsystem with a high voltage and current switching on the same silicon chip is likely to lead to very noisy data – as predicted by the Burns group [28] (they integrated photodiodes but did not integrate the HV subsystem). To the best of our knowledge, to date, there has been no report of the integration of the HV and optical subsystems. We address the challenge of integrating the sensitive detection electronics with the intrinsically noisy high voltage subsystem.

Path Forward: There are many potential paths forward, both in terms of design and integration, but one is typically faced with the need to trade performance for cost. Since the cost is such a driving issue (especially in healthcare), such trade-offs must be explored. A simple way of looking at the problem is to examine the PCR/CE combination that forms the basis of many genetic diagnostics. A LOC infrastructure that could perform such a test could dramatically improve the use of LOC technologies. Hence, we measure our technologies against whether they can implement a PCR/CE diagnostic.

Although a large number of LIF-based CE demonstrations make use of intercalators rather than end-labelled DNA [36] (intercalated DNA is often several orders of magnitude brighter than end-labelled DNA), the use of intercalators requires additional processing steps hence are not as suitable for diagnostic, where rapidity is important [37]. On the other hand, end-labelled DNA is ideally suited for LOC applications based on integration of genetic amplification via PCR and analysis via CE. Integration of end-labelled PCR with CE form the basis of many medical diagnostics to the extent that we considered it a design constraint – i.e. the system must be able to detect end-labelled DNA as would be produced in an on-chip PCR. The sensitivity of microchip electrophoresis is very dependent upon the procedure used to perform the electrophoresis (e.g. the running buffer concentration and how much sample is used). In particular, if the DNA sample has low ionic strength, then sample stacking effects [38] could be used to concentrate the DNA on-chip and to thereby demonstrate better apparent sensitivities. However, unless the means to purify the sample are also to be incorporated on the microfluidic chip, this approach of estimating the sensitivity of the instrument is misleading. Thus, for the present

work we seek to use a PCR sample without any purification/clean-up step.

The LOC technology has not reached a level that would enable a single-chip solution for LIF-CE. Most instrumental infrastructure development work has focused on integrating the optical components, largely relying on external electronics support for HV, signal amplification, data acquisition and overall interface. Apart from our past reports, there are, to our knowledge, no other reports of CMOS-based HV subsystems [35]. Subsequently, using that IC-based HV subsystem with an optical subsystem based on discrete off-chip components, we demonstrated a photodiode-based LIF-CE system [19]. In the present work, we integrate the discrete component-based optical subsystem [19] (photodiode, analogue to digital converter and an amplifier) with the high voltage subsystem, and control and interface subsystem onto a single IC. We thereby demonstrate a LIF-CE instrument consisting of a single IC with only a few additional and inexpensive components – a laser diode (≈$30), a miniaturised lens (≈$20), filter (≈$30) and a few discrete electrical components (i.e. an inductor, resistors, capacitors costing ≈$10). The complete instrument is controlled and powered via a USB connection to a laptop computer. The present work enables extremely compact and inexpensive, portable systems consisting of one or more CMOS chips and several other low-cost components. There are, to our knowledge, no other reports of complete CMOS-based LIF detection (i.e. from photons to digital data). We demonstrate the present system in the analysis of PCR products representative of those in standard medical diagnostics.

6.2 Materials and Methods

6.2.1 Instrument

This instrument is designed to be fully powered and controlled by laptop computer via a USB interface. The IC (Figure 6.1) communicates with a SPI-USB converter module (DLP-2232M-G, FTDI Inc., Glasgow, UK) using a standard serial peripheral interface (SPI) protocol for control, data management. The communication and control interface (CCI) subsystem within the IC decodes the SPI commands. The CCI also controls and monitors the HV generation, HV switches and optical detection circuitry (Figure 6.2a). Since the USB to SPI implementation is not the focus of our demonstration, an off-the-shelf module was used to implement this function.

The functional block shown in Figure 6.2a is assembled in the set-up shown in Figure 6.2b. For experimental purposes it was convenient to use the jig shown in the above figure - this allowed for manual adjustment of the alignment. However, in future the alignment will be performed by a simple holder that properly positions the chips. The simplified optical subsystem (Figure 6.3a, details in Optical Assembly section) consists of a commercial laser diode, an interference filter and a gradient index (GRIN) lens to collimate the emitted light from the microfluidic chip.

6.2.2 Integrated Circuit

The IC is designed and fabricated using DALSA Semiconductor's (Bromont, QC, Canada) three metal layer, triple well, dual gate oxide 0.8 μm 5V HV CMOS/D-MOS (double diffused MOS) process. This microfabrication process technology

supports the integration of both the HV components and low voltage components (for control, data communication, optical transducers and related components) within a single die. This LOC work has required the development of a new design library and VLSI elements, in an ongoing process that is expected to ultimately benefit the wider LOC community.

From an operational perspective, this IC (Figure 6.1) consists of four main subsystems: (a) programmable HV generation module (b) eight independently controlled HV switched-outputs that can be coupled to the microfluidic chip, (c) an optical detection subsystem composed of devices and circuits that transduce, amplify and digitize the fluorescence and (d) an interface subsystem, the communication and control interface (CCI) that controls and monitors the IC functionality. The HV subsystem is formed from the generation and switching modules. For convenience, the chip was placed in a 40-pin DIP package.

6.2.3 HV Generation and Switching

To generate the required electric potentials, a non-isolated inductive DC-DC converter is implemented within the IC. This DC-DC converter circuit converts the 5 V input supply (from the USB interface) to up to 300 V at the output. Briefly, the principle of this conversion is based on the rectification of the back-electromotive force created by periodically interrupting the current through an external inductor and storing this energy into an external HV capacitor. The detailed operation and working principle is described in Chapter 5.

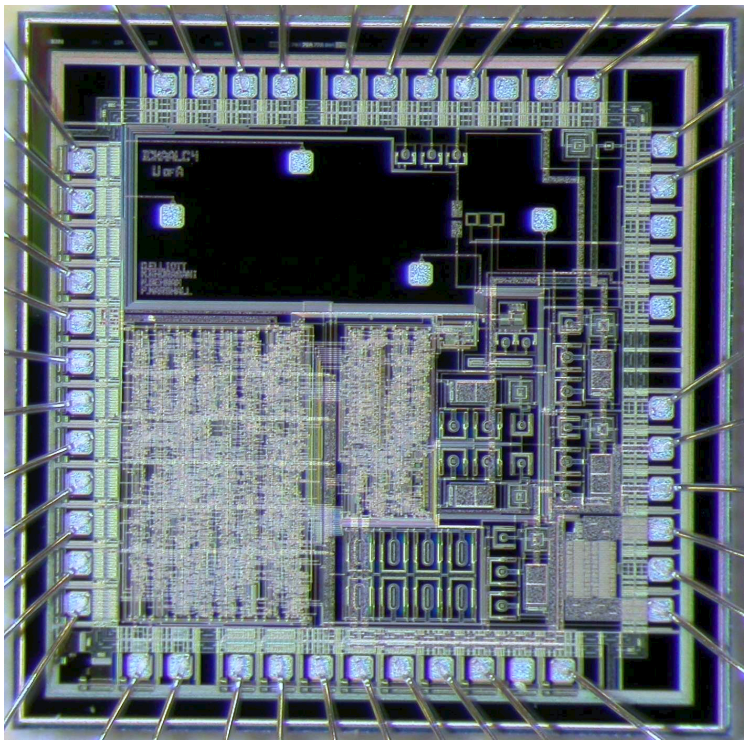

Figure 6.1: Photograph of one of our HV ICs (with total silicon area of $<$0.25 cm^2) comprising of the high voltage capability and optical electronics integrated on the same silicon die.

In this design, to implement a broad range of microfluidic applications, eight independent 300 V HV switches are included that could be coupled to the microfluidic chip. Five of these switches can set their respective outputs to positive high voltage supply, ground (0V), or high impedance (float). These HV switches consist of an output stage and a level-shifter stage. The output stage has one pull-down and one pull-up transistor. By setting these transistors (set by the user using custom software that communicates with the IC), the output (ground, high voltage, and high impedance states) of the HV switch can be determined. The level-shifter stage changes the logic control signal (from control and interface sub-system, 0-5V) to an appropriate level to control the output stage transistors. To minimise silicon area

and cost, an additional three switches are designed such that their respective outputs can be set only to either a ground or high impedance state. Detailed designs for these switches have been reported elsewhere [35].

6.2.4 Photodiode and Transimpedance Amplifier

A 150 μm x 150 μm Si p-n photodiode was fabricated on the IC. The anode is a p-well and the cathode is n+ diffusion. The photodiode is placed in its own p-well, isolating it from all other circuit components, this reduces the current leakage to/from other junctions. The photodiode is used in a photoconductive mode and is connected to the transimpedance amplifier as shown in Figure 6.2a, in which the photodiode is biased across its junction capacitance. As the fluorescently labelled DNA migrates through the CE channels, the emitted fluorescence reaching the photodiode generates photocurrent and discharges the photodiode junction capacitance, thus reducing its voltage. The change in photodiode capacitance voltage is tracked and amplified by a common source amplifier (this amplifier design is similar to the design used in a CMOS camera pixel) whose signal is then digitized by the internal ADC. Experimentally, the responsivity of the photodiode was found to be 0.35 A/W (at 600 nm) by applying a known optical power (30.4 pW) to generate a photocurrent of 10.6 pA.

6.2.5 Analogue to Digital Converter

The ADC architecture here is based on successive approximation architecture. Although we could have designed and integrated a higher resolution ADC (i.e. 12-bit

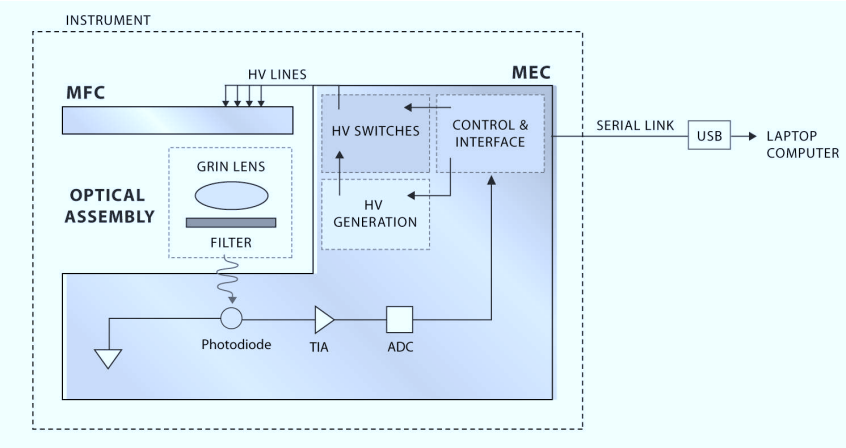

(a)

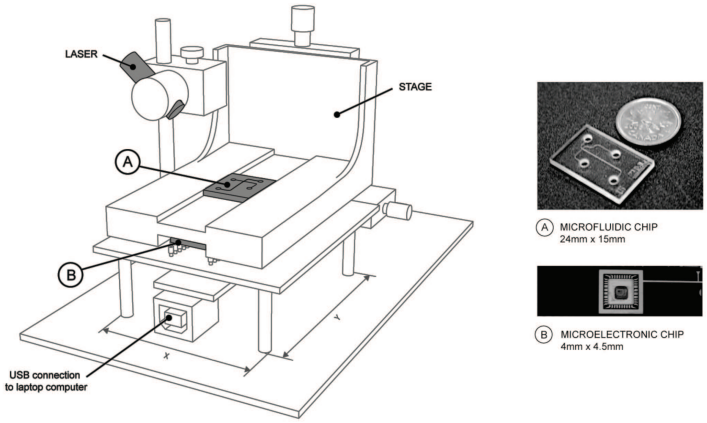

(b)

Figure 6.2: (a) Functional block diagram of the CE instrument, (b) the experimental set-up consists of an IC, a microfluidic chip, a laser diode and simplified optics (a single GRIN lens and an interference filter). This stage has been built for flexibility, primarily for optical alignment. Once packaged, such an optical stage will not be necessary. The detailed optical assembly is shown in Figure 6.3a (MEC and MFC refer to the microelectronic (i.e. the IC) and microfluidic chip respectively).

or 16-bit), in order to save both power and silicon area, in this prototype IC, we include only an 8-bit ADC (average error $\pm$ 1 least significant bit). This ADC sequentially converges to a digital value that represents the analogue input in 8-cycles

by performing a binary search algorithm as detailed in [39]. This ADC architecture is suitable for 8-16 bit resolutions at moderate operating frequencies, has low power consumption and requires minimal silicon area. In this integration we must balance the cost of higher resolution against the usefulness of higher resolution in acquiring higher sensitivity (the area of the ADC typically scales nearly linearly with the number of bits. In this present chip design the ADC occupies ≈21% of Si area used by low voltage components).

6.2.6 Isolation Between High Voltage and Optical Electronics

The integration of noisy circuits (i.e. HV supply switching and digital logic) with highly sensitive optical detection circuits is a key challenge. In this demonstration, a standard isolation technique of placing the photodiode in a dedicated isolated well [40] is implemented to minimise the noise coupling between the HV and the optical circuit. The photodiode was then connected to an integrating amplifier and then to the ADC. In order to save silicon area and pin-count we decided on a design that did not also isolate the amplifier and ADC from other circuits (this allowed us to have multiple uses for these circuits).

6.2.7 Optical Assembly

We make use of a highly simplified optical assembly (Figure 6.3a) consisting of a focusable 6mW commercial red laser (635 nm, Part # 59089, Edmund Optics, Barrington, NJ, USA) that excites the fluorescently tagged bio-molecules, an interference filter (HQ660LP, Chroma Technology Corporation, VT, Rockingham, USA)

that selectively transmits light of a specific wavelength (≈670 nm) and a gradient index (GRIN) lens (LGI630-6, Newport Corporation, Irvine, CA, USA) to collimate the emitted light from the microfluidic chip onto the photodiode.

During assembly, the lens is placed on top of the interference filter that is aligned to the photodiode (Figure 6.3a). A standard glass-glass microfluidic chip is used [35]. The spacing between the lens and photodiode is such that the microfluidic channel is in focus when viewed from the photodiode. To achieve this, after removing the interference filter, the spacing between lens and IC (which contains the photodiode) was set to observe the image of the photodiode (through the lens) on the microfluidic channel Figure 6.3b. This procedure of optical alignment is discussed in detail in our earlier report [19].

6.2.8 Capillary Electrophoresis Protocol

Electrophoresis is performed using a microfluidic chip that has two intersecting channels (Figure 6.4a). The injection channel is 16 mm long, and the separation channel is 21 mm long, both with a cross section of 90 μm (width) and 40 μm (depth). These channels link four fluid reservoirs. Adjacent to the separation channels, a 110 nm thick masking layer of chromium is patterned. This masking layer minimises the incident light, both directly from the laser diode and from the scatter from the microfluidic channels onto the photodiode.

We make use of a standard CE protocol consisting of injection and separation steps (Figure 6.4b). As in our earlier reports [19, 35] we adapted our CE protocols

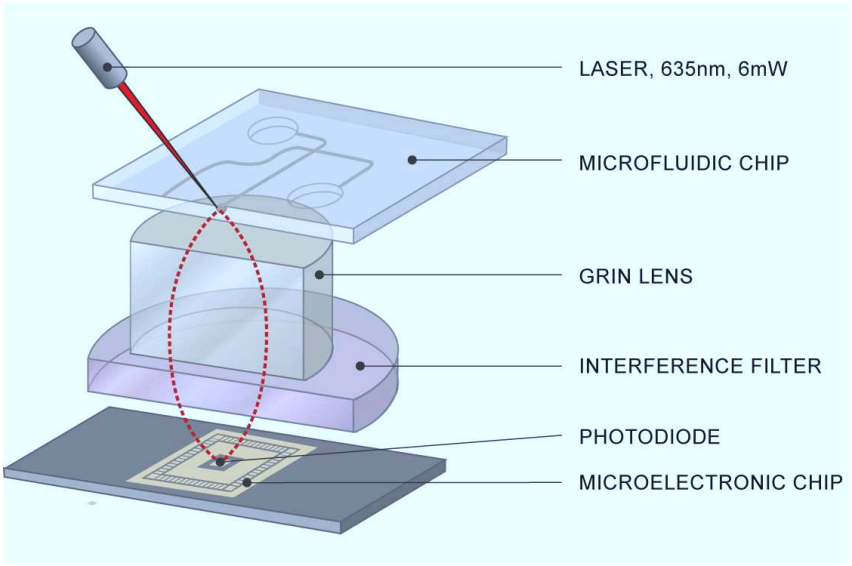

(a)

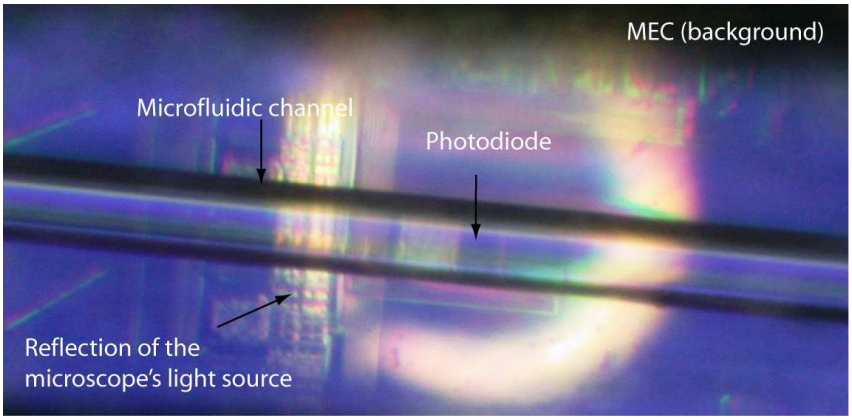

(b)

Figure 6.3: (a) The optical path consists of the microfluidic chip, a GRIN lens, an interference filter and the custom-designed IC. (b) Image of the photodiode as seen through the GRIN lens when in focus with the microfluidic channel. The photodiode is the area surrounded by the metallic contact ring. The ring-like image is the reflection of the microscopes light source and is not the outline of the GRIN lens. The metallic pad at the left of the photodiode is for characterization and interface purposes.

to perform electrophoresis at short distances with 200 V (detection at 13 mm along the CE channel). The HV output from the IC are coupled to the microfluidic chip

using platinum wire electrodes that are lowered into the fluidic reservoir using a gantry. As part of the CE protocol, a commercial dynamic coating (the Gel Co., San Francisco, CA; Cat# DEH-100) was applied to the microchannel [41]. Subsequently, channels were filled with a 4% linear polyacrylamide (LPA, MW 600,000 - 1,000,000, 10% solution in water, Polysciences, PA, USA) polymer matrix. The buffer, sample waste and buffer waste reservoirs were then filled with 3.0 μL of a 1 x TTE buffer solution and the sample well was filled with 2 μL of 0.1 x TTE, 1.0 μL DNA sample. TTE (Tris-taps-edta) buffer was prepared from 0.01 mM EDTA (ethylene diamine tetraacetic acid, Sigma, USA), 0.5mM TAPS ([(2-Hydroxy-1, 1-bis(hydroxymethyl)ethyl) amino]-1-propanesulfonic acid, N-[Tris(hydroxymethyl) methyl]-3-aminopropanesulfonic acid, Sigma, USA) and 0.5 mM Tris (tris (hydroxymethyl) aminomethane, Fisher Scientific, Canada). The sample is a PCR product (amplified from genomic DNA) with a final concentration of 13 μg/mL. The primer sequence (tagged with Cy5) uniquely identifies a β2 microglobulin gene (273 bp) from genomic DNA. Further details about the PCR protocol can be found elsewhere [18]. The time for injection, separation, optical integration and the sampling frequency were set using a custom-built graphical user interface (GUI) running on a laptop computer, which communicates these parameters to the IC via the USB link (Figure 6.2a).

6.3 Results and Discussion

6.3.1 Signal Processing and Noise Characterisation

It was found empirically that the least noise was present in the signal when sampled at 6.4 Hz, corresponding to a 150 ms sampling time plus 6 ms reset and communi-

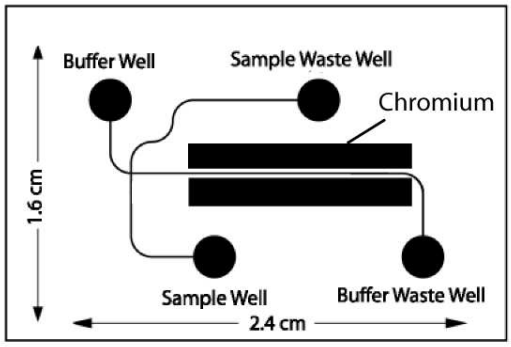

(a)

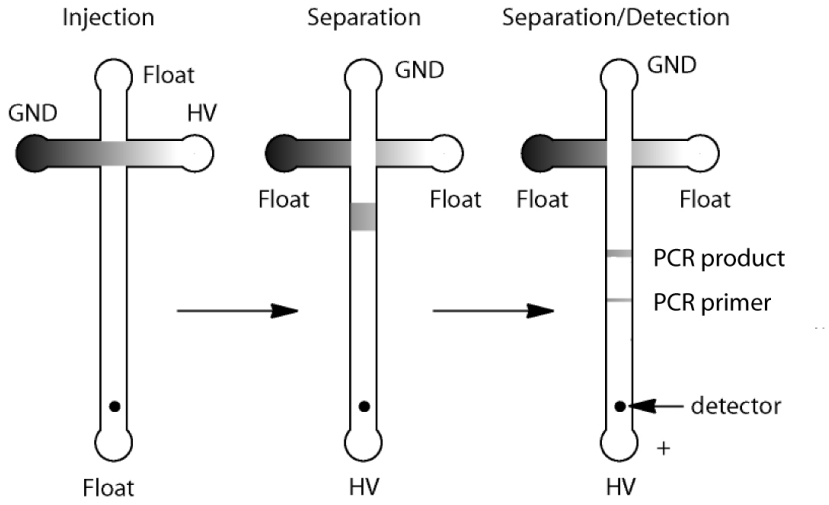

(b)

Figure 6.4: (a) Diagram of a standard glass-glass CE chip with 40 μm deep channels (90 μm wide channel) and 2 mm wide wells/ports. These chips are patterned with a 110 nm chromium layer that is photolithographically patterned on the bottom surface of the microchip. (b) In the injection stage of CE, positive HV is applied to the sample waste well, while ground state is applied to the sample well and a floating state (high impedance) to both buffer well and buffer waste well initiating electrophoretic migration of DNA. Injection is performed for 100 s at 200 V. During the separation step, the buffer well is connected to ground and positive HV is applied to the buffer waste well, while the sample well and sample wastes well are set to a float state. Separation is performed for 200 s at 200 V.

cation time. In the sampling period, a precharged capacitor gets discharged through a photodiode in photoconductive mode, and in the reset period, the capacitor is

charged (explained in the photodiode and transimpedance amplifier section). This integration time strikes an optimal balance between ensuring sufficient gain and avoiding ADC saturation – either of which would generate clipping of the signal. It was verified that the raw data from each electropherogram did not contain clipping in or near the arrival times of the primer or product peak. After analyzing the raw data of successive electropherograms, we found that the signal contained a noise contribution with the strongest contribution at 0.8 Hz and with successively smaller contributions at higher order harmonics. This was determined to originate from variations in the laser optical output power.

Since the data of interest is slowly varying (nearly DC, established from past work [18, 19, 42] and for the electrophoretic conditions used here the peaks corresponding to DNA are about 3 seconds in duration) we make use of a low pass filter. We designed a standard low-pass finite impulse response (FIR) equiripple filter (order of 20) with attenuation initiated at 0.8 Hz and a cut-off frequency of 1.0 Hz (implemented using MATLABs filter design and analysis tool, FDATOOL). This LP filter attenuates the frequencies above 0.8 Hz caused by the laser variation, and other high frequency resulting in a smooth electropherogram (Figure 6.5). (The amplitude of the 0.8 Hz signal was large enough that it was sometimes clipped, however this clipping generated higher frequency components that were readily removed by the filter.) The baseline variation, which is primarily due to both the laser module and the photodiode, is suppressed by subtracting the median of the nearest 29 data points (corresponding to 4.53 s), a window sufficiently wide to not affect the data of interest.

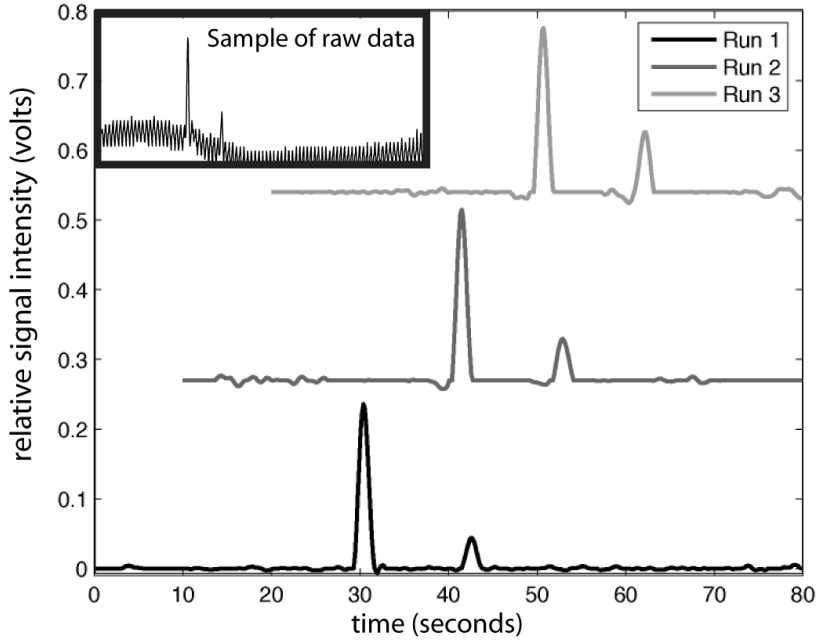

Figure 6.5: End-labelled PCR product representing the presence of the β2 microglobulin gene (β2M), was electrophoretically separated on a microfluidic chip operated by an IC-based instrument. The relative fluorescence signal collected by the IC is plotted against the time axis in seconds. Three consecutive CE runs demonstrate the repeatability of the peak arrival times. Within each run, the first peak (left) is the primer peak (20 bps) and the second peak (right) is the PCR product peak (≈273 bps). The minor dip in the electropherogram (before the PCR primer and product peak arrivals) below the baseline (i.e. zero) is an artefact introduced by the digital filter used to remove the 0.8 Hz noise. Given that this artefact is small and proportional to the following peak, its presence does not affect the limit of detection. The inset (top left) shows representative unprocessed data.

6.3.2 Single and Dual Chip Operation

Characterization of the acquired data revealed that acquiring the signal when the HV generation module was operational caused large variations in the measurement. This is due to noise coupling from the HV subsystem to the optical measurement circuits (amplifier and ADC). There are several ways of dealing with this large source of noise. In the "single IC" approach the HV and optical subsystems of a

single chip are used simultaneously. In this approach we found that the standard deviation of the acquired data (i.e. the signal) was 0.431 ± 0.004 V (based on three runs).

We also tested an approach in which we deactivated the HV generation module briefly while the optical measurement is being performed. When the HV subsystem is turned off the standard deviation of the signal is 0.064 ± 0.015 V (i.e. $\approx$7 times lower than when the HV is turned on). However, deactivating the HV for the 150 ms sampling time results in an unacceptable drop of the HV subsystem output voltage. In a third approach, the dual IC approach, we used two identical ICs, one with an active optical subsystem and the other with an active HV subsystem. With this configuration the standard deviation of the acquired signal was the same as the HV off case. Given that this was the most sensitive and robust approach, further testing was performed with this configuration.

As shown in Figure 6.5, the system can reliably detect the products of an end-labelled PCR reaction. CE results are commonly characterised with metrics such as the signal-to-noise ratio (SNR), the limit of detection (LOD) and the resolution (in base pairs for DNA) of electrophoretic separation. The average SNR for the DNA sample used (consisting of a PCR primer and product peak) for three consecutive CE runs (Figure 6.5) is calculated to be 98. The baseline of the electropherogram is calculated by estimating the noise in the data from the first 20 seconds of the CE run, long before the DNA peaks of interest arrived. Along with the amplitude of the PCR product peak, this is used to estimate the SNR. We earlier established that such a SNR is adequate for medical diagnostic applications [18]. Additionally,

under similar CE conditions and using the same microfluidic chip, electrophoresis was performed with a commercial confocal CE system (the Microfluidic Tool Kit (μTK), Micralyne, Edmonton, Canada), resulting in an average SNR value of $\approx$300 (data not shown). This indicates that using the IC with highly simplified optics (using the CE protocol outlined in the methods section) gave a SNR comparable to that of a commercial system (confocal and PMT-based system).

Limit of detection: We demonstrate the systems performance by operating directly on a PCR product of representative strength, rather than using a calibration standard directly. In this way we could be certain that no sample stacking effects could lead to misleadingly good sensitivity estimates. We calibrated our system against a commercial instrument (the μTK) by comparing sample peak heights with the same microfluidic chips and protocols. Briefly, we first calibrated the μTK by purifying a PCR product to remove its primers and unincorporated nucleotides before measuring the UV absorbance. In this standard method, the ionic strength of the buffer was maintained (i.e. before and after purification the sample had the same salt concentration). From this, the concentration of PCR product was found to be $\approx$13 μg/mL, a concentration typical of PCR products generated in clinical tests.

We use a standard definition for the LOD, i.e. the amount of sample that is required to produce a peak height that is equal to three times the standard deviation (3σ) in the baseline of the electropherogram. Using the filtered data (Figure 6.5) after removing the baseline variation by means of subtracting the median over 29 points ($\approx$4.5 s), the standard deviation for the first 20 s before the arrival of the DNA peaks was calculated. From the observed product peak amplitude and known

amount of DNA, the LOD was calculated to be ≈1 ng of end-labelled DNA. As our standard CE protocol makes use of 1 μL of sample, this corresponds to approximately 1 ng/μL (if we were working with intercalators then we would expect approximately 100 times more fluorophores per molecule, and hence a LOD of about 10 pg/μL). The dominant uncertainty in these calculations is thought to arise from the calibration process and this is estimated as 30% (a calculation error in our earlier report [19] gave rise to an overly pessimistic estimate of our LOD).

The estimated sensitivities of the system are shown in Table 6.1. In the operating range of the optical detection subsystem, used in this experiment, the ADC output is linear to the optical intensity detected by the photodiode. Hence we extrapolate the LOD for a single IC given that the level of noise is seven times higher by the same factor. The dual ICs approach was found to be more sufficient for the analysis of a PCR reaction of typical strength. It is clear from Table 6.1 that the use of standard isolation methods for the photodiode alone did not completely suppress the noise pickup. Although the single IC approach was not sufficiently sensitive to analyse a typical end-labelled PCR sample with our present methodology, it could be used to analyse a strong end-labelled PCR product or an intercalator-labelled product. With such higher concentrations, although it might be possible to optimize the integration times to better acquire data, such concentrations were too high to be relevant – i.e. higher than could be obtained in a standard PCR without adding sample purification. Therefore, we chose to proceed with dual-IC approach. As we continue to develop the design libraries and new elements for this CMOS technology we will investigate approaches to increase the sensitivity, but our primary goal is to improve the noise isolation between the HV and optical subsystems through

the use of dedicated amplifier and ADC circuits and by placing these in their own dedicated isolation wells (as opposed to only the photodiode). Moreover, in future designs, separate digital and analog power supply pins will be used (the IC will still be operated using a single USB interface), this will minimise the digital switching noise.

Table 6.1: Estimated limits of detection of end-labelled DNA.

Approach	*Noise Level (V)*	*LOD (ng µL)*
Dual ICs	0.064±0.015	1±30%
Single IC	0.431±0.004	7±30%

The resolution (calculated according to the procedure detailed in [37]) was found to be ≈30 bps. This resolution was adequate to differentiate the PCR product peak from the primer peak. The repeatability of the electrophoretic performance was demonstrated by the peak arrival times for five consecutive CE runs (three consecutive runs plotted in Figure 6.5) demonstrating a variation less than 0.4 seconds. The commercial system (μTK) with a similar microfluidic chip gave an improved resolution (10 bps [42]) suggesting that this reduction in resolution is likely due to the size of the detector and the selection of the filter for data processing (since the designed LP filter is similar to the sample averaging, this tends to make the peaks broader, hence reduces the resolution during signal conditioning.

6.3.3 Conclusion

We have shown that our IC-based system could perform the microfluidic electrophoresis needed for a demonstration of a PCR/CE-based medical diagnostic.

By adapting a new HV-CMOS technology to LOC applications we have demonstrated that a single IC can essentially integrate (almost) all of the instrumentation required for microchip electrophoresis. Through the development and integration of devices in this CMOS technology, and by applying noise isolation techniques, we have overcome some of the central challenges preventing the wider use of the LOC technologies.

As we build progressively less expensive LOC-based CE instruments with increased level of integration and functionality being ported onto the integrated circuits [19, 35] we also seek to boost performance. Cost reduction is another important consequence of integrating the optical detection components (photodiode, amplifier, ADC, control and communication interface) on a single IC. This integration results in the reduction in power usage such that the instrument is now fully powered (and controlled) through a USB connection to a laptop computer.

The present demonstration suggests it may now be feasible to build a CE instrument that is the size and cost of a USB memory key. The cost for a CMOS chip is directly related to the area of silicon used. For high-volume manufacture of CMOS chips of this area, a cost on the order of dollars is typical. We estimate the cost of this chip in volume production as being $<$\$10, making such CMOS-based instruments inexpensive and well-suited for POC diagnostic applications. With the present level of integration, our IC-based instruments are approaching the LOC ideal, where the major functionality resides upon the chips and with minimal overall off-chip infrastructure. We expect that this level of integration will promote the wider use of the LOC technologies.

Bibliography

[1] P. Yager, T. Edwards, E. Fu, K. Helton, K. Nelson, M. R. Tam, and B. H. Weigl, "Microfluidic diagnostic technologies for global public health." *Nature*, vol. 442, no. 7101, p. 412, 2006.

[2] J. P. Landers, "Molecular diagnostics on electrophoretic microchips," *Analytical Chemistry*, vol. 75, no. 12, pp. 2919–2927, 2003.

[3] C. J. Easley, J. M. Karlinsey, J. M. Bienvenue, L. A. Legendre, M. G. Roper, S. H. Feldman, M. A. Hughes, E. L. Hewlett, T. J. Merkel, J. P. Ferrance, and J. P. Landers, "A fully integrated microfluidic genetic analysis system with sample-in-answer-out capability," *Proceedings of the National Academy of Sciences of the United States of America*, vol. 103, no. 51, pp. 19 272–19 277, DEC 19 2006.

[4] R. G. Blazej, P. Kumaresan, and R. A. Mathies, "Microfabricated bioprocessor for integrated nanoliter-scale Sanger DNA sequencing," *Proceedings of the National Academy of Sciences of the United States of America*, vol. 103, no. 19, pp. 7240–7245, MAY 9 2006.

[5] M. L. Hupert, H. Wang, H. Chen, W. Stryjewski, D. Patterson, M. A. Witek, P. Datta, J. Goettert, M. C. Murphy, and S. A. Soper, "A field-deployable system for automated molecular testing using modular microfluidics," in *Twelfth International Conference on Miniaturized Systems for Chemistry and Life Sciences*, L. E. Locascio, M. Gaitan, B. M. Paegel, D. J. Ross, and W. N. Vreeland, Eds., vol. 2, San Diego, USA, 2008, pp. 1046–1048.

[6] M. E. Johnson and J. P. Landers, "Fundamentals and practice for ultrasensitive laser-induced fluorescence detection in microanalytical systems," *Elec-*

trophoresis, vol. 25, no. 21-22, pp. 3513–3527, 2004.

[7] M. Asogawa, M. Sugisawa, K. Aoki, H. Hagiwara, and Y. Mishina, "Development of portable and rapid human dna analysis system aiming on-site screening," in *Twelfth International Conference on Miniaturized Systems for Chemistry and Life Sciences*, vol. 1, October 2008, pp. 1072–1074.

[8] R. Renzi, J. Stamps, B. Horn, S. Ferko, V. VanderNoot, J. West, R. Crocker, B. Wiedenman, D. Yee, and J. Fruetel, "Hand-held microanalytical instrument for chip-based electrophoretic separations of proteins," *Analytical Chemistry*, vol. 77, no. 2, pp. 435–441, JAN 15 2005.

[9] R. J. Meagher, A. V. Hatch, R. F. Renzi, and A. K. Singh, "An integrated microfluidic platform for sensitive and rapid detection of biological toxins," *Lab on a Chip*, vol. 8, no. 12, pp. 2046–2053, 2008.

[10] G. T. Roman and R. T. Kennedy, "Fully integrated microfluidic separations systems for biochemical analysis," *Journal of Chromatography A*, vol. 1168, no. 1-2, pp. 170–188, OCT 19 2007.

[11] D. Jackson, J. Naber, T. Roussel, M. Crain, K. Walsh, R. Keynton, and R. Baldwin, "Portable high-voltage power supply and electrochemical detection circuits for microchip capillary electrophoresis," *Analytical Chemistry*, vol. 75, no. 14, pp. 3643–3649, 2003.

[12] C. D. García, Y. Liu, P. Anderson, and C. S. Henry, "Versatile 3-channel high-voltage power supply for microchip capillary electrophoresis," *Lab on a Chip*, vol. 3, no. 4, pp. 324–328, October 2003.

[13] T. Kappes, B. Galliker, M. Schwarz, and P. Hauser, "Portable capillary electrophoresis instrument with amperometric, potentiometric and conductometric detection," *TrAC Trends in Analytical Chemistry*, vol. 20, no. 3, pp. 133–139, MAR 2001.

[14] D. Erickson, D. Sinton, and D. Li, "A miniaturized high-voltage integrated power supply for portable microfluidic applications," *Lab on a Chip*, vol. 4, no. 2, pp. 87–90, April 2004.

[15] G. E. Collins, P. Wu, Q. Lu, J. D. Ramsey, and R. H. Bromund, "Compact, high voltage power supply for the lab-on-a-chip," *Lab on a Chip*, vol. 4, pp. 408–411, March 2004.

[16] L. Jiang, X. Jiang, Y. Lu, Z. Dai, M. Xie, J. Qin, and B. Lin, "Development of a universal serial bus-powered mini-high-voltage power supply for microchip electrophoresis," *Electrophoresis*, vol. 28, no. 8, pp. 1259–1264, 2007.

[17] E. Lagally, J. Scherer, R. Blazej, N. Toriello, B. Diep, M. Ramchandani, G. Sensabaugh, L. Riley, and R. Mathies, "Integrated portable genetic analysis microsystem for pathogen/infectious disease detection," *Analytical Chemistry*, vol. 76, no. 11, pp. 3162–3170, JUN 1 2004.

[18] G. V. Kaigala, V. N. Hoang, A. Stickel, J. Lauzon, D. Manage, L. M. Pilarski, and C. J. Backhouse, "An inexpensive and portable microchip-based platform for integrated RT-PCR and capillary electrophoresis," *Analyst*, vol. 133, no. 3, pp. 331–338, 2008.

[19] G. V. Kaigala, M. Behnam, C. Bliss, M. Khorasani, S. Ho, J. N. McMullin, D. G. Elliott, and C. J. Backhouse, "Inexpensive, universal serial bus-powered and fully portable lab-on-a-chip-based capillary electrophoresis instrument," *IET Nanobiotechnology*, vol. 3, no. 1, pp. 1–7, MAR 2009.

[20] J. Webster, M. Burns, D. Burke, and C. Mastrangelo, "Monolithic capillary electrophoresis device with integrated fluorescence detector," *Analytical Chemistry*, vol. 73, no. 7, pp. 1622–1626, 2001.

[21] P. Liu, T. S. Seo, N. Beyor, K.-J. Shin, J. R. Scherer, and R. A. Mathies, "Integrated portable polymerase chain reaction-capillary electrophoresis microsystem for rapid forensic short tandem repeat typing," *Analytical Chemistry*, vol. 79, no. 5, pp. 1881–1889, MAR 1 2007.

[22] E. Lagally and H. Soh, "Integrated genetic analysis microsystems," *Critical Reviews in Solid State and Materials Sciences*, vol. 30, no. 4, pp. 207–233, OCT-DEC 2005.

[23] V. Namasivayam, R. Lin, B. Johnson, S. Brahmasandra, Z. Razzacki,

D. Burke, and M. Burns, “Advances in on-chip photodetection for applications in miniaturized genetic analysis systems,” *Journal of Micromechanics and Microengineering*, vol. 14, no. 1, pp. 81–90, JAN 2004.

[24] B. Kuswandi, Nuriman, J. Huskens, and W. Verboom, “Optical sensing systems for microfluidic devices: A review,” *Analytica Chimica Acta*, vol. 601, no. 2, pp. 141–155, 2007.

[25] O. Hofmann, X. H. Wang, A. Cornwell, S. Beecher, A. Raja, D. D. C. Bradley, A. J. deMello, and J. C. deMello, “Monolithically integrated dye-doped pdms long-pass filters for disposable on-chip fluorescence detection,” *Lab on a Chip*, vol. 6, no. 8, pp. 981–987, 2006.

[26] E. Thrush, O. Levi, L. J. Cook, J. Deich, A. Kurtz, S. J. Smith, W. E. Moerner, and J. S. Harris, “Monolithically integrated semiconductor fluorescence sensor for microfluidic applications,” *Sensors and Actuators B-Chemical*, vol. 105, no. 2, pp. 393–399, 2005.

[27] S. Balslev, A. M. Jorgensen, B. Bilenberg, K. B. Mogensen, D. Snakenborg, O. Geschke, J. P. Kutter, and A. Kristensen, “Lab-on-a-chip with integrated optical transducers,” *Lab on a Chip*, vol. 6, no. 2, pp. 213–217, 2006.

[28] M. Burns, B. Johnson, S. Brahmasandra, K. Handique, J. Webster, M. Krishnan, T. Sammarco, P. Man, D. Jones, D. Heldsinger, C. Mastrangelo, and D. Burke, “An integrated nanoliter DNA analysis device,” *Science*, vol. 282, no. 5388, pp. 484–487, OCT 16 1998.

[29] G. Minas, J. S. Martins, J. C. Ribeiro, R. F. Wolffenbuttel, and J. H. Correia, “Biological microsystem for measuring uric acid in biological fluids,” *Sensors and Actuators a-Physical*, vol. 110, no. 1-3, pp. 33–38, 2004.

[30] T. Kamei and T. Wada, “Contact-lens type of micromachined hydrogenated amorphous Si fluorescence detector coupled with microfluidic electrophoresis devices,” *Applied Physics Letters*, vol. 89, no. 11, SEP 11 2006.

[31] P. Pittet, J. M. Galvan, G. N. Lu, L. J. Bum, and B. D. Leca-Bouvier, “Cmos lif detection system for capillary analysis,” *Sensors and Actuators B*, vol. 97,

pp. 355–361, 2004.

[32] J. M. Song and T. Vo-Dinh, "Integrated cmos microchip system with capillary array electrophoresis," *Analytical Bioanalytical Chemistry*, vol. 373, pp. 399–403, 2002.

[33] N. Manaresi, A. Romani, G. Medoro, L. Altomare, A. Leonardi, M. Tartagni, and R. Guerrieri, "A CMOS chip for individual cell manipulation and detection," *IEEE Journal of Solid-State Circuits*, vol. 38, no. 12, pp. 2297–2305, 2003.

[34] G. Minas, G. de Graaf, R. F. Wolffenbuttel, and J. H. Correia, "An MCM-based microsystem for colorimetric detection of biomolecules in biological fluids," *IEEE Sensors Journal*, vol. 6, no. 4, pp. 1003–1009, 2006.

[35] M. Behnam, G. V. Kaigala, M. Khorasani, P. Marshall, C. J. Backhouse, and D. G. Elliott, "An integrated CMOS high voltage supply for lab-on-a-chip systems," *Lab on a Chip*, vol. 8, no. 9, pp. 1524–1529, SEP 2008.

[36] H. S. Rye, S. Yue, D. E. Wemmer, M. A. Quesada, R. P. Haugland, R. A. Mathies, and A. N. Glazer, "Stable fluorescent complexes of double-stranded dna with bis-intercalating asymmetric cyanine dyes - properties and applications," *Nucleic Acids Research*, vol. 20, no. 11, pp. 2803–2812, 1992.

[37] V. J. Sieben and C. J. Backhouse, "Rapid on-chip postcolumn labeling and high-resolution separations of DNA," *Electrophoresis*, vol. 26, no. 24, pp. 4729–4742, 2005.

[38] R. Chien, "Sample stacking revisited: a personal perspective," *Electrophoresis*, vol. 24, no. 3, pp. 486 – 497, 2003.

[39] P. E. Allen and D. R. Holberg, *CMOS analog circuit design*. New York, USA: Oxford University Press, 2002.

[40] M. Nagata, J. Nagai, K. Hijikata, T. Morie, and A. Iwata, "Physical design guides for substrate noise reduction in CMOS digital circuits," *IEEE Journal of Solid-State Circuits*, vol. 14, no. 3, pp. 539–549, 2001.

[41] N. M. Toriello, C. N. Liu, and R. A. Mathies, "Multichannel reverse transcription-polymerase chain reaction microdevice for rapid gene expression and biomarker analysis," *Analytical Chemistry*, vol. 78, no. 23, pp. 7997–8003, 2006.

[42] G. V. Kaigala, R. J. Huskins, J. Preiksaitis, X.-L. Pang, L. M. Pilarski, and C. J. Backhouse, "Automated screening using microfluidic chip-based PCR and product detection to assess risk of BK virus-associated nephropathy in renal transplant recipients," *Electrophoresis*, vol. 27, no. 19, pp. 3753–3763, 2006.

Chapter 7

Summary and Future Research Direction

7.1 Thesis Summary

Realizing practical lab-on-chip solutions for point-of-care disease diagnostics is only feasible only if miniaturized, integrated, automated, and cost effective instruments are developed. In this thesis, microfluidic and microelectronic technologies required to build such systems are presented. To facilitate this development, a scalable, general purpose microfluidic platform that performs all the required functionalities for *sample-in-answer-out* genetic-based diagnostics was designed, built, and tested. These functionalities include microchip-based sample preparation, genetic amplification via polymerase chain reaction (PCR) and detection via laser-induced-fluorescence (LIF) capillary electrophoresis (CE). This bench top system, with a component cost on the order of few hundreds of dollars, could be effectively used for performing genetic testing in places with minimal (or no) supporting infrastructure such as a physician's office or mobile laboratories. This system is fully validated against convectional molecular diagnostics equipment and protocols by performing a complete genetic-based analysis on a raw human sample.

We demonstrated the scalability of this technology by building custom microelectronics chips, which integrated the functionality required for genetic analysis, for a handheld (i.e., USB-key sized) instrument. At the time of writing this thesis, we have successfully demonstrated capillary electrophoresis, laser-induced-fluorescence detection, and thermocycling using these chips. The technology (i.e. CMOS) used for fabrication of these microelectronic chips permits instruments built around these chips to outperform discrete component-based instruments in several aspects: (1) orders of magnitude lower in cost; (2) lower power, allowing for battery powered operation; (3) size reduction by several orders of magnitude; (4) higher repeatability; and (5) fully automated manufacturing.

This thesis has demonstrated the technologies to realize *true* LOC diagnostics, where not only the fluidic manipulation functionalities are miniaturized and integrated into a microfluidic chip but also the required external infrastructures are miniaturized, integrated, and automated. By combining microelectronics and microfluidics, a path for future evolution of highly inexpensive and small genetic analysis instruments has been established. The end goal is to develop an inexpensive handheld, low power instrument (similar to a off-the-shelf home pregnancy test) that can perform all the required steps for genetic-based diagnostics. Our demonstrations have shown many of the subsystems and suggest the feasibility of a USB-key sized device that performs all the required steps in molecular diagnostics and costs on the order of few tens of dollars.

7.2 On-going Projects

As this thesis is being reviewed, another two manuscripts are being prepared by the author that describe further development in the technologies discussed in this thesis.

7.2.1 A Bench-Top Integrated Instrument for Sample Preparation, Realtime PCR, and Melting Point Analysis

This instrument performs all the steps required for a complete genetic diagnostics procedure based on realtime quantitative polymerase chain reaction (rqPCR) and melting point analysis (MPA) with minimal manual intervention starting from a patient's raw sample.

The rqPCR is an advancement to PCR that facilitates simultaneous amplification and quantification of a sample. In this technique the fluorescence intensity emitted by excited DNA strands, which are labeled by intercalator fluorescent dyes, is measured and plotted against the PCR cycles. Hence, the increase in fluorescence level relates to increase in the PCR product concentration (i.e. quantity).

MPA is a technique used for genotyping (studying the gene expression) of a DNA sample. In this technique, the temperature of PCR product is slowly increased (or decreased) by $\approx 0.5^{\circ}$/sec while the relative fluorescence emission is measured. A sudden change in fluorescence indicates the melting temperature of the sample or the temperature at which the negative derivative of detected florescence intensity versus temperature reaches its maximum.

In order to prove the functionality of this system, in a collaboration with Provincial Laboratory for Public Health (Dr. Yanow), we are adapting conventional macular diagnostics protocols to genotype four different types of Malaria.

7.2.2 Monolithic Microfluidic and Microelectronic Chip

As it has been discussed in chapters 5 and 6, microelectronic technology provides an excellent platform for miniaturization and high-volume production. ICs for biological applications have already been built that incorporate capacitive sensor arrays [1] and photodiodes for detection; DEP (dielectrophoresis) [2] and magnetic means [3] for actuation of molecules and cells, and fluidic components over CMOS using SU-8 epoxy [4] for sample storage and transport. On the similar line, Balslev demonstrated SU-8 microfluidic channels fabricated on a silicon wafer and sealed with a glass layer [5]. However, to date, no single monolithic solution has been developed that integrates all of these components. The key challenges limiting developments are difficulties in fabrication and integration of microfluidics at microelectronic dimensions using high-volume CMOS wafer manufacturing methods and adaptation of conventional molecular diagnostic protocols to millimeter scale microchannels.

In this demonstration, we present a CMOS-based lab on chip (LOC) device with mm-scale (mm-scale in length and μm-scale in width of depth) microfluidics that performs capillary electrophoresis (CE). The microchannels are wafer level-bonded to a LV/HVCMOS microelectronic chip detailed in chapter 5. Combining key functionalities of a standard electrophoretic instrument onto a monolithic LOC enables

the reduction of several orders of magnitude in cost of medical diagnostic instruments, size from benchtop to USB memory key dimensions and power consumption to allow for mobile operation, all of which are necessary to enable point-of-care genetic diagnostics. This work is the starting point for integration of polymer based fluidics atop of microelectronics, detailed in 7.3.1.

Enclosed microfluidic channels over Si-CMOS are fabricated using volume wafer fabrication equipments. Microfluidic channels are made of KMPR polymer; a negative photoresist (similar to SU-8), with high aspect ratio and high chemical and plasma resistance. Fabrication involves applying and patterning the polymer on Si-CMOS wafer to introduce the floor and channel walls, followed by a polymer-polymer bonding to enclose the channels. There are openings in the floor polymer that act as an interface between the integrated CMOS electrodes and the fluid, as well, there are openings on the ceiling layer for reagent filling.

7.3 Future Paths

7.3.1 Polymer-based Microfluidic Structures

The number of LOC diagnostics applications is limited by the cost of the glass chip, interfacing, and instrument. In this thesis, we have addressed the instrument cost by first introducing an inexpensive discrete component based device followed by instruments based on custom microelectronic (CMOS) chips. The remaining obstacles are the cost of the fluidic chip and its interface. Glass has been used extensively for microfluidics due to well-established microfabrication protocols and suitable chemical/optical properties. However, in mass production the commercial

use of glass is hindered by the cost of the material, lengthy/costly fabrication techniques, and the challenge of interfacing a glass chip with the operating instrument. If the technical challenges related to integrating microfluidic structures fabricated from polymers and CMOS technologies on a single mm-scale chip are addressed, this would enable far less expensive (and potentially disposable) microfluidic instruments for POC applications. Polymers such as KMPR are ideal for this integration due to its excellent adhesion to metals, CMOS compatibility and excellent aspect ratios and optical properties all of which are required for realizing monolithic microfluidic-microelectronic devices with an optical detection mechanism.

To achieve similar functionality as our glass microfluidics chip, we are integrating various components into our polymer-based chips. These components include, but are not limited to heaters, temperature sensors, optical filters, and valves/pumps (explained in section 7.3.2).

7.3.2 Integrated Electrically Actuated Valves and Pumps

Integrated valves/pumps are necessary for on-chip fluidic manipulation. Although our current design of valves/pumps is efficient, it requires air pressure and vacuum sources, increasing the cost, size, and power consumption of the instrument. Moreover, interfacing the air pressure/vacuum to microfluidic chips hinders higher level of integration. To realize a highly miniaturized monolithic device similar to what was presented in section 7.2.2, a low power, miniaturized, CMOS compatible electrically actuated valve is necessary.

As DALSA HV CMOS process offers required voltages for high electric fields (few thousands V/cm), an electrostatic valve with a polymer membrane (i.e. KMPR) is an ideal candidate. At the time of writing this thesis, we are in the process of integrating electrostatic valves into our microfluidic chips.

7.3.3 On-chip Reagent Storage

Reagent storage and transportation at room temperature is one of the main bottlenecks for extensive use of LOC-based diagnostics in remote areas. One potential solution is to spot lyophilize (i.e. freeze-dry) reagents on microfluidics chips. Lyophilization enables reagents to be transported at room temperature and also increases the shelf-life of the reagents. In a collaboration with Dr. Sigurdson (Mechanical Engineering), we are investigating the possibility of including lyophilized reagents on our microfluidics chips.

7.3.4 Test Multiplexing on a Single Instrument

Clinical diagnostics often require several tests to be done on a single sample simultaneously. These tests can be either positive/negative control tests for a single pathogen and/or examining for multiple pathogens. While our focus has been on developing single reaction instruments, the modular scheme of our instruments enables integration of several reaction chambers (i.e. PCR) with a negligible technical difficulties.

7.3.5 LED-based Light Source for LIF-CE and rqPCR

Although laser diodes have been used extensively as excitation sources for LIF-based CE and rqPCR due to their confined beam, and precise wave length, high cost and optical power output instability (especially for inexpensive uncooled lasers) limit their use for sensitive LOC application. Advancements in light emitting diode (LED) fabrication technology in recent years have paved the way for using LEDs as a light source for LOC applications. Similar to many other research groups, we are actively investigating using LEDs for excitation sources by addressing central technical challenges including light collimation and spectral specificity through optical filtering.

Bibliography

[1] A. Romani, N. Manaresi, L. Marzocchi, G. Medoro, A. Leonardi, L. Altomare, M. Tartagni, and R. Guerrieri, "Capacitive sensor array for localization of bioparticles in cmos lab-on-a-chip," in *Solid-State Circuits Conference, 2004. Digest of Technical Papers. ISSCC. 2004 IEEE International*, Feb. 2004, pp. 224–225 Vol.1.

[2] N. Manaresi, A. Romani, G. Medoro, L. Altomare, A. Leonardi, M. Tartagni, and R. Guerrieri, "A cmos chip for individual cell manipulation and detection," in *Solid-State Circuits Conference, 2003. Digest of Technical Papers. ISSCC. 2003 IEEE International*, 2003, pp. 192–487 vol.1.

[3] H. Lee, Y. Liu, E. Alsberg, D. Ingber, R. Westervelt, and D. Ham, "An ic/microfluidic hybrid microsystem for 2d magnetic manipulation of individual biological cells," in *Solid-State Circuits Conference, 2005. Digest of Technical Papers. ISSCC. 2005 IEEE International*, Feb. 2005, pp. 80–586 Vol. 1.

[4] Z. Peng, Z. Ling, M. Tondra, C. Liu, M. Zhang, K. Lian, J. Goettert, and J. Hormes, "CMOS compatible integration of three-dimensional microfluidic systems based on low-temperature transfer of SU-8 films," *Journal of Microelectromechanical Systems*, vol. 15, no. 3, pp. 708–716, JUN 2006.

[5] S. Balslev, A. M. Jorgensen, B. Bilenberg, K. B. Mogensen, D. Snakenborg, O. Geschke, J. P. Kutter, and A. Kristensen, "Lab-on-a-chip with integrated optical transducers," *Lab on a Chip*, vol. 6, no. 2, pp. 213–217, 2006.